UNIVERSITY OF SOUTHAMPTON

Bone & Joint Research Group

School of Medicine

BONE TISSUE ENGINEERING: EXPERIMENTAL STRATEGIES & CLINICAL APPLICATION

by

Alexander Aarvold

Thesis for the degree of Doctor of Medicine

June 2011

Thesis Abstract

Skeletal stem cell based therapies offer tremendous potential for regeneration of a patient's bone. With the demographics of an ageing population, the demand for skeletal reconstruction to replace lost or damaged bone is expanding dramatically. Novel bone tissue engineering techniques offer the opportunity to push the boundaries of bone regeneration, yet few strategies have been translated to clinical practice.

This thesis aims to explore novel bone regeneration strategies *in vitro* and *in vivo*, and details the clinical application of those techniques. The effects of skeletal stem cells, growth factors and material properties on osteogenesis of bone tissue engineering constructs were explored:

- Skeletal stem cells and human fibronectin were shown to augment the biomechanical characteristics of impacted allograft.
- Alteration of porosity in a synthetic ceramic scaffold had an effect on osteogenesis.
- Innovative technology for enriching the skeletal stem cell fraction from aspirated bone marrow was successfully trialled on bone marrow from an elderly cohort of patients, reaching a therapeutic cellular concentration.
- A pathological role for osteogenic cells was demonstrated in unicameral bone cysts, with up-regulation of RANKL related cytokines and stimulation of osteoclastic activity.
- Retrieval of tissue from an early translated tissue engineering case provided the opportunity for *ex vivo* analysis, with discussion on lessons that can be learned for future translation.
- A novel tissue engineering strategy, to augment the biological and mechanical characteristics of impacted allograft, was subsequently translated to a case series of four patients with avascular necrosis of the femoral head. Surgical technique, clinical follow-up and analysis of retrieval tissue is described.

This study has shown the efficacy of skeletal stem cells for bone regeneration *in vitro* and *in vivo*, and explored techniques to further augment their osteogenic capacity on bone graft extenders. The translational potential of this bone tissue engineering technology has been realised from the bench to the clinic.

Table of Contents

List of Figures

List of Tables

Declaration

I hereby declare that this thesis is composed entirely of my own work, as a member of a research group. Contributions from other members of the research group, and collaborations with other institutions, are acknowledged in the appropriate sections where this has occurred. I have not submitted this thesis in candidature for any other degree, diploma or professional qualification

……..……...

Mr Alexander Aarvold MBChB, BSc(Hons), MRCS

Acknowledgements

To my mum and dad, whose values and attributes I have striven to emulate, and who have supported me unquestioningly. I would further like to acknowledge the following for their support, advice, discussions and assistance:

Supervisors:
Professor Richard OC Oreffo, Mr Douglas G Dunlop

Bone & Joint Research Group:
Mr James Smith, Mr Edward Tayton, Mr Andrew Jones
Esther Ralph, Joanna Greenhough, Carol Roberts, Kate Murawski, Stefanie Inglis
Dr Jon Dawson, Dr Stuart Lanham, Dr Janos Kanczler, Dr Rahul Tare

Bioengineering Science Research Group:
Dr Adam Briscoe, Professor Mark Taylor

Biomedical Research Unit:
Jas Barley, Kerry Taylor

Southampton University Hospitals Trust:
Mr David Higgs, Mr Ed Gent, Miss Caroline Edwards, Dr Darren Fowler, Mrs Sue Hill

Smith & Nephew UK Ltd and Technology Strategy Board:
Dr Steve Curran, Dr Jon Ridgway, Bridget Mathews

University of Bath:
Dr Irene Turner, Mrs Ursula Potter, Dept of Mechanical Engineering
Professor Julian Chaudhuri, Department of Chemical Engineering

Holly Tree Cottage
Alice Aarvold – for her unerring support and for almost single handedly looking after first Benjamin, then Eliza, who were both born during the preparation of this thesis.

Abbreviations

ALP	alkaline phosphatase
AVN	avascular necrosis
A/S	Alcian blue / Sirius red
BMA	Bone marrow aspirate
c	*circa*
CFU-F	Colony forming unit - fibroblast
CTG-EH	CellTracker Green – Ethidium Homodimer
DNA	Deoxyribonucleic acid
ECM	Extra-cellular matrix
FCS	Foetal calf serum
HFN	Human Fibronectin
IBG	Impaction Bone Grafting
IL	Interleukin
μCT	micro Computed Tomography
MCP-1	Monocyte chemotactic protein - 1
M-CSF	Macrophage colony stimulating factor
MEM	Modified Eagle's medium
MIP-1α	Macrophage inflammatory protein - 1
OPG	Osteoprotegerin
ppi	pores per inch
RANKL	Receptor Activated by NFκB Ligand
RGD	Arginyl-Glycyl-Aspartic acid
SEM	Scanning electron microscopy
SSC	Skeletal stem cell
TGF-β	Transforming growth factor - β
THR	Total hip replacement

Publications & Book chapters

Publications

1. "Skeletal stem cells and bone regeneration: Translational strategies from bench to clinic
   Tare RS, Kanczler JM, **Aarvold A**, Jones AMH, Dunlop DG, Oreffo ROC
   Proc. IMechE 2010;224(12) Part H: J.Engineering in Medicine:1455-70. Review
2. "Taking tissue engineering principles into theatre: retrieval analysis from a clinically translated case"
   Aarvold A, Smith JO, Tayton ER, Tilley S, Dawson JI, Briscoe A, Lanham SA, Dunlop DG, Oreffo ROC
   Regen Med 2011;6(4):461-7
3. "Skeletal tissue regeneration – current approaches, challenges and novel reconstructive strategies for an ageing population"
   Aarvold A, Smith JO, Tayton ER, Dunlop DG, Oreffo ROC
   Tiss Eng Part B Rev 2011;17(5):307-20
4. "From bench to clinic and back: skeletal stem cells and impaction bone grafting for regeneration of bone defects"
   Aarvold A, Smith JO, Tayton ER, Jones AMH, Dawson JI, Briscoe A, Lanham SA, Dunlop DG, Oreffo ROC
   Submitted with revisions Oct 2011, J Tiss Eng Regen Med
5. "The effect of scaffold porosity on skeletal stem cell growth and differentiation"
   Aarvold A, Smith JO, Tayton ER, Lanham SA, Chaudhuri J, Turner IG, Oreffo ROC
   Submitted Oct 2011, Biochem Biophys Res Comm
6. "The pathogenesis of unicameral bone cysts is driven by osteoblast-osteoclast signalling"
   Aarvold A, Smith JO, Tayton ER, Edwards C, Fowler D, Gent ED, Oreffo ROC
   Submitted Sept 2011, JBJS(Am)

Abstracts

1. "The optimisation of polymer type and chain length for use as a biological composite graft in impaction bone grafting: a mechanical and bio-compatibility analysis"
   J Bone Joint Surg (Br), Proceedings (BOA 2011)
   Tayton ER, Fahmy S, **Aarvold A**, Smith JO, Dunlop DG, Shakesheff K, Howdle S, Oreffo ROC
2. "Does increasing PLA scaffold porosity using supercritical CO_2 strategies enhance the characteristics for use as an alternative to allograft in impaction bone grafting?"
   J Bone Joint Surg (Br), Proceedings (BOA 2011)
   Tayton ER, Purcell H, **Aarvold A**, Smith JO, Dunlop DG, Shakesheff K, Howdle S, Oreffo ROC
3. "Tantalum trabecular metal - Addition of skeletal stem cells to enhance the bone-implant interface"
   J Bone Joint Surg (Br), Proceedings (BOA 2011)
   Smith JO, Sengers B, **Aarvold A**, Tayton ER, Dunlop DG, Oreffo ROC
4. "Enrichment of skeletal stem cells to enhance skeletal regeneration – a novel clinical technique"
   J Bone Joint Surg (Br), Proceedings (BORS / BRS 2011)
   Smith JO, Dawson JI, **Aarvold A**, Dunlop DG, Ridgway J, Curran S, Oreffo ROC

5. "The optimisation of polymer type and chain length for use as a biological composite graft in impaction bone grafting: a mechanical and bio-compatibility analysis"
   J Bone Joint Surg (Br), Proceedings (BORS / BRS 2011)
   Tayton ER, Fahmy S, **Aarvold A**, Dunlop DG, Shakesheff K, Howdle S, Oreffo ROC
6. "Does increasing PLA scaffold porosity using supercritical CO_2 strategies enhance the characteristics for use as an alternative to allograft in impaction bone grafting?"
   J Bone Joint Surg (Br), Proceedings (BORS / BRS 2011)
   Tayton ER, Fahmy S, **Aarvold A**, Dunlop DG, Shakesheff K, Howdle S, Oreffo ROC
7. "A tissue engineering strategy for the treatment of osteonecrosis: evaluation of efficacy in four patients"
   Aarvold A, Smith JO, Tayton E, Dawson JI, Briscoe A, Lanham SA, Dunlop DG, Oreffo RO
   J Bone Joint Surg (Br), Proceedings (EFORT 2011)
8. "Optimisation of polymer and stem cell technology to produce substitute allograft for use in impaction bone grafting"
   Tayton ER, Fahmy S, **Aarvold A**, Shakesheff K, Howdle S, Oreffo ROC, Dunlop DG
   J Bone Joint Surg (Br), Proceedings (EFORT 2011)
9. "Biological augmentation of impaction bone grafting: retrieval analysis of human tissue engineered specimens
   Aarvold A, Smith JO, Tayton ER, Briscoe A, Lanham S, Dawson JI, Oreffo RO, Dunlop DG
   J Bone Joint Surg (Br), Proceedings (BHS 2011)
10. "Cyst fluid and stem cells: why unicameral bone cysts are so hard to treat"
    Aarvold A, Smith JO, Edwards CJ, Tayton ER, Gent ED, Oreffo ROC
    J Bone Joint Surg (Br), Proceedings (BSCOS 2011)
11. "The development of a custom-made IM nail for use in an ovine tibial segmental defect model"
    Briscoe A, **Aarvold A**, Street M, Tayton E, Smith JO, Dunlop DG, Oreffo ROC
    J Biomech 2010;43:Supp I:71
12. "The use of impaction bone grafting and skeletal stem cells for the treatment of avascular necrosis of the femoral head
    Aarvold A, Jones AMH, New A, Oreffo RO, Dunlop DG
    J Bone Joint Surg (Br), Proceedings (BORS 2010)

Book Chapters

1. "Bone Tissue Engineering"
   Dawson JI, Kanczler J, Smith JO, **Aarvold A**, Dunlop DG, Oreffo RO
   In: Comprehensive Biotechnology
   Editors. Z Cui & L Brandon, Publisher: Elsevier, 2011
2. "Skeletal stem cells: phenotype, nanotopography, biomimetic niche and translational biology"
   Dawson JI, Kanczler J, **Aarvold A**, Kingham EJ, Oreffo RO
   In: Stem Cells: Basic Biology and Clinical Applications,
   Editor: M Kassem, Publisher: King Saud University Press, 2011
3. "Clinical applications for skeletal / mesenchymal stem cell therapy"
   Tayton ER, Smith JO, **Aarvold A**, Oreffo RO, Zaleh W, Kassem M
   In: Stem Cells: Basic Biology and Clinical Applications,
   Editor: M Kassem, Publisher: King Saud University Press, 2011

Presentations

1. "Tantalum trabecular metal - Addition of skeletal stem cells to enhance the bone-implant interface"
   BOA, Dublin, 15/9/11
   Podium – James Smith
2. "The optimisation of polymer type and chain length for use as a biological composite graft in impaction bone grafting: a mechanical and bio-compatibility analysis"
   BOA, Dublin, 14/9/11
   Podium – Ed Tayton
3. "Does increasing PLA scaffold porosity using supercritical CO_2 strategies enhance the characteristics for use as an alternative to allograft in impaction bone grafting?"
   BOA, Dublin, 14/9/11
   Podium – Ed Tayton
4. "Exploring the pathogenesis of unicameral bone cysts"
   Gauvain, 17/6/2011
   Podium presentation
5. "Retrieval analysis of clinically translated human tissue"
   Gauvain, 17/6/2011
   Podium presentation
6. "A tissue engineered substitute for allograft to use in impaction bone grafting"
   Gauvain, 17/6/2011
   Podium presentation – Ed Tayton
7. "The exothermic effects of setting bone cement"
   Gauvain, 17/6/2011
   Podium presentation – Ed Tayton
8. "Extending the role of tantalum trabecular metal using tissue engineering strategies"
   Gauvain, 17/6/2011
   Podium presentation – James Smith
9. "Clinical Translation of Bone Tissue Engineering"
   Medicine & Biological Sciences Postgraduate Conference, Southampton, 8/6/11
   Podium presentation
10. "Optimisation of polymer and stem cell technology to produce substitute allograft for impaction bone grafting"
    Medicine & Biological Sciences Postgraduate Conference, Southampton, 8/6/11
    Poster presentation
11. "A clinical strategy to concentrate aspirated bone marrow for skeletal stem cells to enhance skeletal regeneration"
    Tissue Engineering & Regenertive Medicine International Society (TERMIS), Granada, Spain, 7/6/11
    Podium – Jon Dawson
12. "A tissue engineering strategy for the treatment of osteonecrosis: evaluation of efficacy in four patients"
    EFORT, Copenhagen, 3/6/11
    Podium presentation
13. "Optimisation of polymer and stem cell technology to produce substitute allograft for use in impaction bone grafting"
    EFORT, Copenhagen, 3/6/11
    Podium presentation – Ed Tayton
14. "Novel technology for enrichment of skeletal stem cells from bone marrow"

EFORT, Copenhagen, 2/6/11
E-poster presentation

15. "Evidence based reduction in prophylactic antibiotic use for elective orthopaedic surgery: a single centre audit cycle"
    EFORT, Copenhagen, 2/6/11
    E-poster presentation
16. "A tissue engineering strategy for the treatment of AVN: clinical translation and analysis of retrieval specimens"
    Orthopaedic Research Society (ORS), Long Beach, California, 13-16/1/11
    Poster presentation
17. "The optimisation of polymer type and chain length for use as a biological composite graft in impaction bone grafting: a mechanical and bio-compatibility analysis"
    British Orthopaedic Research Society (BORS), Cambridge, 27/6/11
    Podium presentation – Ed Tayton
18. "Does increasing PLA scaffold porosity using supercritical CO_2 strategies enhance the characteristics for use as an alternative to allograft in impaction bone grafting?"
    British Orthopaedic Research Society (BORS), Cambridge, 27/6/11
    Podium presentation – Ed Tayton
19. "Enrichment of skeletal stem cells to enhance skeletal regeneration – a novel clinical technique"
    British Orthopaedic Research Society (BORS), Cambridge, 27/6/11
    Podium presentation – James Smith
20. "A tissue engineering approach with tantalum trabecular metal to enhance bone-implant integration"
    British Orthopaedic Research Society (BORS), Cambridge, 28/6/11
    Oral poster presentation – James Smith
21. "Retrieval analysis of tissue engineered bone: a clinical and laboratory study"
    British Orthopaedic Research Society (BORS), Cambridge, 27/6/11
    Poster presentation
22. "Enrichment of skeletal stem cells from bone marrow to enhance skeletal regeneration – a novel clinical technique"
    UK National Stem Cell Network (UKNSCN), York, 30/3/11
    Poster presentation, Pfizer Award for Best Clinical Translation Poster
23. "Biological augmentation of impaction bone grafting: retrieval analysis of human tissue engineered specimens?"
    British Hip Society (BHS), Research Prize Session, Torquay, 2/3/11
    Podium presentation
24. "Cyst fluid and stem cells: why unicameral bone cysts are so hard to treat"
    British Society for Children's Orthopaedic Surgery (BSCOS), Sheffield, 28/1/11
    Podium presentation
25. "From bench to clinic – retrieval of human tissue engineered bone"
    University of Southampton Translational Research Conference, 16/11/10
    Poster Presentation
26. "Development of a novel strategy for enrichment of skeletal stem cells for clinical application"
    University of Southampton Translational Research Conference, 16/11/10
    Poster Presentation
27. "The use of Impaction Bone Grafting and skeletal stem cells for the treatment of AVN of the femoral head – evaluation of efficacy in 4 patients"
    Gauvain, 16/7/2010

Podium presentation

28. "Novel Technology to provide an enriched therapeutic skeletal cell concentrate from bone marrow aspirate"
    Gauvain, 16/7/2010
    Podium presentation – James Smith
29. "The use of impaction bone grafting and skeletal stem cells for the treatment of avascular necrosis of the femoral head"
    British Orthopaedic Research Society (BORS), Cardiff, 13/7/10
    Podium presentation
30. "The development of a custom-made IM nail for an ovine tibial segmental defect model"
    International Conference on Orthopaedic Biomechanics, Clinical Applications and Surgery (OBCAS), Brunel University, London, 7/6/10
    Podium presentation – Adam Briscoe
31. "The use of autologous stem cells to treat AVN of the femoral head"
    Technology for Young Adult and Sports Hip Pathology, Warsaw, 23/4/10
    Podium presentation, Invitational Lecture
32. "Use of skeletal stem cells and impaction bone grafting in treatment of avascular necrosis"
    University of Southampton Translational Research Conference, 4/11/09
    Poster Presentation, 2nd Prize

Prizes

1. Pfizer Award, Best Clinical Translation Poster,
   UK National Stem Cells Network Annual Conference, York, 31/3/11
2. No.1 invention, 'Top Ten of 2010' Medical Device Developments, Orthopaedic Stem Cell Concentrator. Page 16, http://edition.pagesuite-professional.co.uk/launch.aspx?referral=other&pnum=&refresh=9Fe10q8Z6Ng0&EID=944749fd-1399-4f9a-bd83-faf9ba078b1b&skip=
3. Winner, Medical & Healthcare Category: 'The Engineer' Technology & Innovation Awards 2010; 'Development of a Novel Orthopaedic Stem Cell Concentrator'
4. Winner, Grand Prix: 'The Engineer' Technology & Innovation Awards 2010; 'Development of a Novel Orthopaedic Stem Cell Concentrator'
5. NHS Education South Central (NESC) Travelling Fellowship
   Visit to Rizzoli Orthopaedic Institute, Bologna, Italy, Oct 2009
6. Gauvain 2011, 2nd Prize
7. Gauvain 2010, 3rd Prize
8. University of Southampton Translational Research Conference, 4/11/09
   Poster Presentation, 2nd Prize

'The Engineer' awards ceremony at The Royal Society, London, Friday 3rd December 2010.

From left to Right, Alex Aarvold, Jon Dawson, Robert Llewellyn, James Smith

www.theengineerawards.co.uk

Chapter I

Introduction

Introduction

1.1 Bone tissue regeneration

The concept of tissue regeneration has been around since Greek mythology when the great Titan, Prometheus, was punished by Zeus for giving the gift of fire to mankind. Tied to a rock on Mount Kaukasos, an eagle would come and eat his liver, only for it to regenerate overnight and for him to undergo the same fate the next day and for eternity (**Fig.1**).

Figure 1: 'Prometheus Bound', Oil on Canvas c1640 by Jacob Jordaens (1593-1678).

Tissue engineering can be defined as the application of scientific principles to the design, modification, growth and maintenance of living tissues (Langer & Vacanti 1993). The science of tissue engineering has expanded dramatically in recent years, notably in orthopaedic applications, for therapeutic, not punitive application, and there is intense

interest in harnessing the potential of tissue engineering to replace lost bone stock with a patient's own regenerated bone. There are three elements central to the science of bone tissue engineering:

1) **Osteoconduction** – scaffolds / allograft provide a matrix for cell growth.
2) **Osteoinduction** – bone growth factors induce differentiation of cells into the osteoblastic phenotype.
3) **Osteogenesis** – osteoblasts are required for generation of osteoid, and are derived from skeletal stem cells.

Skeletal stem cells were first identified by Friedenstein and colleagues, who described a population of spindle-shaped stromal cells present in the bone marrow that had the capacity for self renewal, differentiation into more than one cell type and maintain the capacity for cell division throughout life. These cells can be made to differentiate along multiple mesodermal lineages to generate cartilage, bone, myelosupportive stroma, adipocytes and fibrous connective tissue (**Fig.2**) (Friedenstein *et al.* 1968;Friedenstein 1976;Friedenstein *et al.* 1978;Lajtha 1979). These stromal cells are multipotent, rather than pluripotent like foetal stem cells, but exist in post-natal bone marrow. Thus their use avoids the ethical controversies of embryonic stem cells. A variety of terms have been applied including mesenchymal stem cells, osteogenic stem cells, osteoprogenitor cell, marrow stromal fibroblastic cells, human bone marrow stromal cells and skeletal stem cells (Bianco & Robey 2001), the latter term being used in this thesis.

Figure 2: Multipotent differentiation lineages of post-natal bone marrow derived SSCs (adapted from Bolland *et al.* 2007).

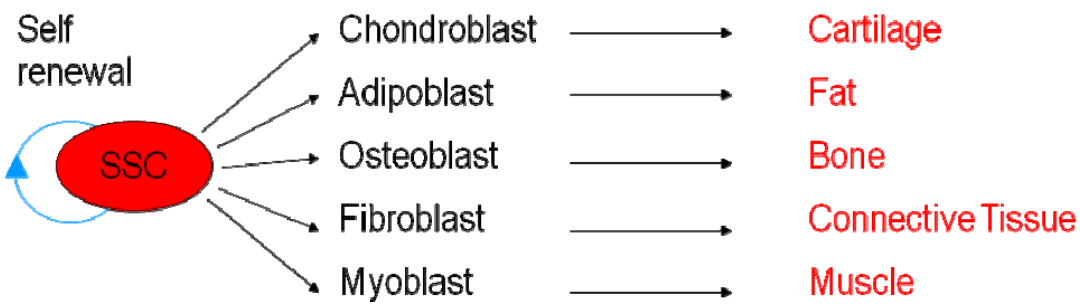

1.2 Burden of Problem

Bone loss as a consequence of trauma, injury or disease represents a significant cause of chronic morbidity, impacting not only on an individuals' mobility, but additionally affecting their wider health, social and economic status (Kilgore *et al.* 2009;Heckman & Sarasohn-Kahn 1997;Dahabreh, Dimitriou, & Giannoudis 2007). Although current strategies to replace or restore lost bone can be successful, the approaches come with substantial limitations and inherent disadvantages that may in themselves contribute to patient morbidity. It is now clear that the challenges of an increasingly ageing demographic, along with changing clinical scenarios and rising functional expectations provide the imperative for new, more reliable bone regeneration strategies. Approaches to treat the traditional causes of bone loss such as trauma, infection, inflammation and the treatment of tumours are now also being adapted to treat the elective cohort of patients who require bone defect reconstruction during revision arthroplasty surgery (McNamara 2010). The proportion of people in Britain aged over 65 years is projected to increase by nearly 50% in the next 25 years, and a concomitant increase in such orthopaedic revision surgery can be expected (Office for National Statistics 2008). Although primary hip arthroplasty was successfully introduced around fifty years ago, many of the techniques, prostheses and instruments had not yet been refined. Consequently increasing numbers of patients are now presenting who require challenging revision surgery due to extensive bone loss around loose implants (**Fig.3A-B**). Over 72,000 total hip replacement procedures were performed in 2009 in the United Kingdom in comparison to just 30,000 in 2003, and the number of revision hip procedures more than doubled over this period, to 7,136 (National Joint Registry 2010). In addition, knee arthroplasty is now performed more often than hip arthroplasty, thus the true scale of the problem of inadequate bone stock in revising total knee replacements will only emerge in the years to come (**Fig.3C**).

Figure 3A: Antero-posterior radiograph of a right hip cemented hemi-arthroplasty. B: Radiograph of the same prosthesis with progressive osteolysis, seen as a lucency surrounding the prosthesis, marked with arrows. C: Anteroposterior and lateral radiographs of a patient's left knee, showing a revision total knee replacement with significant loss of bone stock, marked with arrows. Such scenarios are becoming increasingly common in clinical practice, causing significant symptoms and presenting a surgical challenge to reconstruct the joint in order to restore quality of life for the patient. Images courtesy of Southampton University Hospitals NHS Trust.

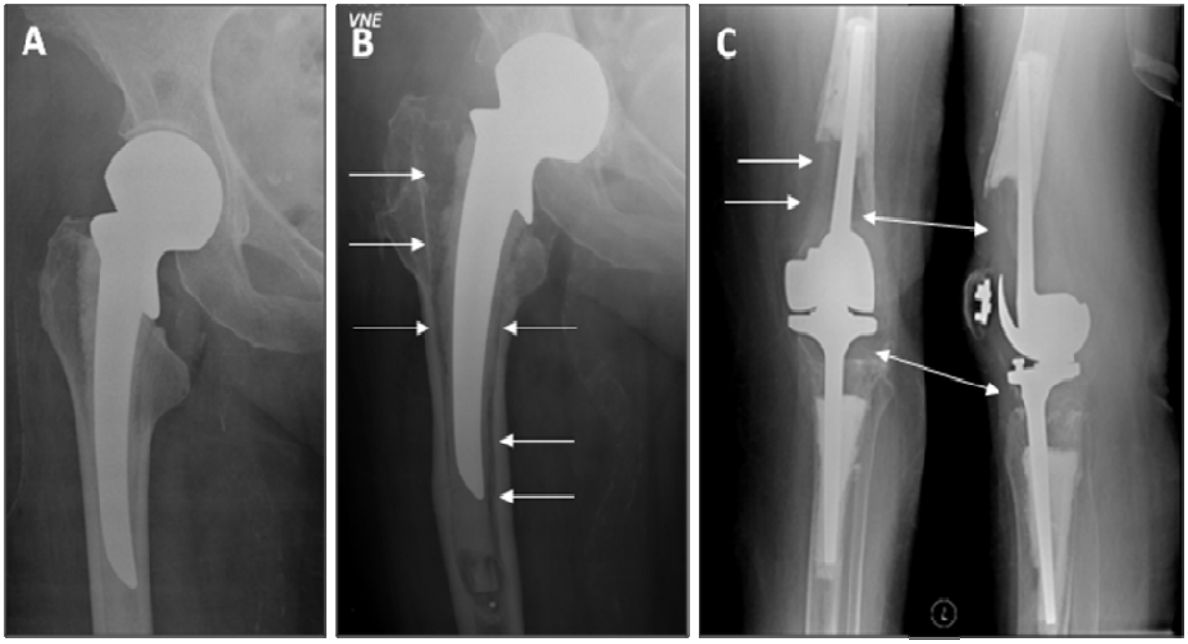

Current approaches in clinical practice for replacement of lost skeletal tissue are outlined below, along with a discussion of the significant hurdles, challenges and drawbacks of current strategies. Innovative approaches for *de novo* skeletal tissue generation offer exciting potential, but remain confined to the laboratory due to practical and financial constraints. Thus most scientific potential falls into the 'Valley of Death', unable to scale up to large animal trials nor clinical practice (Reichert *et al.* 2009). However, some bone tissue engineering strategies have made the transition to clinical practice, and these are reviewed below.

1.3 Current bone tissue reconstruction strategies and their limitations

Many procedures to reconstruct bone defects have developed from the challenges of treating congenital deformities or tumours, and from experiences in wartime (Hindle 2010;Saleh, Yang, & Sims 1999;Aronson 1997;Eward *et al.* 2009;Kanakaris *et al.* 2007;Parsons & Strauss 2004;Brown & Shaw 2010;Swennen *et al.* 2001). Trauma accounts for many such situations as non-union may follow any fracture and major injury with significant bony comminution, devascularisation or frank bone loss can leave a defect too large for bridging callus. Surgically-induced bone defects may be caused following resection of tumours, debridement of osteomyelitis, osteoarthritis and inflammatory arthritis or in the treatment of congenital defects, notably in maxillofacial surgery. Furthermore, the loss of bone stock around prosthetic implants, as illustrated in **Figure 2**, has become an additional factor driving the mandate to develop better reconstructive techniques (Halliday *et al.* 2003;Schreurs *et al.* 2009;Bolland *et al.* 2007).

Reconstructive solutions currently include distraction osteogenesis (DO) and bone grafting using autologous bone, allograft or synthetic biomaterials. DO was first described by Codivilla in 1905 to allow for gradual lengthening of soft tissues alongside correction of severe bone deformities (Codivilla 2008). Ilizarov refined the technique and apparatus, demonstrating successful healing of established fracture non-unions (Rozbruch & Ilizarov 2007). Patients are now routinely treated by this osteotomy-distraction technique to regenerate bone lost through surgical debridement, fracture non- and mal-union, congenital deformity, for limb lengthening in dwarfism and for some skeletal sequelae of poliomyelitis (Aronson 1997). Ring external fixators stabilise the affected area and are distracted at a rate of 1mm per day, generating healing and ossification by microfractures (Shearer, Roach, & Parsons 1992). This technique takes advantage of the regeneration

potential of bone without the use of bone graft and allows large skeletal defects to be healed with some excellent functional outcomes (Schep *et al.* 2009). However, the healing index is just 2-3 months per centimetre of bone lengthened, so patients often require treatment for many months. Furthermore, successful outcomes of DO are dependent on intensive patient education and co-operation, high levels of specialist support, frequent hospital visits and often multiple procedures. Complications are frequent, with pin tract infection in up to 95% of patients as well as cellulitis, osteomyelitis, non- and mal-union and psychological consequences (Aronson 1997).

Autologous bone graft, either vascularised or free, represents the current clinical gold standard for treating bone defects (Marino & Ziran 2010). It provides an osteoconductive three-dimensional scaffold with osteoinductive properties through growth factors and vascularisation, whilst retaining native cells with osteogenic potential (Delloye *et al.* 2007). It can be harvested and implanted during the same operation, and because no new material is introduced, it provokes no immunogenic reaction at the recipient site. However, associated donor site morbidity limits its application (Ahlmann *et al.* 2002). The development of free vascularised bone grafts has facilitated autograft use in larger defects, particularly where structural support is also required, for example in limb salvage and reconstruction (Taylor, Miller, & Ham 1975). Autologous vascularised fibula, scapula, iliac crest, and rib transplant have been used to repair major discontinuity defects of over 5cm, such as those which exist after ablative tumour surgery (Warnke *et al.* 2004). The proximal fibula is a particularly good candidate for such interventions, as it functions mainly as an attachment for muscles, and removal leads to minimal donor site morbidity (Muramatsu *et al.* 2004). In a series of patients with surgically-induced long bone segmental defects following tumour resection, treatment with vascularised fibular grafts

produced primary union in 23 out of 30 patients (77%) at a mean of six months. However, over half of these patients suffered complications and 40% required re-operation for non-union, graft fracture or infection (Eward *et al.* 2009). The technique has been refined by placing the fibular autograft within the intramedullary space of a structural cortical allograft shell to aid initial stability and promote the biology and regeneration of host bone. However, the technical difficulty and high complication rates of such procedures, and the additional problems inherent in using both autograft and allograft remain (Innocenti *et al.* 2009;Capanna *et al.* 2007;Abed *et al.* 2009). For these reasons, allograft alone is generally favoured for the treatment of expansive defects despite significant biological, economic and practical disadvantages to its use (Emms *et al.* 2009).

Allograft has been shown to initiate a healing response, inducing cells from surrounding soft tissue to produce new bone at the host-graft interface, which then progresses into the graft material. However, this requires a contiguous vascular supply and adequate mechanical stability to allow vessel in-growth and eventual bone remodelling (Hernigou *et al.* 2005b;Stevenson, Emery, & Goldberg 1996). These conditions are often absent, particularly in traumatic defects, where surrounding soft tissue disruption and instability are expected.

Allograft can be milled and impacted to provide a mechanically solid graft and this has been used in revision hip surgery for over forty years as a 'void filler' to support the prosthesis in the context of loss of bone stock (Slooff *et al.* 1984). Survivorship of relatively small defects around acetabular and femoral components at 10 and 20 years respectively is encouraging (99% (Halliday *et al.* 2003) and 87% (Schreurs *et al.* 2009). However, such results have not always been replicated outside major centres or for the

treatment of larger defects, possibly because the surgery is technically demanding and operator-dependent (Eldridge *et al.* 1997;van Haaren *et al.* 2007).

Allograft may be obtained from cadavers or live donors, for example patients undergoing hip replacement surgery where the femoral head would routinely be removed and discarded. However, given the concerns of potential pathogen transmission, strictly regulated regional 'bone banks' have been introduced to screen and store freeze-dried, fresh-frozen or irradiated allograft for future use. This system has the advantage of providing a ready supply of screened and quarantined bone, however the mechanical, biological and immunological properties of allograft may be affected differently by each storage process (Schreurs *et al.* 2004). Although it can act as an osteoconductive scaffold, the requirement to process allograft for safe storage and to reduce its immunogenic reactivity, removes much of its inherent osteoinductive properties. Nevertheless, despite stringent processing and donor screening there remains the possibility of carriage of bacteria, viruses and prions, some of which may yet be discovered. Following the introduction in the UK of the Human Tissue Act in 2004, legislation to ensure traceability of allograft has complicated the process (Her Majesty's Stationery Office 2004). Furthermore, the logistics of acquisition, transport and storage of allograft make it a costly exercise, and as requirements increase, supply will soon be outstripped by demand (Delloye *et al.* 2007).

As a consequence of the inherent disadvantages of autograft and allograft, there has been a significant drive for the development of synthetic scaffold materials, including bio-resorbable polymers (e.g. polylactic acid), naturally occurring polymers (e.g. hydrogels, collagen) and ceramics (e.g. hydroxyapatite, beta-tricalcium phosphate), which aim to

mimic the beneficial characteristics of biological material whilst avoiding their drawbacks (Hutmacher *et al.* 2007). Synthetic scaffolds can be fabricated to possess desirable osteoconductive properties and these materials are readily available subject to manufacturing processes, although work is ongoing to improve structural, osteoinductive and bioresorptive properties. Advances have also been made in the generation of osteoconductive metals, particularly with hydroxyapatite coatings and porous trabecular metals, for the management of lost bone stock (Levine *et al.* 2006). Hydroxyapatite coatings are used in revision hip surgery and for reconstruction after tumour resection, to promote bone in-growth and reduce the rate of aseptic loosening (Trikha *et al.* 2005;Spiegelberg *et al.* 2009). The osteoconductive properties of tantalum trabecular metal have been exploited in many areas of orthopaedic surgery including spinal fusion, primary and revision hip and knee arthroplasty, for the treatment of femoral head avascular necrosis and for custom tumour implants in limb salvage surgery (Bobyn *et al.* 2004;Findlay *et al.* 2004). In a series of 23 revision hip replacements with Paprosky Type III defects that were treated with tantalum components, none has shown mechanical failure at 35 months follow up (Flecher, Sporer, & Paprosky 2008).

The osteoconductive nature of trabecular metals has been applied to clinical practice, and there is growing evidence of osteoinductive properties of tantalum and titanium, with hetereotopic bone growth induced in vivo without supplementation with osteoinductive or osteogenic factors (Habibovic *et al.* 2006a;Fellah *et al.* 2008;Yuan *et al.* 2010;Ripamonti *et al.* 2009;Fujibayashi *et al.* 2004). However, in a goat femoral diaphyseal defect model, the use of trabecular tantalum cylinders required the preservation of native periosteum in order to achieve bony union (Bullens *et al.* 2009). This indicates potential limitations in the application of tantalum to long bone traumatic, infective or neoplastic cases where the

periosteum is typically absent. Furthermore, metals are not biodegradable and removal can cause considerable collateral damage to surrounding bone should subsequent revision be required.

The treatment of femoral head avascular necrosis using trabecular tantalum rods represents a pragmatic alternative to vascularised fibular grafting, and has potential advantages of immediate construct stability, expediting safe weight-bearing and return to function (Veillette *et al.* 2006). The procedure can be performed using a minimally-invasive technique and without the disadvantage of donor site morbidity, however in cases where subchondral bone collapse does occur, the implant may become proud, causing pain and marked acetabular erosion. On subsequent removal of the metal implant to allow joint reconstruction, the result is a sizeable defect that ultimately requires further grafting and may contaminate the replacement with metal debris caused by the difficulty in extraction.

The inherent disadvantages of metal implants, autograft and allograft, combined with the ageing population, a progressive increase in musculoskeletal pathology and patient expectations, highlight a pressing need to augment or replace current bone reconstruction strategies with osteoregenerative techniques.

From a patient's perspective, the ultimate goal is replacement of damaged skeletal tissues with autogenous material harvested with minimal morbidity, and this has further driven research activity to harness the potential of skeletal stem cells (SSCs) in bone regeneration, particularly centred upon strategies that couple material science with the autogenous cells as true tissue engineering constructs. SSCs appear particularly suitable as targets for tissue engineering in general, as they are responsible for the unique capacity of normal bone to

regenerate without scarring (Tare *et al.* 2008). The relative accessibility of an autologous osteoprogenitor population, which is able to replenish the osteoblasts to form mineralised bone matrix, has resulted in significant translational steps towards clinical application (Sacchetti *et al.* 2007). Research into novel, effective bone regeneration strategies has remained predominantly in the realm of laboratory based *in vitro* experimentation and *in vivo* animal modelling, although more recently a number of research centres have bridged the translational gap from bench to clinic, outlined below (Hibi *et al.* 2006;Vacanti *et al.* 2001;Quarto *et al.* 2001;Marcacci *et al.* 2007;Warnke *et al.* 2004;Warnke *et al.* 2006;Hernigou *et al.* 2005a;Hernigou *et al.* 2005b;Ueda *et al.* 2005;Bolland *et al.* 2006;Tilley *et al.* 2006;Jones *et al.* 2009;Morishita *et al.* 2006;Kitoh *et al.* 2007;Sobajima *et al.* 2008;Hartmann *et al.* 2009;Alsousou *et al.* 2009;Hernigou *et al.* 2009;Hibi *et al.* 2006;Ohgushi *et al.* 2005). In addition to the need to reconstruct bone defects, much orthopaedic pathology is derived from cartilage and tendon disease. It is envisaged that novel strategies to address bone defects will also be readily transferable to these applications (Khan, Johnson, & Hardingham 2010;Getgood *et al.* 2009).

1.4 Clinical Translation of novel bone tissue engineering techniques

There is intense interest in cell and scaffold based bone reconstruction techniques, which can be combined as a self-contained implantable unit (Watt & Driskell 2010). Research behind scaffolds and cell based tissue engineering has culminated in their application to a number of human cases, which are discussed below and summarised in **Table 1**.

Table 1: Clinically translated tissue engineering strategies for bone regeneration

RECONSTRUCTIVE STRATEGY		SITE	PATHOLOGY	REFERENCE
Cells	**Scaffold/ Technique**			
Autologous periosteum-derived cells	Hydroxyapatite	Thumb - distal phalanx	Trauma	(Vacanti *et al.* 2001)
Autologous marrow-derived cells	Hydroxyapatite	Long bones	Defects following osteotomy for lengthening/ trauma	(Quarto *et al.* 2001) (Marcacci *et al.* 2007)
Autologous bone marrow	Hydroxyapatite & titanium	Mandible	Oral neoplasia	(Warnke *et al.* 2004) (Warnke *et al.* 2006)
Autologous concentrated bone marrow aspirate	Percutaneous injection	Tibia	Non-union following trauma	(Hernigou *et al.* 2005a)
Culture-expanded skeletal stem cells	Alumina-ceramic prosthesis	Ankle	Osteoarthritis	(Ohgushi *et al.* 2005)
Autologous stem cells and platelet-rich plasma	Hydroxyapatite	Maxilla	Reduced alveolar bone crestal height	(Ueda *et al.* 2005)
Autologous bone marrow aspirate	Impaction bone grafting of allograft	Femoral head	Cyst / osteonecrosis	(Bolland *et al.* 2006) (Tilley *et al.* 2006)
Concentrated autologous bone marrow aspirate	Local application	Femoral head	Osteonecrosis	(Hernigou *et al.* 2009)
Culture-expanded autologous skeletal stem cells	Hydroxyapatite	Femur/ tibia	Benign bone tumours	(Morishita *et al.* 2006)
Culture-expanded skeletal stem cells and platelet-rich plasma	Titanium mesh plate	Alveolar cleft	Congenital cleft lip and alveolus	(Hibi *et al.* 2006)
Skeletal stem cells and platelet-rich plasma	Distraction osteogenesis	Femur/ tibia	Achondroplasia/ hypochondroplasia	(Kitoh *et al.* 2007)
Platelet-rich plasma	Local application	Spine/ mandible/ maxilla	Degenerative/ congenital	(Vadala *et al.* 2008) (Hartmann *et al.* 2009) (Alsousou *et al.* 2009)

Following successful animal trials of a hydroxyapatite scaffold seeded with *ex vivo* culture-expanded autologous marrow-derived osteoprogenitor cells (Kon *et al.* 2000), this concept was translated to three patients with large segmental defects (4 to 7 cm) in long bones. Abundant callus formation and new host bone integration within two months of surgery was observed with a subsequent return to function (Quarto *et al.* 2001) and ongoing mid-term success at 6-7 year follow-up (Marcacci *et al.* 2007). A human distal phalanx has also been created using *ex vivo* culture-expanded periosteum-derived cells seeded onto a porous hydroxyapatite scaffold and encapsulated within a hydrogel coating (Vacanti *et al.* 2001).

The treatment of benign bone tumours using tissue-engineered implants has also recently been successful. Morishita *et al* seeded *ex vivo* osteogenic culture-expanded SSCs derived from iliac crest aspirates onto a hydroxyapatite scaffold in three patients with benign long-bone tumours (aneurysmal bone cyst within proximal tibia, giant cell tumour of proximal tibia, and fibrous dysplasia of proximal femur) (Morishita *et al.* 2006). Weight bearing was commenced in all cases within 2-3 weeks with no adverse clinical or radiological sequelae, demonstrating excellent early mechanical strength. The same group successfully applied a tissue engineering approach to arthroplasty in an attempt to reduce the rate of aseptic loosening associated with ankle prostheses (Ohgushi *et al.* 2005). They culture-expanded SSCs from iliac crest aspirate in osteogenic conditions, then applied these to the ceramic bone-contacting surfaces of the prosthesis, culturing *ex vivo* for a further 2 weeks before implanting the construct. The authors highlight several drawbacks of the study, including lack of a control group, a small cohort with short patient follow-up and the need for an additional procedure to harvest the bone marrow. Nevertheless, this highlights an exciting new technique to enhance the integration at the prosthesis-bone interface.

The osteogenic nature of skeletal stem cells can be used to augment the properties of impaction bone grafting (IBG). Cells survive the impaction process and promote the generation of new bone on the impacted allograft, to provide a solid graft mantel to support a prosthetic joint replacement (Bolland *et al.* 2007;Korda *et al.* 2008;Korda *et al.* 2006). The addition of SSCs has been shown not only to improve the biological characteristics, but also to augment the shear strength of the impacted construct (Bolland *et al.* 2006). These findings have been translated to theatre for the treatment of a benign bone cyst and for post-traumatic osteonecrosis of the femoral head (Tilley *et al.* 2006).

The tissue engineering paradigm has recently been applied to DO to improve the healing index and clinical outcomes, whereby supplementation of the defect with concentrated autologous platelet-rich plasma (PRP) and SSCs from the iliac crest accelerates bone formation (Kitoh *et al.* 2007). In their study comparing 24 femora and tibiae treated with concentrated PRP and SSCs with 32 control osteotomies (i.e. without additional cell therapy) the healing index dropped from 36.2 to just 27.1 days/cm. The considerable complication rates in DO correlate with the total treatment time, so reducing the latter will have significant beneficial effects (Aldegheri 1999).

A number of bone growth factors have been shown to be sequestered in bone and expressed during the course of fracture healing, suggesting a potential role in bone and cartilage formation and in fracture repair. Bone morphogenetic proteins (BMPs), originally identified as constituents which could induce new cartilage and bone formation in non-bony tissues, are key osteoinductive factors pivotal in the recruitment, commitment and differentiation of bone progenitors. Whilst a variety of BMPs are used clinically, this approach has significant cost implications (Cahill *et al.* 2009). The use of extracellular

matrix proteins such as laminin-1, fibronectin, vitronectin and collagen sub-types have been reported to promote adhesion and osteogenic differentiation of SSCs (Mizuno & Kuboki 2001;Salasznyk *et al.* 2004;Globus *et al.* 1998;Cool & Nurcombe 2005). Work within the Bone and Joint Research Group in Southampton has shown that pre-coating allograft with Type I Collagen prior to seeding with skeletal progenitor populations not only enhanced osteogenic differentiation in basal culture but, furthermore, augmented the mechanical properties of the allograft (Jones *et al.* 2009).

Platelet-rich plasma (PRP) has been used in orthopaedic applications to promote spinal fusion (Vadala *et al.* 2008;Hartmann *et al.* 2009) and fracture union (Kitoh *et al.* 2007), although the first clinical studies to use PRP in bone reconstruction therapy were in maxillofacial surgery for reconstruction of mandibular and periodontal defects (Intini 2009). The effects of PRP are mediated through growth factors, which are released from the α-granules of platelets upon activation during clotting and are known to contribute to tissue healing. They include vascular endothelial growth factor (VEGF), transforming growth factor beta (TGF-β), insulin like growth factor (IGF), epidermal growth factor (EGF) and platelet derived growth factor (PDGF). The combination of PRP with induced autologous SSCs derived from iliac crest in a nine year old girl was successfully applied with a titanium mesh scaffold as an alveolar cleft osteoplasty (Hibi *et al.* 2006). A further study to evaluate the combination of autologous SSCs, PRP and hydroxyapatite as grafting materials for maxillary sinus floor augmentation, or 'onlay plasty', was successful in 20 patients (Ueda *et al.* 2005). However, despite some good clinical outcome data, controversy remains over the therapeutic effects of PRP, as the growth factors within it have a short half-life and many *in vitro* and *in vivo* studies to date are inconclusive (Alsousou *et al.* 2009). Furthermore, clinical studies are restricted to case reports or limited

series, and many strategies simultaneously use skeletally derived cells, so confounding the attributable cause of any benefit seen (Cenni *et al.* 2009).

Hernigou and colleagues have used concentrated osteoprogenitor cells in the treatment of osteonecrosis and fracture non-union. Enduring bone architecture was maintained with this treatment in femoral head osteonecrosis (Hernigou *et al.* 2009), and by injecting into established atrophic tibial non-unions of sixty patients, union was achieved in fifty three cases (Hernigou *et al.* 2005a). Interestingly, the seven cases with persistent non-union were all implanted with lower SSC concentrations, indicating a requirement for delivery of a critical concentration of progenitor cells to the defect site. This concentration exceeds numbers of stem cells present in iliac crest aspirate, emphasising the need for the development of cell enrichment strategies (Hernigou *et al.* 2005a).

The field of maxillofacial surgery has provided further novel strategies of skeletal regeneration. Most cited examples are small *in vivo* case-based studies, however they do demonstrate proof of concept and provide a valuable platform from which to progress. In 2004 Warnke *et al* grew a patient's mandible *de novo* (Warnke *et al.* 2004). A titanium mesh external scaffold filled with recombinant human BMP-7 coated hydroxyapatite blocks and seeded with autologous bone marrow was grown within the latissimus dorsi muscle prior to implantation into the defect site. Complications included heterotopic ossification, fracture of the mesh and infection, but the procedure has subsequently been repeated on a second patient (Warnke *et al.* 2006). Transference of this technique to more load-bearing bones in an orthopaedic context may prove even more difficult as Warnke provided no direct evidence that a normal mandibular structure or integration with surrounding tissue had been established (Gronthos 2004).

In 2006, Heliotis *et al* went further and demonstrated that BMP-7 with hydroxyapatite has the ability to induce osteogenesis outside the skeleton, without the addition of cortical bone, bone marrow aspirates or any other bone precursors to the implant (Heliotis *et al.* 2006). As a reconstructive strategy for a mandibular defect following resection of squamous cell carcinoma, they placed a hydroxyapatite/BMP-7 implant into a patient's pectoralis major muscle for three months. The graft was then raised as a myo-osseo-hydroxyapatite flap pedicled on the thoracoacromial artery, and secured to the existing mandibular stump. Unfortunately, despite good initial clinical results, the graft became infected and had to be removed after 5 months. More recently, mandibular defects have been reconstructed in pigs using autoclaved autogenous mandibular grafts loaded with collagen matrix and autogenous bone marrow cells harvested from the pigs' tibiae (von Wilmowsky *et al.* 2009). Additional clinical applications for this technique include bone tumour surgery (the affected bone can be re-introduced after destruction of tumour cells by autoclaving, with a low incidence rate of local tumour recurrence) or after open fractures (as steam sterilisation of the bone segment removes microbiological load, but preserves the bone morphology and osteoconductivity).

1.5 Major Null Hypothesis

Skeletal stem cells can not be used to augment bone formation.

1.6 Aims of Thesis

Current strategies for the treatment of lost bone stock have inherent disadvantages, and in view of ever increasing demand as a consequence of demographics, there is a pressing need for novel treatment modalities. The approaches outlined in this Introduction provide a snapshot of future potential, but the scarcity of cases in the literature and the absence of reliable controls prohibit the routine clinical use until large scale clinical trials have been performed. However, the application of these novel techniques has afforded the opportunity to push the boundaries of tissue engineering strategies in clinical practice, where current treatment strategies are insufficient.

This thesis aims to investigate, *in vitro*, *in vivo* and through to clinical translation, skeletal stem cell derived tissue engineering strategies for bone reconstruction.

1.7 Objectives

1. To investigate techniques for augmentation of the biomechanical characteristics of impacted bone graft, by the addition of skeletal stem cells and human fibronectin protein.
2. To examine the effect of changes in porosity of a ceramic scaffold on osteogenesis.
3. To explore novel technology for the enrichment of the skeletal stem cell fraction from aspirated bone marrow, in a rapid single step process for facile clinical application.
4. To evaluate the efficacy of autologous bone marrow seeded onto milled allograft as a novel clinically translated tissue engineering strategy, by analysis of retrieved bone tissue.
5. To investigate the effect of the cyst fluid from unicameral bone cysts on osteoblast and osteoclast activity and signalling.
6. To examine the treatment of avascular necrosis of the femoral head using skeletal stem cells and impacted allograft, translated to four patients.

Chapter II

Biological Augmentation of Scaffolds for Bone Regeneration

PART 1: Effect of Skeletal Stem Cells and Human Fibronectin on the Biomechanical Properties of Impacted Bone after Impaction Bone Grafting

I am grateful to Dr Adam Briscoe, Bioengineering Science Research Group, for assistance with the mechanical testing and the Mohr-Coulomb equation calculations.

PART 2: The Effect of Scaffold Porosity on Skeletal Stem Cell Growth and Differentiation

This work was performed in collaboration with Dr Irene Turner (University of Bath Department of Mechanical Engineering) and Professor Julian Chaudhuri (University of Bath Department of Chemical Engineering) who produced the scaffolds and subsequently performed the SEM. I am grateful to Dr Janos Kanczler for assistance with the *in vivo* work and Dr Stuart Lanham for the μCT scans and analysis.

PART 1: Effect of Skeletal Stem Cells and Human Fibronectin on the Biomechanical Properties of Impacted Bone after Impaction Bone Grafting

2.1.1 Introduction

While traditional causes of bone loss such as trauma, infection and tumours present ongoing challenges, there is now a growing cohort of patients who require bone defect reconstruction during revision arthroplasty surgery. The proportion of people in Britain aged over 65 is projected to increase by nearly 50% in the next 25 years (Office for National Statistics 2008), and a concomitant increase in arthroplasty surgery can be expected. In 2008 in England and Wales, there were approximately 65,000 primary hip replacements performed in comparison to just 30,000 in 2003, and the number of revision hip procedures doubled over this period, to 6,600 (National Joint Registry 2009). Given these demographic changes as well as the observation that joint replacements are being increasingly performed in younger patients, the number of people outliving their prosthesis can be projected to increase. Patients now present in increasing numbers, often with extensive bone loss around loose implants, providing a substantial orthopaedic challenge in revision surgery. Furthermore, knee arthroplasty is now performed more frequently than hip arthroplasty (National Joint Registry 2009), thus the true scale of the problem of inadequate bone stock in revising total knee replacements will only emerge in years to come. Furthermore, the patient of today has higher expectations of medical intervention (Nilsdotter, Toksvig-Larsen, & Roos 2009) and a deteriorating, painful prosthetic joint will often be poorly tolerated in the context of bone loss occurring as a result of a previous therapeutic intervention.

Impaction bone grafting (IBG) using fresh frozen morselised allograft remains the current gold standard for replacement of bone stock encountered during revision hip surgery and has been used as a void filler as such for over forty years (Slooff *et al.* 1984). Survivorship for acetabular and femoral components at 20 and 10 years respectively is encouraging (87% (Schreurs *et al.* 2009) and 99% (Halliday *et al.* 2003)), although such results have not always been repeated outside specialist centres (Eldridge *et al.* 1997;van Haaren *et al.* 2007). The technique, which employs fresh frozen morselised allograft as a passive 'void filler', endeavours to recreate a solid, adaptive mantle into which the implant can sit

securely, immediately withstanding forces associated with normal implant use. The ability of the graft bed to resist such forces and form a new living bone construct is a critical factor for the long-term success of the revision implant. However, all histological specimens taken from revision hip IBG reveal fibrous and necrotic tissue amongst areas of graft integration (van Haaren *et al.* 2007;van der Donk *et al.* 2002;Ling, Timperley, & Linder 1993).

Factors such as preparation of graft, constituent particle size, chemical additions and local fluid drainage are known to affect the performance of IBG (Dunlop *et al.* 2003;Bolland *et al.* 2007). The application of tissue engineering strategies to promote the generation of host bone, and thereby improve the biomechanical characteristics of the graft, has the potential to improve the outcomes of this demanding technique. The accepted method for replacement of allograft in IBG is via creeping substitution, however the concept of a living graft which becomes incorporated into, rather than replaced by the surrounding host tissue presents a paradigm shift to the concept of allograft use. This would bring the osteogenic characteristics of autograft to the application of allograft, whilst avoiding the inherent donor site morbidity of autograft. Recent work, including within the Bone & Joint Research Group, University of Southampton, has now identified biological factors that can be modulated to augment the structure and performance of bone graft extenders (Bolland *et al.* 2006;Jones *et al.* 2009;Hutmacher *et al.* 2007;Tsai *et al.* 2010).

Multipotent skeletal stem cells (SSCs) present in bone marrow not only survive the impaction process and continue to proliferate on allograft, but also improve the mechanical (shear) characteristics of the construct (Bolland *et al.* 2006;Mushipe *et al.* 2006;Korda *et al.* 2006;Green *et al.* 2009;Jones *et al.* 2009). SSCs have the potential, however, to differentiate along a number of different stromal cell lineages including osteoblasts, chondrocytes, fibroblasts and adipocytes. In IBG it is desirable to maximise the differentiation of these stem cells to form bone and thus a solid osseous construct, rather than fibrous tissue. Whilst it is straightforward to encourage differentiation into the osteogenic lineage *in vitro* by modulation of growth conditions and media constituents, many of these methods (e.g. the addition of dexamethasone, or the creation of a hypocapnic environment) are not transferable to clinical practice due to local and systemic side effects.

Osteoinductive factors provide potential for *in vivo* enhancement of cellular differentiation along an osteogenic lineage, resulting in improved mechanical and biological properties of the IBG composite, without toxicity (Baas 2008). Collagen Type I, an extra-cellular matrix protein, has been shown to induce osteoblastic differentiation *in vitro* and on scaffold surfaces (Tsai *et al.* 2010;Mizuno & Kuboki 2001;Salasznyk *et al.* 2004). Jones et al have used Collagen Type 1 to coat milled allograft, prior to seeding with SSCs and impaction. This resulted in increased osteogenic differentiation of the SSCs and improved mechanical strength of the IBG construct compared to SSCs alone (Jones *et al.* 2009). In parallel studies, SSCs were treated with hydroxyapatite nanoparticles (HAp), which pushed cells along an osteogenic lineage, resulting in improved shear strength of the graft (Jones *et al.* 2009).

The integration and biocompatibility of allograft is dependent on the adhesion and differentiation of SSCs to osteoblasts. The augmentation of SSC adhesion, proliferation and osteoblastic differentiation is thought to be mediated through the adhesion motif Arg-Gly-Asp (RGD), found in a number of bone ligands including osteopontin, thrombospondin and bone sialoprotein (Yang *et al.* 2001). The extra-cellular matrix (ECM) protein Human Fibronectin (HFN) contains the RGD sequence and has been shown to play a central role in facilitating osteoblast adhesion, proliferation, differentiation, function and survival (Globus *et al.* 1998;Yang *et al.* 2001). The addition of HFN to bone marrow SSCs in culture has been demonstrated to enhance osteogenic differentiation, as determined by expression of bone specific markers RUNX-2, Type I collagen, alkaline phosphatase and osteocalcin (Cool & Nurcombe 2005). Furthermore, this effect was shown to be augmented when the cells were under strain (Huang *et al.* 2009), suggesting a beneficial behaviour ideally suited to the conditions in IBG around a revision hip prosthesis. Enhanced cell adhesion, spreading and differentiation as a result of HFN, and the RGD adhesion motif, has been demonstrated on a 3D biomimetic scaffold (Yang *et al.* 2001). Although HFN has FDA approval for use in clinical application, the effect of HFN on the IBG construct has not previously been defined.

2.1.2 Aims

This study aims to examine the biomechanical effects on the impacted allograft construct following the addition of human fibronectin (HFN), in combination with SSCs, to improve cell adhesion, activity and graft-cell composition.

2.1.3 Null Hypothesis

1. HFN-coating of milled allograft, prior to seeding with SSCs, will not enhance cellular differentiation along the osteogenic lineage on the impaction bone graft construct.
2. HFN-coating of milled allograft, prior to seeding with SSCs, will not augment the mechanical properties of the impaction bone graft construct.

2.1.4 Materials and Methods

Allograft was divided into four groups, for coating with HFN, seeding with SSCs, both HFN-coating and SSC-seeding, plus a negative control (**Table 1**). Each group contained 16 aliquots of 10cc of loosely-packed milled allograft for impaction.

Table 1: Illustration of arms of the impaction bone graft study.

Group	*10cc of milled allograft*	*HFN-coating*	*SSC-seeding*
1	✓	X	X
2	✓	✓	X
3	✓	X	✓
4	✓	✓	✓

Reagents, hardware & software

Tissue culture reagents including alpha-Modified Eagle's Medium (α-MEM), fetal calf serum (FCS) and all staining agents were purchased from Sigma-Aldrich Ltd. (Gillingham, UK), unless otherwise stated. Human fibronectin (HFN) was purchased from Chemicon International, Temecula, USA. CellTracker Green (CMFDA, 5-chloromethylfluorescein diacetate) and Ethidium Homodimer-1 (CTG-EH) were purchased from Molecular Probes (Leiden, Netherlands). Impactors, acrylic chambers and the cam shear tester were custom manufactured by the University of Southampton Bioengineering Science Research Group.

Alkaline phosphatase stain of in vitro monolayer cell culture

For assessment of the effects of HFN on cell characteristics, *in vitro* monolayer culture was performed. Tissue culture plastic wells were coated with HFN (n=3) for 60 minutes, according to manufacturers instructions, then SSCs in basal media (α-MEM, 10% FCS, 2% penicillin-streptomycin) were added. Non HFN-coated wells, with cells at identical seeding density, were used as controls (n=3). Cells were cultured for two weeks until confluent, fixed in 95% ethanol and stained with Naphthos AS-MX and Fast Violet B Salts for alkaline phosphatase.

Allograft preparation and milling

Highly washed morselised allograft was obtained from fresh frozen femoral heads that had been stored at -80°C. These had been retrieved with the consent of patients undergoing elective or traumatic hip surgery after approval of the local ethics committee (LREC 194/99/1). Under sterile conditions in theatre femoral heads were defrosted and processed in accordance with standard clinical practice (Halliday *et al.* 2003). Cartilage and most subchondral bone were removed using an oscillating bone saw (Stryker, Newbury, UK) (**Fig.1A**) and the femoral heads were milled using the Noviomagus bone mill (OrthoLink Ltd, Prestonpans, UK) (**Fig.1B**). Milled bone graft was soaked in 6% hydrogen peroxide for 30 minutes to remove fat and marrow (**Fig.1C**), washed repeatedly with normal saline, soaked in antibiotic/antimycotic solution for 24 hours (**Fig.1D**), re-washed in phosphate-buffered saline (PBS) and immersed in α-MEM in 10 cm^3 aliquots. For each experimental arm or control group 16 aliquots were prepared in order to provide 12 discs for mechanical testing, 3 for biochemical analysis and one for histology and examination of cell viability.

Figure 1A: Removal of cartilage and soft tissue from the femoral head, leaving only sub-chondral and cancellous bone. B: Milling of human femoral head allograft using the Noviomagus bone mill. C: Washing milled allograft in 6% H_2O_2. D: Soaking in antibiotic-antimycotic solution.

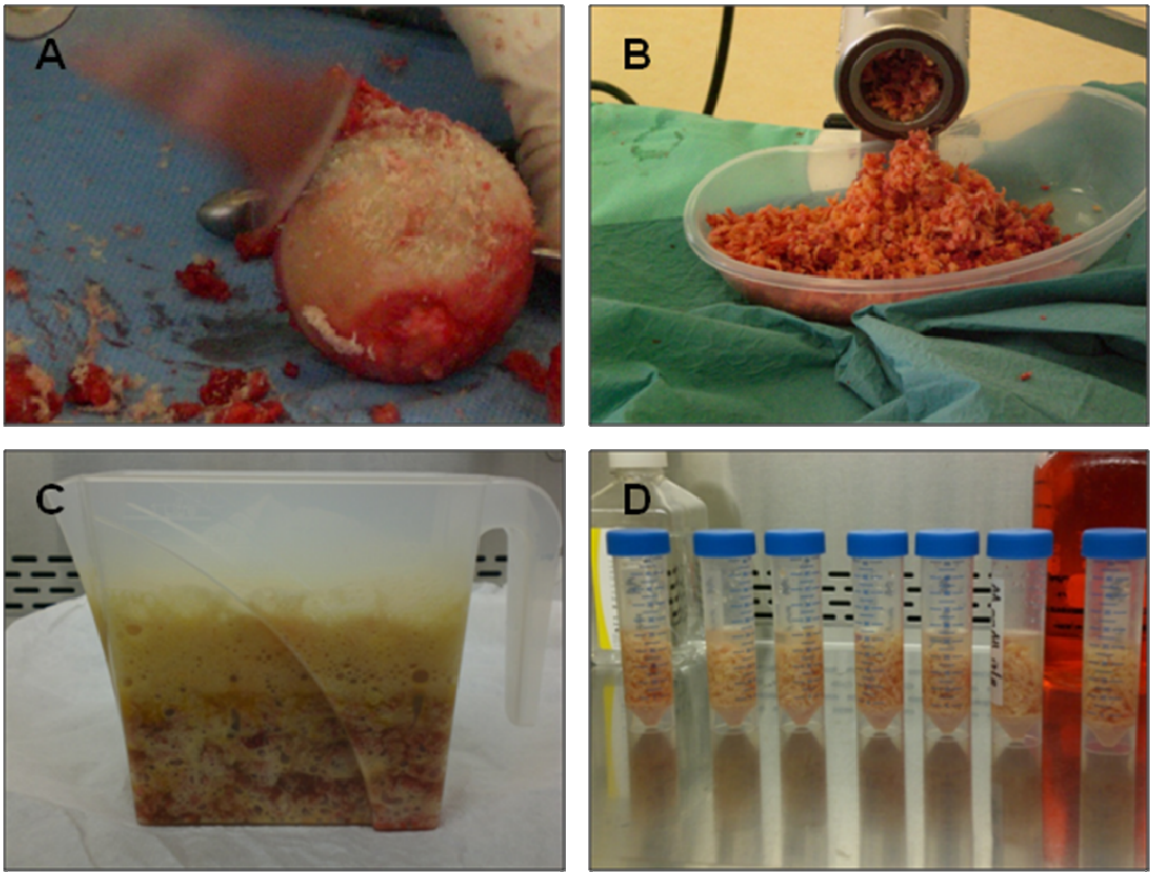

HFN-coating of allograft

5mg of human plasma fibronectin purified protein (Chemicon International) was suspended in 96ml of basal media. Aliquots of 6ml were applied to 10cc aliquots of loosely packed milled allograft (= 312.5µg HFN on 10cc allograft) and left for 60 minutes to allow adsorption onto the allograft surface, according to manufacturer's instructions.

Skeletal stem cell culture

Only first-passage cultured SSCs were used in all studies. Bone marrow samples were obtained from haematologically normal patients undergoing routine total hip replacement surgery with the approval of the local ethics committee (LREC194/99/1). SSCs were harvested by repeatedly washing the marrow in α-MEM, removing the washed cell population prior to centrifugation at 1100 rpm for 5 minutes at 4ºC. The cell pellet was resuspended in 10 ml α-MEM and passed through a 70µm filter. The cell fraction was plated into tissue culture flasks in basal media and incubated at 37ºC in 5% CO_2. Cells

were washed in PBS and media changes were repeated every 3-4 days. Upon confluence the cells were released using trypsin in EDTA (ethylene diamine tetra-acetic acid), centrifuged, re-suspended in basal media and the total count using a haemocytometer determined prior to seeding onto morcelised, prepared allograft.

SSC-seeding of milled allograft

SSCs were seeded at the specific seeding density of $5x10^4$ cells / cc of loosely packed milled allograft. Following trypsinisation from tissue culture flasks, cell number was determined using a haemocytometer and cells were suspended in equal aliquots of $5x10^5$ cells in 6 ml basal media (to cover 10 cc of milled allograft). Cell suspensions were added to sterile pots containing milled allograft and placed on an agitator (Belly Dancer, Stovall Life Sciences, Greensboro., NC, USA) within the incubator for one hour to optimise cell adherence prior to impaction. This period was limited to one hour in order to simulate time that would be available intra-operatively, thereby ensuring relevance for clinical translation. For all experimental groups with SSCs, cell seeding density was kept constant at $5x10^4$ cells / cc, according to previously defined methods (Jones *et al.* 2009).

In vitro impaction of milled washed human allograft

An *in vitro* model has been developed to replicate the femoral IBG process, whereby a standard femoral impaction has been previously determined using force plate analysis to be equivalent to a 1.98kg mass falling 65mm onto a 60mm diameter circular base plate (BB06). The custom-manufactured impactor device used in this study was appropriately scaled and consisted of a graft chamber 25mm in diameter, a piston with a 344g free sliding weight, and a drop height of 65mm (**Fig.2A-B**). Impaction chambers were sterilised in 95% ethanol and under UV light, and the impactor device by steam autoclaving. 10cc of loosely packed milled allograft was impacted into these in three layers, with three sets of 24 impactions applied at a frequency of 1Hz to ensure even graft compaction (**Fig.2C-D**). The graft was contained in a scaffold chamber consisting of a base, ring and lid machined from cast acrylic rod, with perforations to allow extrusion of liquid during compaction, and diffusion of media and metabolites during cell culture (**Fig.2E**). When assembled, the three components enclosed a cylinder of scaffold 25mm in diameter and 10mm high, a volume of 4.9cm³. All samples were cultured in basal media for 2 weeks with washes and change of media every 3-4 days (**Fig.2F**).

Figure 2: *In vitro* replica of impaction bone grafting; A-B: Impactions at 1Hz. C: First layer of graft impacted 24 times. D: Third layer of graft impacted 24 times, ensuring even graft compaction throughout the construct. E: Acrylic chamber with perforations. F: Impacted discs in culture media.

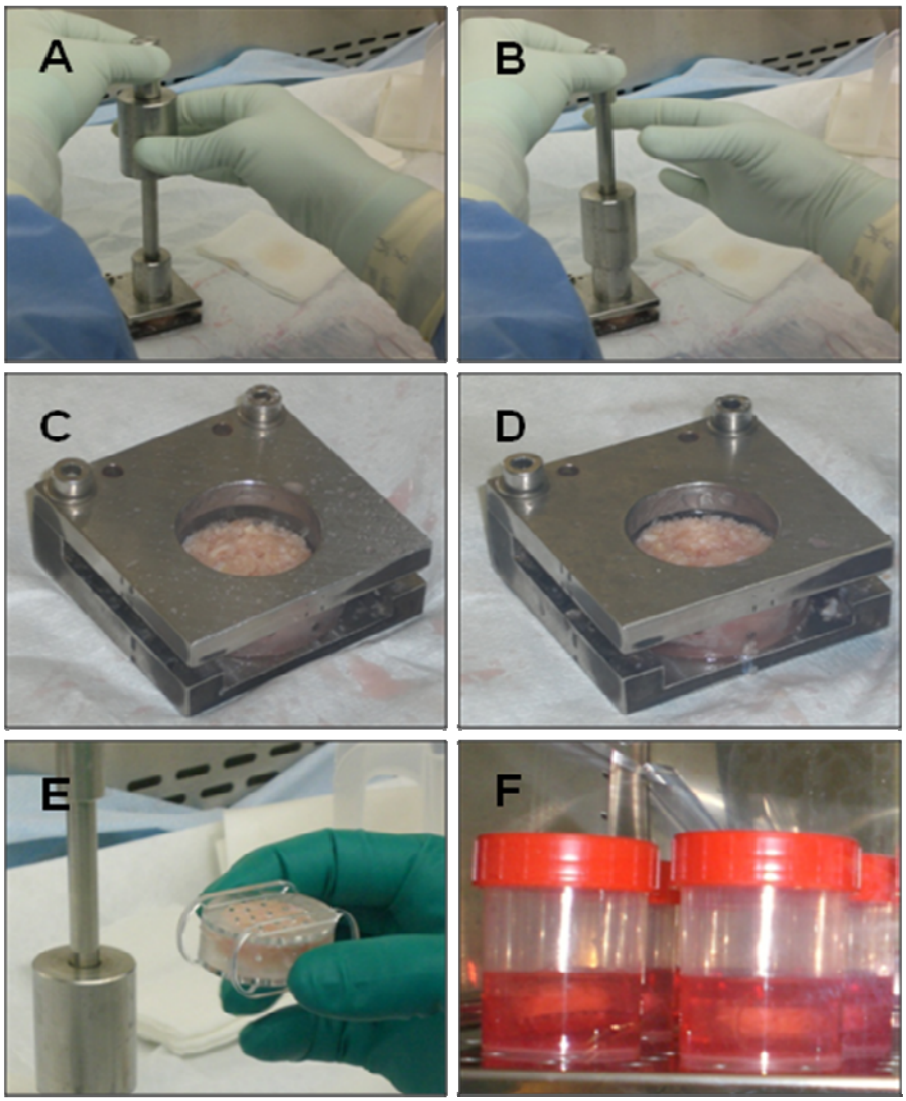

Mechanical shear testing

Following two weeks in culture, impacted discs were transferred to a custom made cam shear tester for mechanical shear testing. This established methodology has been validated previously (BB06, Dunlop thesis, Jones TCES). The chamber size corresponded to the dimensions of the impacted graft samples, with a fixed upper ring and a mobile lower ring (**Fig.3**). Twelve discs from each group were tested by first applying an axial load within the physiological spectrum of compressive stresses, at 50N, 150N and 250N, with four 4 discs per stress. After 5 minutes under the compressive load, each sample was then sheared at a constant rate of 1.2 mm / min using a hydraulic actuator (Instron Ltd, High Wycombe, UK).

Figure 3: Schematic of the custom-made Cam shear tester, demonstrating the position of the impacted allograft disc and the mobile rings that apply the shear stress at a constant rate of displacement.

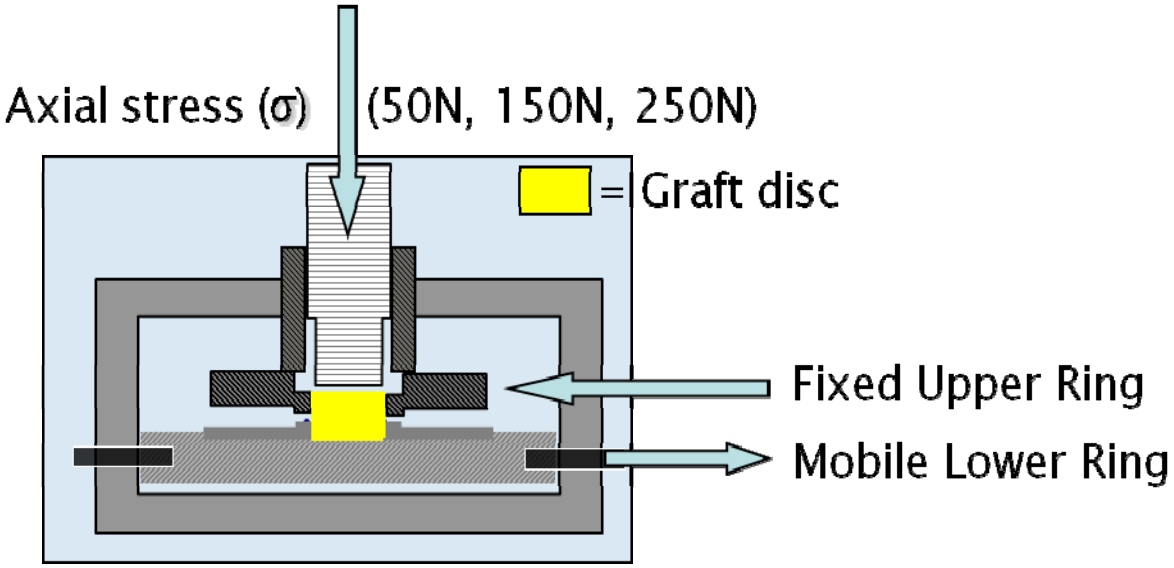

The load applied and resulting displacement of the sample were measured and a family of stress-strain curves were generated from which shear strength at 10% shear strain could be determined, as per industry standards. These were plotted against normal stress and from this data shear strength, inter-particulate cohesion and internal friction angle parameters were calculated using linear regression analysis and the Mohr Coulomb failure law. The shear strength (τ) of a granular aggregate, such as milled allograft, depends on the internal friction (φ), expressed as the angle at which the aggregate will slide, and interlocking of the particles (c), expressed as a stress. The frictional resistance varies in proportion with the compressive stress (σ) applied by the load on the aggregate. The relationship between the parameters can be expressed by the Mohr Coulomb failure equation, '$\tau = c + \sigma \tan \varphi$', allowing the shear strength of the aggregate to be calculated. Statistical significance was calculated by Grouped linear regression analysis (Zar 1984) using Graphpad Prism Ver 3.02.

Cell viability and histology

Following two weeks in culture, one disc from each group was divided for analysis of cell viability and for histology. Cell viability was assessed by staining with CellTracker Green (CMFDA, 5-chloromethylfluorescein diacetate) and Ethidium Homodimer (CTG-EH). Histological analysis was performed following decalcification of the allograft samples in 0.1M TRIS / 5%EDTA solution at pH7.3, verified by Faxitron MX-20 micro X-ray

(Faxitron X-ray, Wheeling, IL, USA) (**Fig.4**). Decalcified samples were embedded in wax, mounted, processed through graded ethanols, sectioned to 7µm thickness, then stained using Alcian Blue and Sirius Red (A/S). Images were viewed using Carl Zeiss Axiovision software Ver 3.0 via an AxioCam HR digital camera on an Axiovert 200 inverted microscope (Carl Zeiss Ltd, Hertfordshire, UK) under white or fluorescent light.

Figure 4: Faxitron MX-20 micro X-ray images of milled allograft decalcification in Tris-EDTA at weekly timepoints, prior to wax embedding and sectioning for histology. Arrows highlight the radio-opaque calcified tissue.

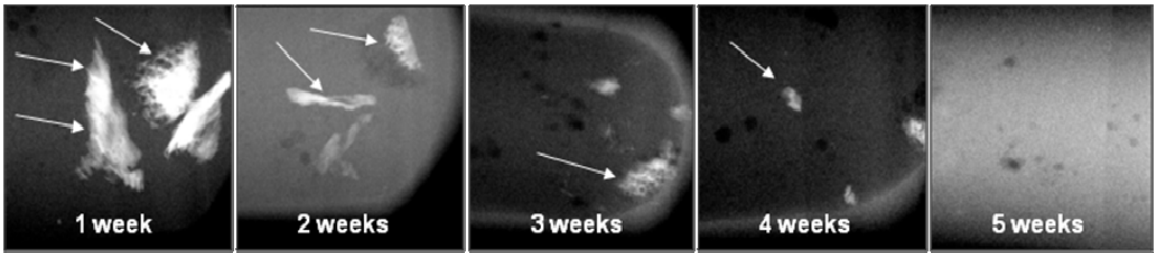

Biochemistry

Three discs were retained for biochemical analysis of DNA content (as a measure of cell number), and specific alkaline phosphatase (ALP) activity (as a measure of osteogenic differentiation). Cells were released from the allograft using trypsin, collagenase and multiple vortexing. Allograft was discarded, cells were fixed in ethanol and cell lysates were obtained via three sequential freeze-thaw cycles in Triton X-100 (BDH Chemical Ltd, Poole, UK). ALP and DNA assays were then performed using 10µl of lysate run in triplicate for each disc on a plate against two standards and read on a BioTek KC4 and FLX-800 microplate fluorescent reader (BioTek, Potton, UK). DNA was measured in nanograms (ng) / ml of lysate and ALP read as nanomoles of p-nitrophenol / ml / hour (nmol pNPP/ml hr^{-1}). Statistics were calculated in Excel and SPSS Ver 18.

2.1.5 Results

Cell viability on impacted allograft

Following 14 days culture of SSCs on milled impacted allograft, representative sections from a single disc in each group were analysed by CTG-EH stain in order to confirm the presence of viable adherent SSCs on allograft from both SSC-seeded groups (Group 3 & 4, Table 1) (**Fig.5**).

Figure 5: Cell viability analysis of SSC-seeded allograft (A) and HFN-coated SSC-seeded allograft (B) confirmed the presence of viable cells (arrows) adherent to the allograft, seen on the graft in fluorescent green. Scale bars = 100µm.

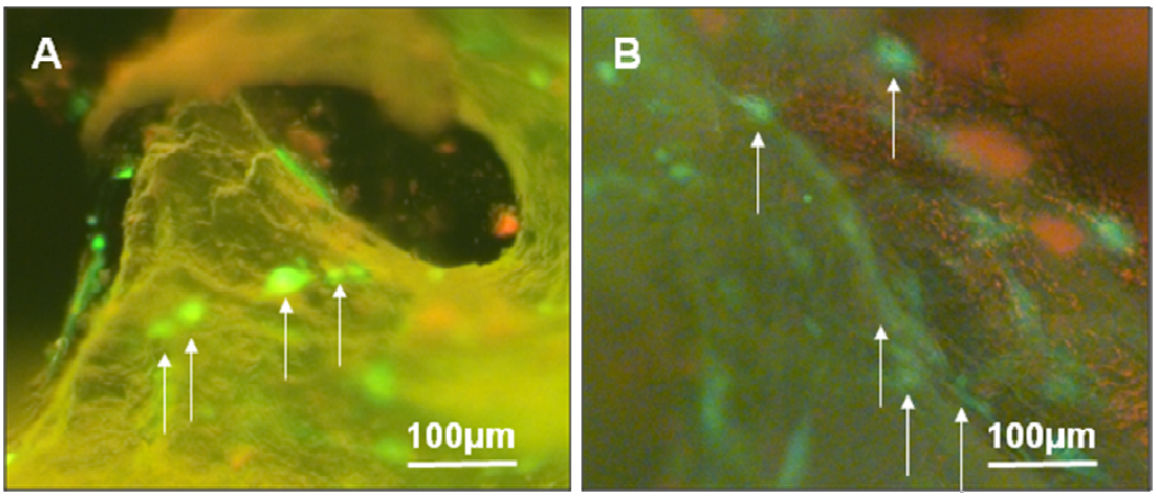

Parallel Monolayer Culture

SSCs were cultured *in vitro* in monolayer for 14 days in basal media on tissue culture plastic to explore the effect of HFN on cell proliferation and differentiation. ALP stain revealed enhanced cell growth and osteoblastic differentiation in the culture wells that had been coated with HFN prior to the addition of SSCs (**Fig.6**).

Figure 6: ALP staining of *in vitro* monolayer culture; A: Macrosopic appearance of SSCs cultured in basal media. B: Macroscopic appearance of SSCs cultured in basal media but on HFN-coated culture wells. Sacle bars = 10mm. C-D: Magnified images of ALP stained SSCs in monolayer, scale bars= 100µm.

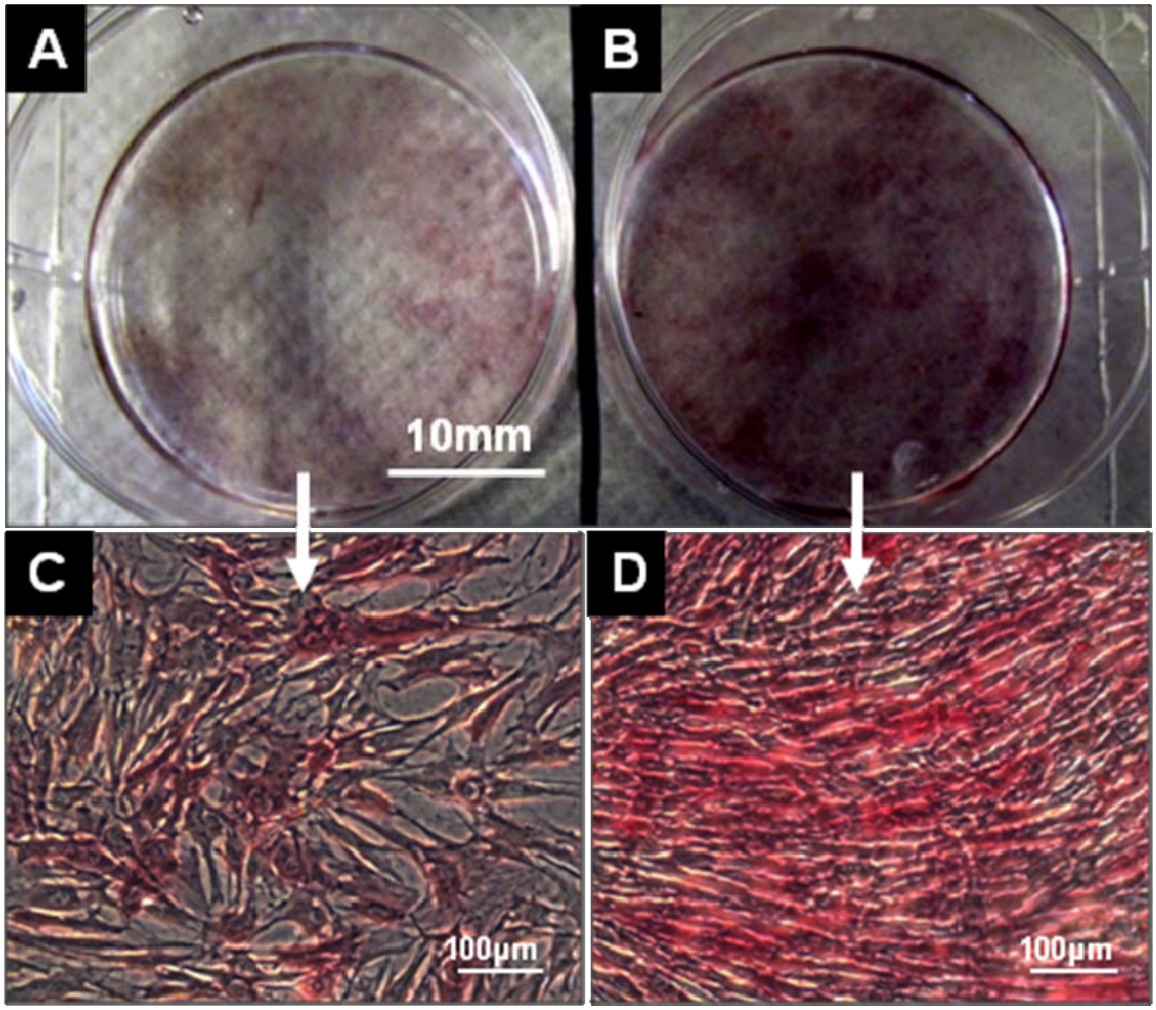

Histology

Viewing of prepared histology slides of A/S stained milled impacted allograft revealed the trabecular structure of cancellous bone, with lamellar micro-architecture, on all specimens. However empty lacunae were observed on the non cell-seeded allograft Groups 1 & 2), indicating an absence of cells (**Fig.7A-B**). This contrasted to SSC-seeded allograft (Group 3) and HFN-coated SSC-seeded allograft (Group 4) which both demonstrated similar architecture, but with cells visible within lacunae (**Fig.7C-D**).

Figure 7: A/S staining of impacted allograft; A: Plain allograft (Group 1). B: HFN-coated allograft (Group 2). Both constructs showed trabecular bone but an absence of cells showing empty lacunae (arrows). This contrasted to the SSC- seeded allograft of Groups 3 and 4, illustrated in 7C and D respectively, which demonstrated similar trabecular micro-architecture, but stained cells were observed within the lacunae (arrows). Scale bars = 100µm.

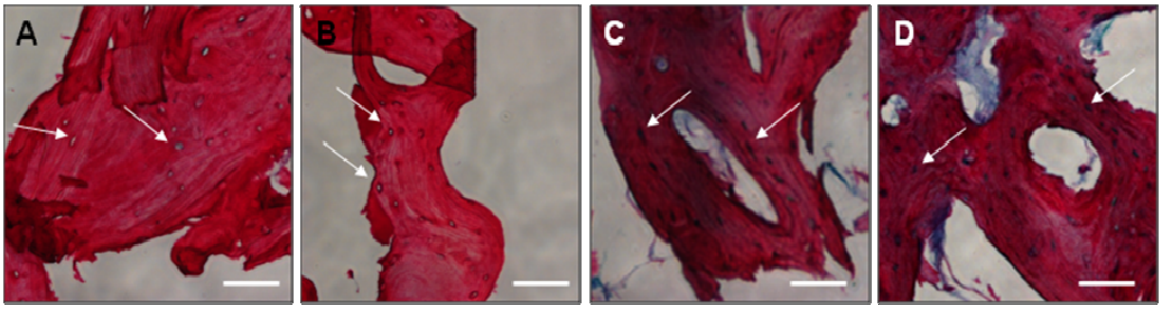

Biochemistry

Analysis of cell proliferation, as measured by DNA assay, confirmed cell growth on the SSC-seeded constructs (Group 3 and Group 4, Table 1). This was significantly greater than the DNA levels on plain impacted allograft (Group 1) ($p<0.001$, independent t-test) (**Fig.8A**). Although allograft is treated with H_2O_2 and multiple washes, some DNA inevitably remains, hence the rare problem in clinical practice of disease transmission and immunogenic reactions (Delloye 2007) and trace levels detected on this *in vitro* study. Despite the increased cell growth induced in monolayer culture by HFN (**Fig.5**), this was not repeated in 3D culture on allograft, with no significant difference between DNA assays of SSC-seeded (Group 3) and HFN-coated SSC-seeded (Group 4) impacted allograft ($p=0.90$) (**Fig.8A**). Measurements of ALP specific activity demonstrated that, in this study, HFN-coating of allograft did not promote osteogenic differentiation of SSCs on impacted allograft, with no significant difference between the ALP specific activity on discs from Group 3 and Group 4 ($p=0.28$) (**Fig.8B**). One disc for biochemical analysis from Group 4 (HFN-coated SSC-seeded) became infected and was therefore discarded from analysis.

Figure 8: Biochemical analysis of impacted allograft discs. Three discs were analysed from every group, with lysates run in triplicate for each disc; A: DNA assay indicated comparable SSC proliferation on Group 3 and Group 4 impacted discs (p=0.90). Only trace DNA levels detected on the non SSC-seeded discs (Group 1) which was significantly lower than the SSC-seeded discs (p<0.001). B: Comparison of ALP specific activity of the SSC-seeded discs with and without HFN-coating, demonstrated no significant difference (p=0.28). Error bars denoted standard deviation. ns = no statistical significance, *** = p<0.001.

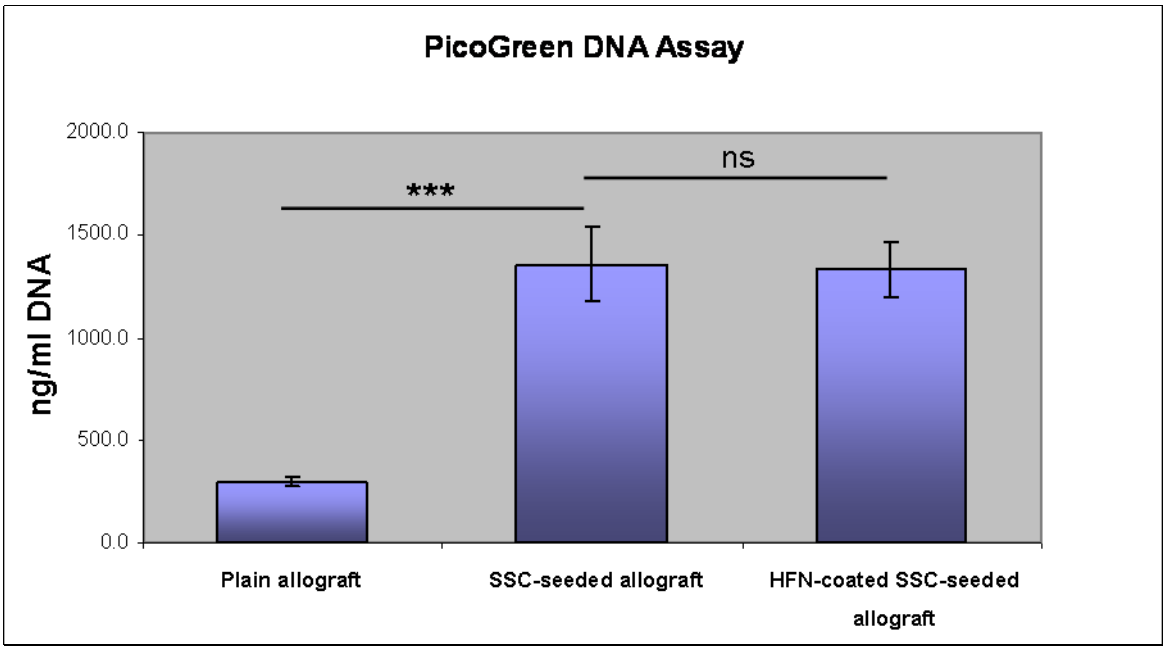

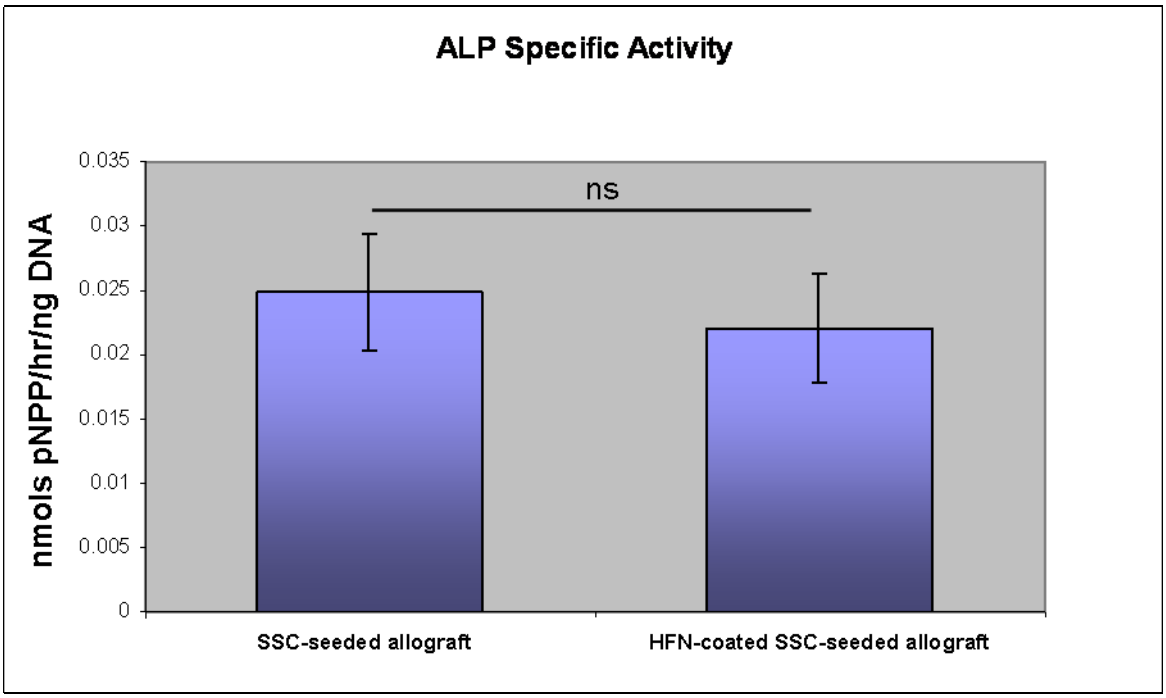

Mechanical Testing

Regression analysis of the shear strength showed a linear increase with compressive stress for all groups (R^2 >0.99) and matching gradients (p=0.85), which represented tan φ, the internal friction angle. This indicated that the grafts satisfied the Mohr Coulomb failure law and were suitable for further analysis (**Fig.9**). Values read from the Mohr-Coulomb curves for shear strength at 350kPa compressive strength (representative of a typical physiological load) are presented for illustration of the differences between the four groups (**Table 2**). The inter-particulate cohesion (c) is the shear stress value when normal stress (x axis on **Fig.9**) equals zero, quantified in **Table 2**. These values demonstrated the trend in increasing shear strength as a result of SSC-seeding and HFN-coating. Mechanical shear-testing revealed significant differences on grouped linear regression analysis between HFN-coated SSC-seeded allograft (Group 4) and both of the non SSC-seeded groups (Group 1&2) (p≤0.0001). The grafts' ability to resist shear after SSC-seeding (Group 3) compared to the current gold standard of plain allograft (Group 1) was increased, although this was not statistically significant (p=0.17). HFN-coating of allograft without the addition of SSCs (Group 2) demonstrated no statistical difference in strength of the construct compared to allograft alone (Group 1) (p=0.09).

Figure 9: Effects on mechanical properties of IBG following HFN coating. Four discs were tested at each of three stresses for every group. Error bars denote Standard Error of mean.

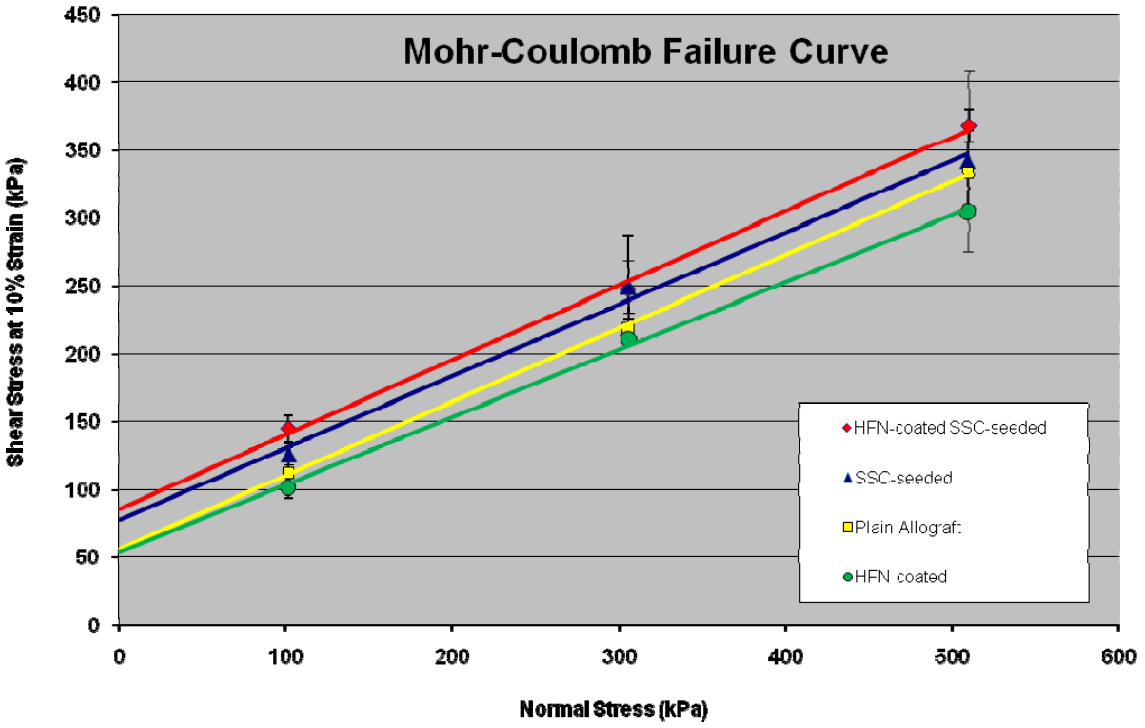

Table 2: Effects on mechanical properties of IBG following HFN-coating and SSC-seeding. Values for shear strength at 350kPa (a typical physiological load during gait) and inter-particulate cohesion (c) determined from the graph to illustrate the differences in mechanical characteristics of each construct.

	R^2 value for linear regression curve	*Inter-particulate Cohesion (c)*	*Shear strength at 350kPa compression*	*Statistical significance (Grouped linear regression analysis)*
Plain Allograft (Group1)	0.9995	55.9	245.7 (±13.8)	
HFN-coated allograft (Group2)	0.9979	53.8	227.8 (±15.6)	vs Group1 p=0.09
SSC-seeded allograft (Group 3)	0.9933	77.3	262.8 (±26.2)	vs Group1 p=0.17 vs Group2 p=0.017
HFN-coated SSC-seeded allograft (Group 4)	0.9976	85.7	277.9 (±8.4)	vs Group1 p=0.0001 vs Group2 p<0.0001 vs Group3 p=0.235

2.1.6 Discussion

The aim of this study was to examine the biomechanical effects that HFN can bring to SSCs seeded onto milled allograft for impaction. The biomechanical augmentation of impacted allograft by the addition of SSCs has been well documented, and it has been postulated that the extracellular matrix produced by the cells crosses the minute gaps between the particles, increasing the inter-particulate cohesion, thus leading to a stronger construct (Bolland *et al.* 2006;Korda *et al.* 2008). HFN is an extra-cellular matrix protein that has been shown to promote osteoblast adhesion, differentiation and proliferation on 3D scaffold surfaces (Yang *et al.* 2001;Cool & Nurcombe 2005), and has FDA approval so would be readily translatable to clinical practice. This study follows previous work in the Bone & Joint Research Group of coating milled allograft with Type 1 collagen, which has been shown to augment the biological and mechanical effect of SSCs on IBG. Both the ALP specific activity and the mechanical strength of the collagen-coated SSC-seeded allograft were significantly increased compared to SSC-seeded impacted allograft ($p=0.001$ and $p<0.05$ respectively) (Jones *et al.* 2009).

This study has demonstrated that HFN increased osteogenic differentiation in monolayer culture (**Fig.6**), in keeping with previous studies (Globus *et al.* 1998;Cool & Nurcombe 2005;Huang *et al.* 2009). However these findings were not replicated in this study when SSCs were cultured on allograft. Comparable cell growth was found on the SSC-seeded allograft (Group 3) to the HFN-coated SSC-seeded allograft (Group 4), as demonstrated qualitatively on CTG-EH stain and A/S stained histology slides (**Fig.5&7**) and quantitatively by biochemical analysis of DNA content (**Fig.8A**). Surprisingly, ALP specific activity of the SSCs on the HFN-coated allograft was not increased (**Fig.8B**). This finding has been reported previously, whereby collagen Type 1, but not fibronectin, was shown to enhance osteogenic differentiation of human SSCs (Tsai *et al.* 2010) but is contrary to most literature.

Confounding factors to these biochemical results include the background level of DNA and ALP activity that was detected from the allograft (**Fig.8A**), despite washing and treatment with H_2O_2. This background level may have been able to influence the result as the SSCs had not reached confluence over the allograft after 2 weeks *in vitro* culture (**Fig.5**). A set seeding density of $5x10^4$ cells / cc of allograft was chosen for this study in accordance with previously validated methods (Jones *et al.* 2009), but culture of SSCs on the scaffold until

confluence would be more likely to demonstrate a difference, thereby minimising the chance of a Type II error, of which this may be.

The control groups of plain allograft (Group 1) and SSC-seeded allograft (Group 3) showed consistent mechanical properties to identical controls performed for previous studies, each of which used n=4 for each group (Bolland *et al.* 2006;Aarvold *et al.* 2011;Jones *et al.* 2009). Thus standard controls have been repeated up to sixteen times, validating of the reproducibility of these methods. The parallel lines produced in all shear strength graphs were evidence that the aggregate behaved as expected, satisfying the Mohr-Coulomb equation. The addition of SSCs to the IBG construct at a seeding density of $5x10^4$ cells / cc of allograft surprisingly did not show significant difference in shear strength to plain allograft (Group 3 *versus* 1) (p=0.17) (**Fig.9 & Table 2**). Previous studies have demonstrated a highly significant difference in mechanical strength when a seeding density of $2x10^5$ cells / cc of allograft was used (p=0.001), with a clear trend in increasing strength from non SSC-seeded allograft, to $5x10^4$ cells / cc, to $2x10^5$ cells / cc (Jones *et al.* 2009). This study used a seeding density of $5x10^4$ cells / cc of allograft as to culture expand $2x10^5$ cells / cc of allograft for the large numbers of discs used (n=16) would be problematic in the confines of a laboratory setting. High passage number risks altering the phenotype of the cells and introducing infection, but for future work either higher seeding density or increased duration of cell culture on allograft would be recommended. In the context of relatively low seeding density used in this study, the biological augmentation demonstrated on the SSC-seeded constructs (**Fig.8A**), and the known trend of SSC-seeding density to mechanical strength (Jones *et al.* 2009), the low significance observed on mechanical testing with the addition of SSCs is likely to be a Type II error.

HFN-coated SSC-seeded allograft (Group 4) showed a statistically significant increase in shear strength compared to allograft alone (Group 1) (p=0.001), indicating a beneficial effect of this tissue engineering approach to IBG. The addition of HFN alone to plain allograft did not demonstrate a statistically significant effect (Group 1 *versus* Group 2, p>0.05) and as described above, SSCs at this seeding density were not able to demonstrate a significant improvement in shear strength over allograft alone (p>0.05). Thus the significant increase in shear strength observed following HFN-coating *and* SSC-seeding of milled allograft (p=0.001) can be attributed to the compounded effect of both. Despite these positive findings, this data did not demonstrate a significant difference between SSC-

seeded allograft with or without HFN coating ($p>0.05$), which may be a Type II error as described above. Chemicon International provide a wide concentration range for HFN solution with which to coat surfaces, too much of which may inhibit cell adhesion (Yang *et al.* 2001). Therefore further work should focus on the optimising this range for clinical practice, as well as SSC seeding density.

The Null Hypothesis that HFN-coating of milled allograft, prior to seeding with SSCs, will not enhance osteoblastic differentiation on the impaction bone graft construct, cannot be rejected on the basis of this study. However this is likely to be a Type II error due to the SSC seeding density used. The Null Hypothesis that HFN-coating of milled allograft prior to seeding with SSCs will not augment the mechanical properties of the impacted bone construct, can be rejected.

As evidence accumulates, it is clear that the traditional concept of impaction bone grafting with allograft can be refined (Dunlop *et al.* 2003;Bolland *et al.* 2006;Jones *et al.* 2009;Korda *et al.* 2006). Studies have shown the potential of ECM proteins in promoting osteogenic differentiation of SSCs (Mizuno & Kuboki 2001;Tsai *et al.* 2010;Globus *et al.* 1998). Cool *et al* have shown increased osteogenic differentiation of SSCs cultured with HFN (Cool & Nurcombe 2005), Salasznyk *et al* have demonstrated increased affinity of SSCs for HFN (Salasznyk *et al.* 2004), and Yang *et al* have demonstrated promotion of both SSC adhesion and osteogenic differentiation on polymer scaffolds following HFN-coating (Yang *et al.* 2001). Thus one might expect that HFN may augment the biological and mechanical effects of SSCs on IBG, as a tissue engineering approach to revision hip surgery.

This study supports previous work that SSCs augment the biological and mechanical characteristics of IBG, which could improve the clinical outcomes of revision hip surgery. Coating of allograft with ECM proteins has a demonstrable effect (Yang *et al.* 2001;Jones *et al.* 2009;Globus *et al.* 1998), but further work is needed to optimise HFN parameters prior to clinical translation. Future work is focused on the use of bone graft extenders in IBG and biological augmentation of these synthetic grafts. Harvest and concentration of autologous SSCs from bone marrow is a facile technique that can be used intra-operatively (see Chapter V), therefore the addition of SSCs to IBG in revision hip surgery is an easily translatable technique that augers well for clinical practice.

PART 2: The Effect of Scaffold Porosity on Skeletal Stem Cell Growth and Differentiation

2.2.1 Introduction

Hydroxyapatite (HA) is the major inorganic component of bone and is widely used, as a natural ceramic, in orthopaedic applications to promote osseo-integration of prostheses (Trikha *et al.* 2005;Spiegelberg *et al.* 2009;Shah, Edge, & Clark 2009). Tricalcium phosphate (TCP) is a synthetic ceramic that is used in scaffolds for bone regeneration. It has a bio-resorption rate 3-12 times that of HA, therefore TCP is more closely matched to the rate of bone repair than HA, while the partial degradation promotes bonding of bone to the scaffold (Habibovic & de Groot 2007;Hutmacher *et al.* 2007). HA and TCP have excellent biocompatibility and compressive strength (Schumacher *et al.* 2010), and when used together in a biphasic scaffold combine the long term stability of HA with the higher solubility and bio-reactivity of TCP (Hutmacher *et al.* 2007;Hsu, Turner, & Miles 2007). The osteoconductive properties of HA and TCP have been well-documented (Shepperd & Apthorp 2005;Hutmacher *et al.* 2007;Habibovic & de Groot 2007), and there is a growing cohort of evidence suggestive of osteoinductivity (Fellah *et al.* 2008;Yuan *et al.* 2010;Habibovic *et al.* 2006a;Ripamonti *et al.* 2009).

Pore size and porosity have been shown to be critical characteristics of scaffolds for bone regeneration, and must allow for cell size and free passage of oxygen, nutrients and waste metabolites while maintaining the structural strength of a scaffold. The porosity of HA/TCP is thought to aid osteoconductivity (and possibly osteoinductivity) as the increased surface area generated within higher porosity scaffolds supports more bone in-growth and exposes cells to greater surface reactivity (Habibovic *et al.* 2006a;Habibovic *et al.* 2006b;Xu *et al.* 2011;Hsu, Turner, & Miles 2007;Hutmacher *et al.* 2007;Yuan *et al.* 2010). This phenomenon of porosity related to osteogenicity has also been demonstrated in titanium (Fujibayashi *et al.* 2004).

Poor bone growth on ceramic scaffolds has been observed in a number of studies, indicating these scaffolds may lack the osteoconductivity needed to repair large bone defects, and remain inferior to the gold standard of autograft (Fellah *et al.* 2008;Habibovic *et al.* 2006a;Yuan *et al.* 2010). Thus seeding biphasic scaffolds with skeletal stem cells

(SSCs) may augment osteogenesis, thereby increasing the application of these scaffolds for clinical practice.

Previous manufacturing techniques to produce porous calcium phosphate granules, such as crushing sintered blocks, hydrothermal conversion of natural corals, dripping, drip casting, gelcasting and stirring mixtures of immiscible liquids, produce either irregularly shaped and sized blocks or scaffolds with isolated pores that are unconnected. To attain interconnected pores by these methods requires such high porosity that the mechanical stability of the material is adversely affected (Hsu, Turner, & Miles 2007). Thus a novel method of production of biphasic calcium phosphate scaffolds has been developed by Dr Irene Turner at the University of Bath Department of Chemical Engineering, which uses vacuum impregnation of polyurethane (PU) foams to create a scaffold with controlled size, shape and porosity. Mechanical testing had been performed on these scaffolds, demonstrating increased stiffness on a die-plunger test compared to the commercially available BoneSave granules (Stryker, Swindon, UK) and no statistical differences in stiffness between the 30 and 45 ppi scaffolds were found (Hsu, Turner, & Miles 2007).

2.2.2 Aims

1. To investigate the potential of a novel porous biphasic HA/TCP scaffold to support skeletal stem cell growth and osteogenic differentiation.
2. To establish whether porosity of an HA/TCP scaffold has an effect on skeletal stem cell growth and osteogenic differentiation.

2.2.3 Null Hypothesis

1. Porous biphasic HA/TCP scaffold does not support human skeletal stem cell growth.
2. The porosity of HA/TCP scaffold has no effect on osteogenic differentiation of skeletal stem cells.

2.2.4 Materials & Methods

Scaffold design & construction

HA/TCP scaffolds were manufactured and produced by Dr Irene Turner (University of Bath Department of Chemical Engineering) using two grades of calcium phosphate powder, TCP 118 and 130. The HA/TCP ratio was controlled by powder ratio and sintering temperature, producing a final phase composition of 37% HA and 63% TCP. Vacuum impregnated PU foams were used to control porosity at either 30 or 45 pores per square inch (ppi), and the PU foam was subsequently completely burnt out during sintering. For assessment of biological augmentation of the scaffolds in this study, equal sized cuboids measuring 5x5x5mm were produced, and the edges smoothed using carbide paper.

Skeletal stem cell isolation and preparation

Human bone marrow was harvested from the femoral canal of a haematologically normal adult undergoing total hip replacement (THR), in accordance with ethical approval LREC194/99/1. The SSC fraction was isolated by repeat washes of the marrow in α-MEM, centrifugation at 1100rpm for 4min, re-suspension of the cell pellet in basal media and passage through a 70μm filter. Cells were plated onto tissue culture flasks, incubated at 37˚C and humidified 4% CO_2 and media changed every 3-4 days until confluent. Cells were released using collagenase and trypsin, re-suspended in basal media and cell count was recorded on a haemocytometer prior to seeding onto the scaffolds.

Seeding of scaffolds with skeletal stem cells

Five 30ppi and five 45ppi scaffolds were seeded with SSCs, and five of each scaffold porosity were used as negative controls. All scaffolds were sterilised in 70% ethanol for 2 hours and washed with sterile phosphate-buffered saline (PBS) to ensure ethanol removal. All twenty scaffolds were incubated in basal media in individual containers for a further 2 hours prior to seeding with SSCs, and divided into four groups of five. Media was removed and five 30ppi and five 45ppi scaffolds were covered with basal media containing $3.6x10^6$ SSCs (2ml) and five 30ppi and five 45ppi scaffolds were covered with plain basal media (2ml) as negative controls (**Table 1**). All scaffolds were incubated in individual containers overnight on a gyrating platform at 37˚C and humidified 4% CO_2.

Table 1: Ten 30ppi and ten 45ppi scaffold cuboids were each divided into 2 groups of five scaffolds. One group of scaffolds of each porosity was seeded with SSCs and one of each used as negative controls. For all groups, n=5.

	Porosity / ppi	*SSC seeding*	*n*
Group 1	30	X	5
Group 2	30	✓	5
Group 3	45	X	5
Group 4	45	✓	5

Analysis of Cell viability

Following 24 hour incubation, one scaffold from each group was removed for staining with CTG-EH and assessed for cell viability using Carl Zeiss Axiovision software Ver 3.0 via an AxioCam HR digital camera on an Axiovert 200 inverted microscope (Carl Zeiss Ltd, Hertfordshire, UK) under fluorescent light.

In-vivo study

The remaining four scaffolds in each group were used for *in vivo* analysis. Male MF-1 nu/nu immunodeficient mice were purchased from Harlan, Loughborough, UK and acclimatized for a minimum of 1 week prior to experimentation. All procedures were performed after prior ethical approval in accordance with regulations specified by the Animals (Scientific Procedures) Act 1986. The animals were weighed and anaesthetised with fentanyl-fluanisone (Hypnorm) (Janssen-Cilag Ltd, High Wycombe, UK) and midazolam (Hypnovel) (Roche Ltd, Welwyn Garden City, UK) in sterile water at a ratio of 1:1 and a dose of 10ml kg^{-1} intra-peritoneally. A longitudinal incision was made on the mouse dorsal flank (**Fig.1A**), and four scaffolds from one group were implanted subcutaneously into the rear flank of the animal. This was repeated on the contralateral side (**Fig.1B**) and wounds were closed with skin clips (**Fig.1C**).

Table 2: Layout of each scaffold Group in the nude mice.

Mouse 1, 38g		**Mouse 2, 45g**	
Left flank	**Right flank**	**Right flank**	**Left flank**
Group 1	**Group 2**	**Group 3**	**Group 4**
30ppi, no cells	**30ppi, SSC-seeded**	**45ppi, no cells**	**45ppi, SSC-seeded**

Figure 1: Intra-operative photographs of sub cutaneous nude mouse operation. A: Longitudinal incision on the dorsal flank. B: Contralateral incision, with cuboid scaffolds visible in the sub-cutaneous pocket. C: Post-operatively with bilateral skin clips.

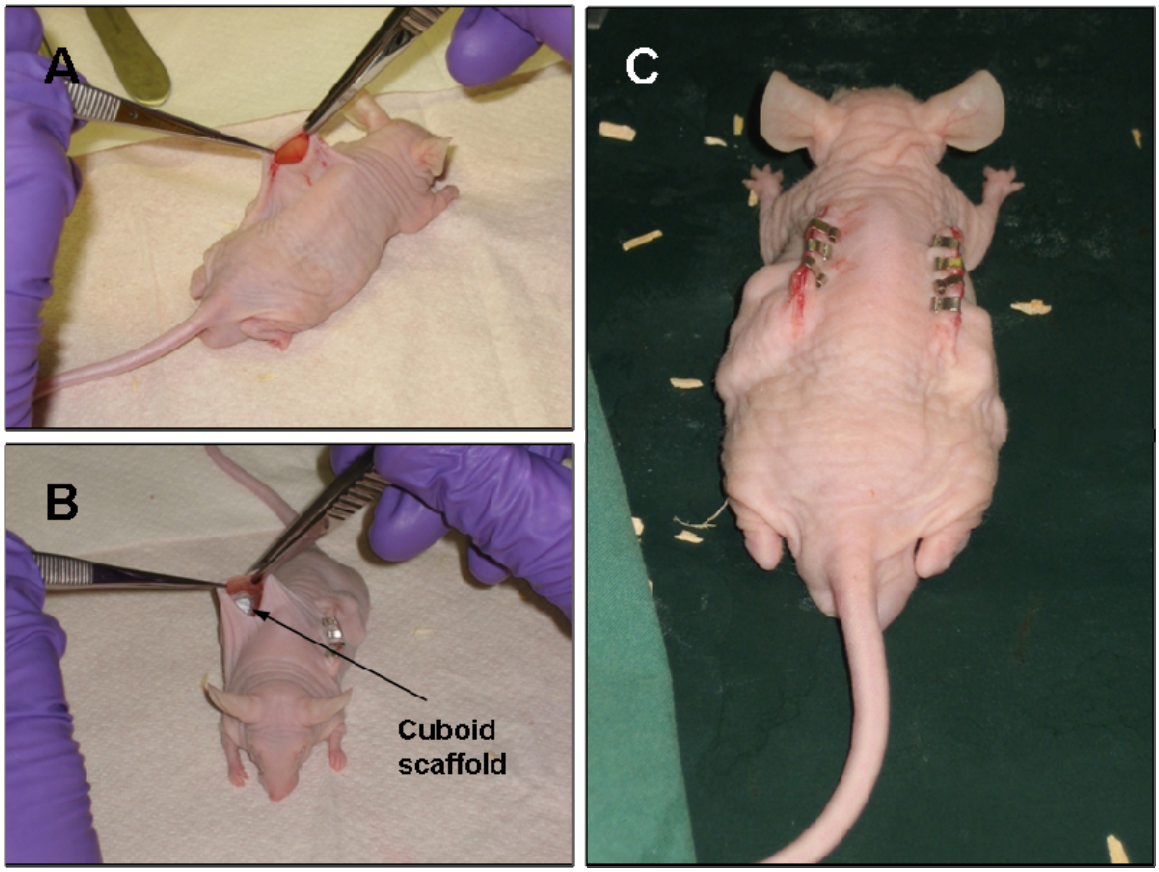

Mice were euthanased at 28 days post-operatively by rising CO_2 and the scaffolds were harvested. Each scaffold was placed in an individual universal container containing fixative as required. One scaffold from each group was fixed in 95% ethanol and three from each group were fixed in 4% paraformaldehyde (PFA). All scaffolds were fixed for 24hrs at 4˚C, then fixative was removed and replaced with 2ml PBS providing graft coverage.

Histology

The scaffolds proved too hard for sectioning for histology slide preparation, and due to the scaffold composition being entirely calcium based, decalcification resulted in dissolution of the scaffold. Therefore analysis by prepared histological slides was not possible.

Scanning electron microscopy

Samples were fixed using 4% paraformaldehyde, as described above, and freeze dried. SEM analysis was performed using a JEOL JSM 6330F Scanning Electron Microscope (JEOL UK Ltd, Welwyn Garden city, UK) and an Oxford Instruments ISIS 300 system (Oxford Instruments, Abingdon, UK) was used to obtain Energy Dispersive X Ray Analysis (EDXA) data of the samples.

Micro Computed Tomography

One scaffold from each group, fixed in 4% PFA, was scanned using an Xtek Benchtop 160Xi scanner (Xtek Systems Ltd, Tring, UK) equipped with a Hamamatsu C7943 X-ray flat panel sensor (Hamamatsu Photonics, Welwyn Garden City, UK). An untreated 30ppi and 45ppi scaffold (not having been *in vivo*) was scanned as a further negative control. All scans were taken to 11micron resolution, at 150kV, 60µA using a molybdenum target with an exposure time of 534ms and 4x digital gain. Reconstructed volume images were analysed using VGStudio Max 1.2.1 software (Volume Graphics GmbH, Heidelberg, Germany). Scaffold and solid tissue was digitally subtracted from 1.5mm^3 regions of each *in vivo* cuboid for analysis of channel dimensions and tissue in-growth.

Biochemistry

The 95% ethanol-fixed scaffold from each group was prepared for biochemical analysis of DNA content (as a measure of cell growth) and ALP activity (as a measure of osteogenic differentiation). ALP specific activity was measured as a proportion of ALP activity to DNA content. Cell lysates were obtained via suspension of the scaffold in 2.0ml Triton X-100 0.05% (BDH Chemical Ltd, Poole, UK) followed by three sequential freeze-thaw cycles with multiple vortexing. The lysate was aspirated, passed through a 70µm filter and the scaffold was discarded. ALP and DNA assays were then performed in a standard manner with 10µl of lysate run in triplicate for each scaffold, on a plate against two standards and read on a BioTek KC4 and FLX-800 microplate fluorescent reader (BioTek, Potton, UK). DNA was measured in nanograms (ng) / ml of lysate and ALP read as nanomoles of p-nitrophenol / ml / hour (nmol pNPP/ml hr^{-1}). Statistics were calculated in Excel and SPSS Ver 18.

2.2.5 Results

Analysis of cell viability

CTG-EH staining confirmed adherent and viable cells on both 30 and 45 ppi scaffolds, with some background luminescence only on the negative controls (**Fig.2**). The SSC-seeded scaffolds were therefore suitable for implantation in vivo.

Figure 2: CTG-EH stain demonstrated background luminescence on the unseeded scaffold (A), with viable cells on the 30ppi (B) and 45ppi (C) SSC-seeded scaffolds (Scale bars = 100µm).

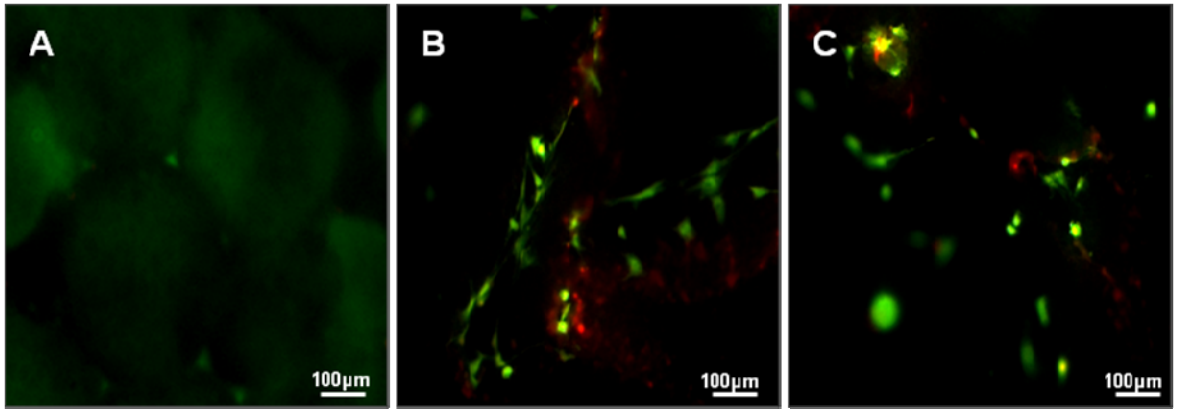

Scanning electron microscopy

Upon removal from the sub cutaneous pocket of the nude mice, all the scaffolds were wrapped in a layer of fibrous tissue (**Fig.3A-B**). This layer was peeled back to expose the underlying pores, for visualisation of representative sections on SEM. Beneath the fibrous layer, erythrocytes could be seen on the surfaces of all the scaffolds (**Fig.3A-D**). High levels of cellular activity were evident on the SSC-seeded scaffolds (**Fig.3C-D**), with tissue ingress into the pores of the 45ppi SSC-seeded scaffolds (**Fig.D**).

Figure 3: SEM images of *ex vivo* scaffolds. Bi-concave disc erythrocytes can be seen on the surface of all scaffolds (thin arrows). SSC seeded scaffolds (C-D) showed erythrocytes and also SSCs adherent to the scaffold surface (thick arrows), with tissue ingress into the pores of the 45ppi SSC-scaffold (D) (Scale bars = 20µm).

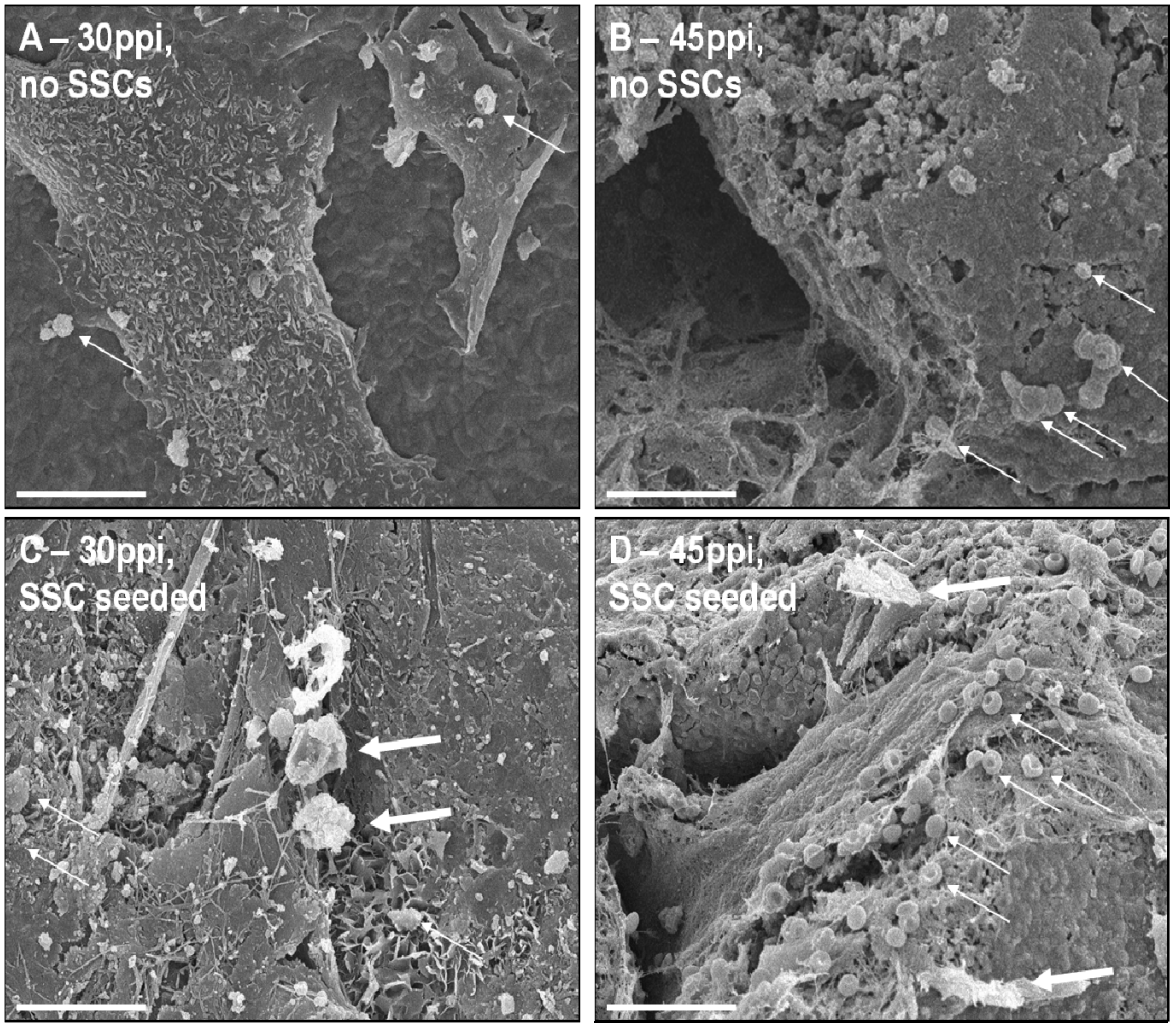

μCT scanning

3D reconstructions of plain untreated scaffolds were performed, illustrating the outer morphology and inner porosity. The porosity is evident within the scaffolds, with the pore pattern maintained throughout (**Fig.4A-D**). Reconstructed volume images of the porous channels without scaffold or soft tissue were produced by digital subtraction (**Fig.4E-H**). Analysis of porous channel characteristics demonstrated negligible difference between the 30ppi scaffolds as a result of SSC-seeding. The data from the 45ppi scaffolds showed that adding SSCs resulted in a reduced overall channel volume, reduced percentage of scaffold that was empty channel, reduced mean channel width and a greater overall length of the channel between the intersects (**Table 3**). Reduced channel dimensions were attributed to generation of new tissue and suggest, on average, there was 0.005-0.01mm of new tissue coating the channel walls of the SSC-seeded 45ppi scaffolds, illustrated schematically in **Figure 5**.

Table 3: Channel dimensions of each scaffold illustrating significant differences seen in the 45ppi scaffold as a result of seeding with SSCs. There was negligible difference observed on the 30ppi scaffold following SSC seeding..

	Group 1 *30ppi, no cells*	*Group 2* *30ppi, SSCs*	*Group 3* *45ppi, no cells*	*Group 4* *45ppi, SSCs*
Mean channel volume / mm^3	0.15	0.16	0.27	0.20
Mean channel width / mm	0.1	0.1	0.09	0.08
Mean channel length / mm	1.06	1.00	0.55	0.69
Proportion of scaffold that is channel / %	4.5	4.8	7.9	5.8

Figure 4: µCT reconstructions of HA/TCP micro-porous scaffolds at 11micron resolution. A-D: Untreated scaffolds illustrate the external morphology and internal porosity which remains uniform throughout. E-F: *Ex vivo* scaffolds demonstrating, by digital subtraction, the interconnected channels. A reduction in channel dimensions was quantified between the non SSC-seeded 45ppi scaffold (4G) and the SSC-seeded 45ppi scaffold (4H), indicative of tissue generation on the channel walls as a result of cell seeding.

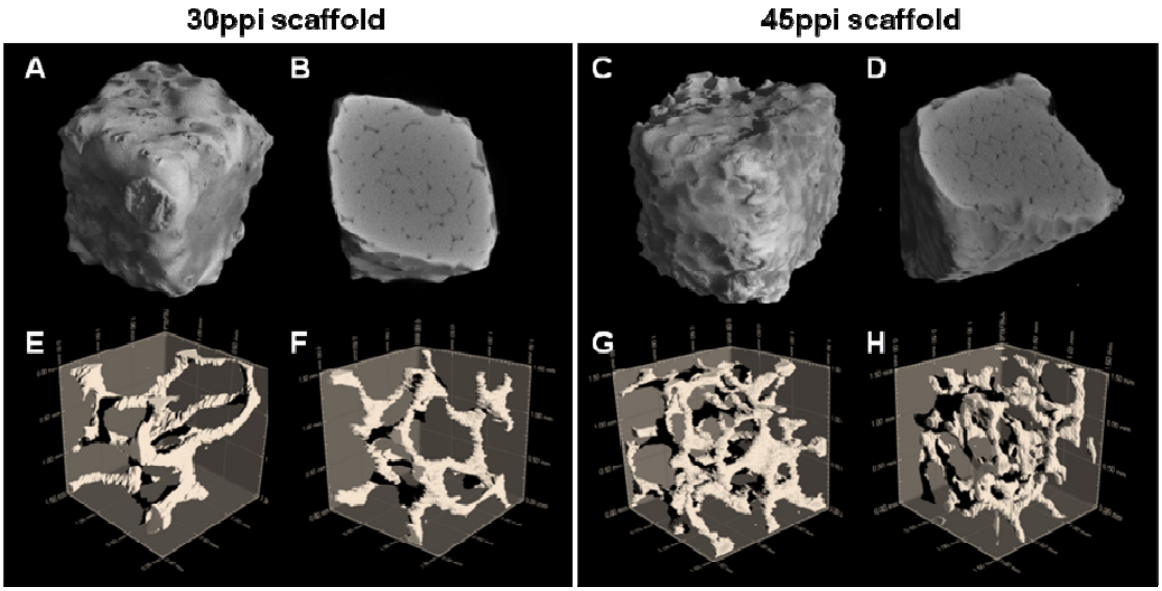

Figure 5: Schematic of tissue formation in the channels of the 45ppi scaffold as a result of seeding with SSCs. The channel dimensions indicated that the channel walls (blue) were augmented by new tissue deposition (red), resulting in a reduced channel width and increased channel length. On average a 0.005-0.01mm layer of tissue was demonstrated.

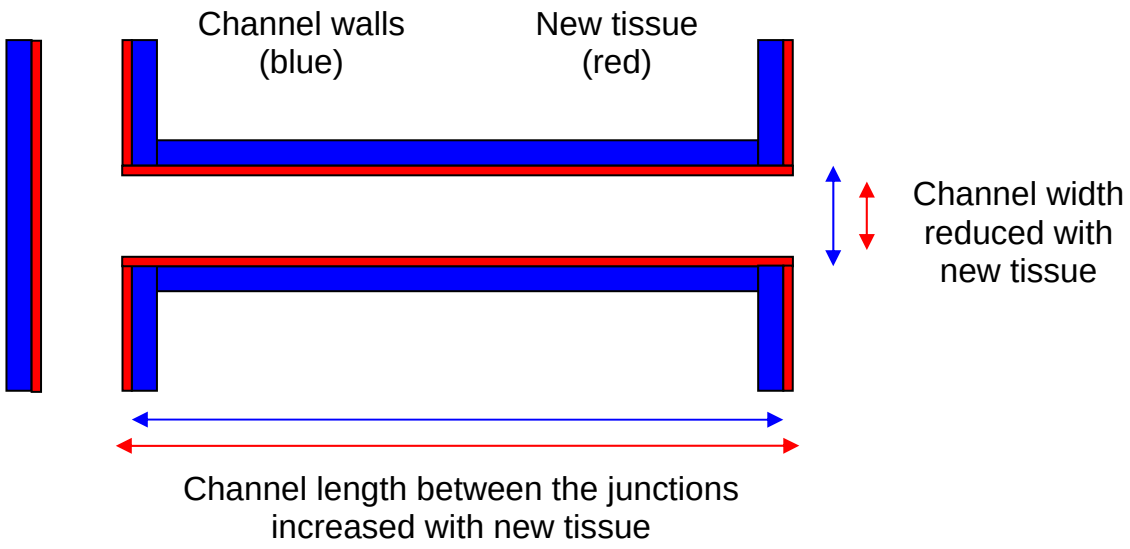

Density analysis of the scaffolds with and without SSC-seeding was performed using Grey Scale value, whereby density of the scaffold corresponded to the peak on the density curve (**Fig.6A-B**). The plain untreated 45ppi scaffold was observed to be less dense than the lower porosity 30ppi scaffold (1995 *versus* 2450 units) (**Table 4**). Both un-seeded scaffolds displayed a small increase in density following 4 weeks *in vivo*, with the 45ppi scaffold maintaining a lower density (2100 *versus* 2695 units). The densities of the 30 and 45ppi SSC-seeded scaffolds following 4 weeks in vivo culture were both increased further, to comparable densities (2820 *versus* 2730 units). The 30ppi SSC-seeded scaffold was observed to have an increased density of 370 Grey Scale units, compared to the 45ppi scaffold which was increased by 735 units. Thus the 45ppi SSC-seeded scaffold supported double the density increase seen in the 30ppi scaffold (x1.99).

Biochemistry

PicoGreen DNA assays demonstrated significant background DNA level on non cell-seeded scaffolds following *in vivo* growth (Groups 1&3), but increased DNA on the SSC-seeded scaffolds (Groups 2&4), indicative of increased cell growth which was statistically significant using unpaired t-test ($p < 0.0005$) (**Fig.7A**). ALP activity, indicating osteogenic differentiation, was increased on the SSC-seeded scaffolds compared to the non cell-seeded controls, and the difference was statistically significant on unpaired t-test for both the 30ppi scaffold ($p=0.001$) and the 45ppi scaffold ($p=0.003$). The 45ppi scaffold demonstrated enhanced ALP activity, which was raised 13.4 fold by the addition of SSCs (4.90nmol pNPP/ml hr^{-1} on the non cell-seeded control *versus* 65.65nmol pNPP/ml hr^{-1}) and 8.7-fold for the 30ppi scaffold (3.45 *versus* 29.86 pNPP/ml hr^{-1}) (**Fig.7B**), which were both highly significant ($p<0.005$). Both 30 and 45ppi SSC-seeded scaffolds demonstrated increased ALP specific activity compared to their non cell-seeded *in vivo* controls, which was highly significant on independent t-test (30ppi, $p=0.007$; 45ppi, $p=0.012$) (**Fig.7C**). The 45ppi scaffold was observed to support double the increase in ALP specific activity (x1.98) of the 30ppi scaffold (0.249nmol pNPP/hr/ngDNA increase *versus* 0.126nmol pNPP/hr/ngDNA).

Figure 6: Density plots of scaffolds following 4 weeks *in vivo* growth with and without prior SSC-seeding (yellow and pink curves respectively). Also plotted is the density curve of each plain scaffold, prior to placement *in vivo*. A: 30ppi scaffolds. B: 45ppi scaffolds.

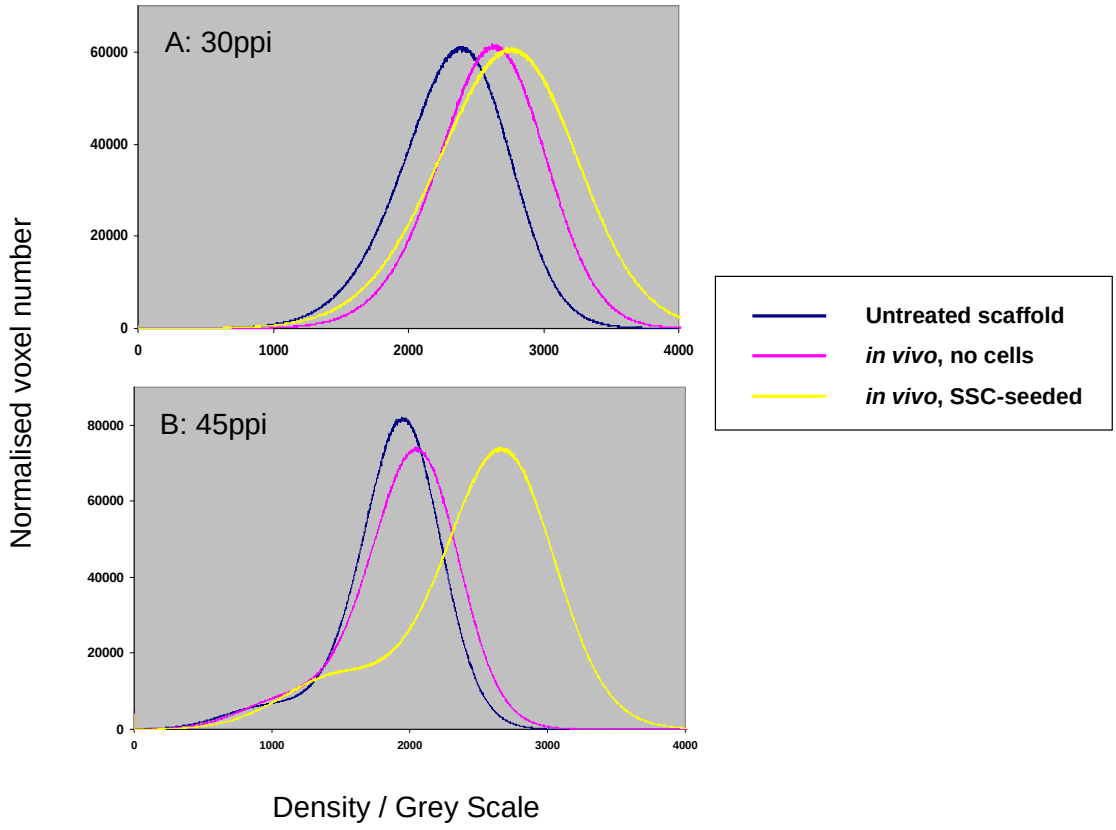

Table 4: Density values in Grey Scale of the scaffolds, read from the peak of the three curves in Figures 6A-B.

	30ppi scaffold	***45ppi scaffold***
Plain untreated scaffold	2450	1995
In-vivo scaffold, no cells	2695	2100
SSC-seeded *in-vivo* scaffold	2820	2730

Figure 7: Biochemical analysis of cellular material on the scaffolds following 4weeks *in vivo* growth. The SSC-seeded scaffolds showed an increase in DNA content compared to the unseeded controls (unpaired t-test, p<0.001). Increased ALP activity was demonstrated on the SSC-seeded scaffolds compared to their negative *in vivo* controls (p<0.001). Enhanced ALP specific activity was observed on both the 30ppi and 45ppi SSC-seeded scaffolds. The 45ppi scaffold supported double the increase in ALP specific activity compared to the 30ppi scaffold. Error bars denote Standard Deviation. *** = p<0.001, ** = p< 0.01, * = p<0.05.

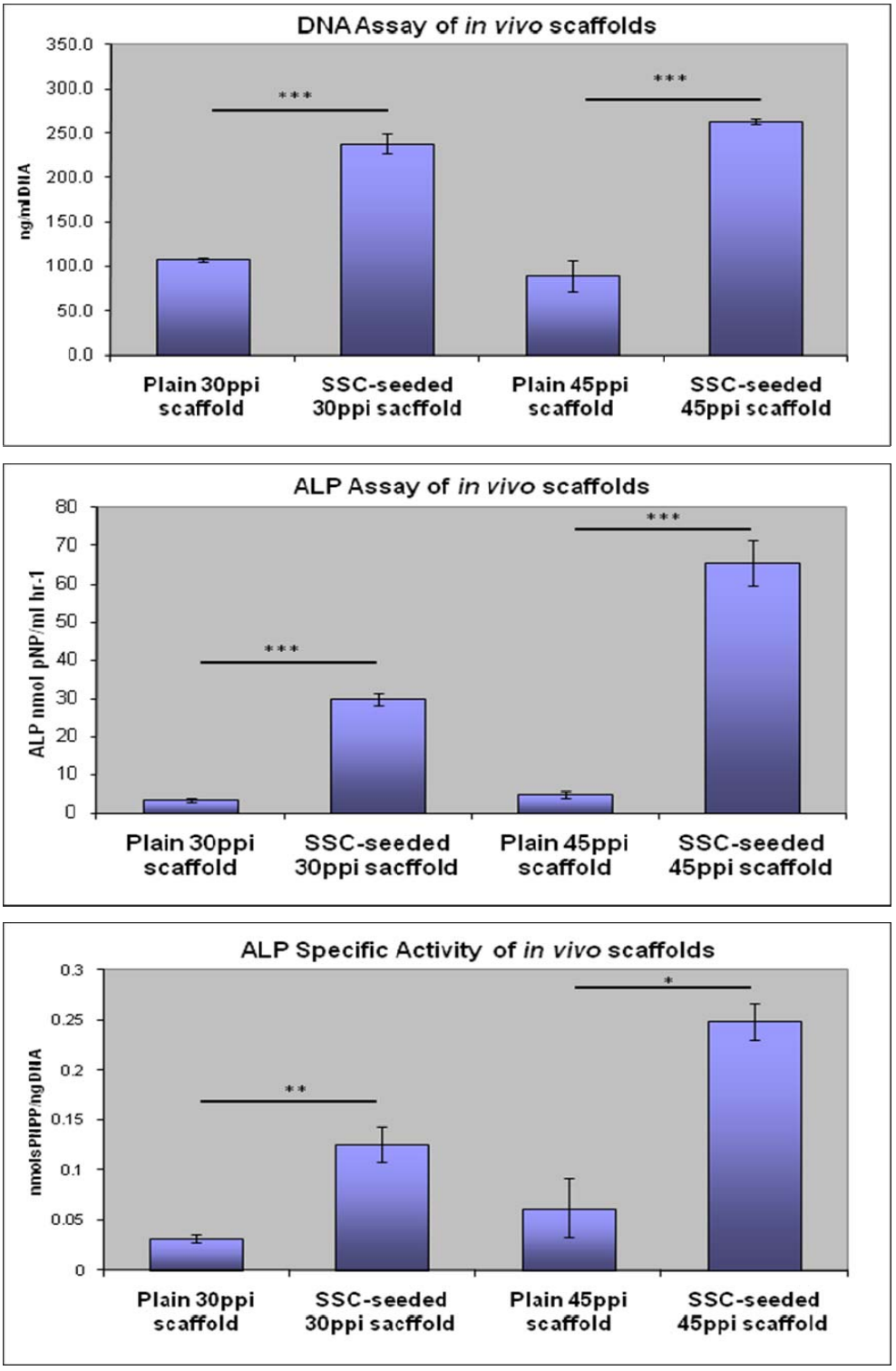

2.2.6 Discussion

This study has demonstrated that a biphasic scaffold material supports human SSC growth, as evidenced by cell viability analysis following 48 hours *in vitro* incubation (**Fig.2**) and biochemical analysis following 4 weeks *in vivo* growth (**Fig.7**). Furthermore, the presence of ALP specific activity signified osteogenic differentiation in this heterotopic sub-cutaneous site. Histological analysis was not possible as the decalcification process prior to sectioning resulted in dissolution of the HA/TCP scaffold, however SEM analysis was used to visualise the scaffold surfaces. Healthy adherent cells were evident on the surfaces of the SSC-seeded scaffolds, with tissue in-growth observed in the pores of the 45ppi SSC-seeded scaffolds (**Fig.3**).

Biochemical assay of DNA content on the scaffolds following *in vivo* culture indicated SSC growth, which was comparable on the 30 and 45ppi scaffolds. The small DNA content detected on the non cell-seeded scaffolds may be attributed to mouse host cells, but this baseline was significantly lower than the DNA content on the SSC-seeded scaffolds (**Fig.7A**). Human SSCs were not labelled prior to seeding (eg. by fluorochrome markers) to confirm their origin, but the non cell-seeded negative controls would suggest that the difference was attributable to human SSC growth. Both SSC-seeded scaffolds demonstrated osteogenic differentiation of the SSCs, as seen by ALP activity (**Fig.7B-C**). The first Null Hypothesis, that this porous biphasic scaffold does not support human SSC growth, can be rejected.

These studies illustrate the porosity of the scaffold was shown to affect SSC differentiation. ALP activity and, crucially, ALP specific activity were enhanced on the highly porous 45ppi scaffold compared to the 30ppi scaffold. This difference was greater by a factor of 1.98 compared to the 30ppi scaffold, indicating that higher scaffold porosity augmented osteogenic differentiation. This may be the result of increased surface area, which exposed the cells to greater surface reactivity of the material, a theory put forward by Habibovic and colleagues (Habibovic & de Groot 2007). Interestingly, the host mouse cells that grew on the non-SSC seeded scaffolds also showed a higher ALP specific activity on the 45ppi compared to 30ppi scaffold (**Fig.7C**), but this was not statistically significant.

This has been hypothesised by Habibovic et al, following implantation of porous ceramic scaffolds intra-muscularly in a goat model, with increased heterotopic bone growth demonstrated on higher porosity ceramic scaffolds (Habibovic *et al.* 2006b). Fellah et al demonstrated that scaffolds lacking such microporosity cannot induce bone growth. This group demonstrated progressive bone growth on microporous ceramic scaffolds, as measured by μCT, EM, histology and histomorphometry, in a goat femoral epiphyseal critical sized defect, but none on the same material lacking the microporous structure. Diffusion chambers were used to remove any osteoconductive effect, indicating that this material and microporosity was osteoinductive in nature (Fellah *et al.* 2008). Osteoinductivity of ceramic materials has been argued by numerous authors who have demonstrated bone growth in non-osseous heterotopic sites. Ripamonti et al inserted HA / calcium carbonate scaffolds into the rectus abdominis muscle of non-human primates, and demonstrated that bone growth was induced in this non-osseus site, on ALP and osteocalcin assays, histology and mRNA expression of Collagen IV and BMP-7, without the addition of osteogenic cells or osteoinductive factors (Ripamonti *et al.* 2009). Such heterotopic bone induction has been demonstrated in canine thigh muscle, which was comparable to bone formation on the same scaffolds placed in the femur. TCP scaffolds demonstrated greater osteoinductivity than HA scaffolds, which the authors believe was due to the inherent osteoinductive nature of the material itself (Yuan *et al.* 2001). Material osteoinductivity has also been suggested in titanium, where heterotopic ossification was demonstrated in porous ceramic scaffolds implanted in the dorsal muscle of beagle dogs. Bone formation occurred despite no supplementation with cells or factors, and was dependent on an interconnected porous architecture and a 3D microporous surface structure (Fujibayashi *et al.* 2004).

Porosity also affected density change of the scaffolds following *in vivo* culture. Whilst both porosity scaffolds demonstrated increased density following SSC growth and differentiation, the 45ppi scaffold showed double (x1.99) the density increase to the 30ppi scaffold. Interestingly, the increase in ALP specific activity of the 45ppi scaffold with the addition of SSCs was also double (x1.98) that seen in the 30ppi scaffold. Thus the difference in density change can be correlated to the difference in osteogenesis, suggesting it was a result of increased bone formation on the higher porosity scaffold. Furthermore, a reduction in dimensions of the porous channel was observed on the higher porosity scaffold following SSC-seeding, as a result of generation of new tissue within the walls of

the scaffold. The biochemical data, notably the greater ALP specific activity on the SSC-seeded 45ppi scaffold, indicated that the tissue that was generated was osteoid, and *de novo* bone formation has occurred. The second Null Hypotheses, that scaffold porosity has no effect on osteogenic differentiation of SSCs, can be rejected.

The affinity of HA/TCP scaffolds for SSC proliferation has been demonstrated *in vitro* and *in vivo*. Their ability to support osteogenic differentiation was observed *in vivo*, with increased porosity found to augment osteogenesis. This phenomenon has been reported in the literature on other materials (Fujibayashi *et al.* 2004;Habibovic *et al.* 2006b;Habibovic *et al.* 2006a;Fellah *et al.* 2008;Ripamonti *et al.* 2009) and may indicate that the material has osteoinductive properties as well as osteoconductive. The preliminary investigation of these scaffolds and their porosity augers well for their use in the clinical treatment of bone defects, and further work is planned in large animal (ovine) studies. This calcium phosphate scaffold can also be impregnated with drugs (eg. antimicrobials, antibiotics, growth factors), offering further potential for stimulation of osteogenesis and widening potential clinical applications.

This novel technique for fabrication of biphasic scaffolds is critical to provide a regular morphology, guarantee of interconnected pores, maintenance of stability and, crucially, control of porosity. The control of porosity, hitherto not possible using existing manufacturing techniques, has been demonstrated in this study to be critical to functionality of the scaffold, and indicates the suitability of this HA/TCP scaffold as a bone graft extender in impaction bone grafting or bone defect repair.

Chapter III

The enrichment of skeletal stem cells from human bone marrow to enhance skeletal repair

This work was performed in conjunction with Dr Jon Dawson and Mr James Smith. We are grateful to Mr Andrew Jones for his preparation of the ethical approval, and to the Technology Strategy Board (TSB) for their peer-reviewed research council funding (Reference AG280K). Marrow aspiration methods were performed and developed in conjunction with Mr Douglas Dunlop and Mr David Higgs. Initial development and testing of the device was performed by Dr Jon Ridgway and Dr Steve Curran from Smith & Nephew UK, prior to the work described in this chapter.

3.1 Introduction

Bone marrow transplantation is an established treatment for leukaemia and multiple myeloma, and the therapeutic potential of autologous bone marrow has now been harnessed for musculoskeletal pathology. Whilst fresh autologous marrow has been used in clinical practice (Warnke *et al.* 2004;Connolly *et al.* 1991;Tilley *et al.* 2006), subsequent investigation by Hernigou and colleagues has established that the skeletal stem cell (SSC) concentration in aspirated marrow is sub-therapeutic for musculoskeletal purposes. Patients with femoral head osteonecrosis or fracture non-union were treated with concentrated autologous bone marrow, and parallel *in vitro* measurement of SSC number by colony forming unit (CFU-F) analysis revealed that all atrophic non-unions that failed to heal had significantly lower CFU-F counts (Hernigou *et al.* 2005a). This indicated a requirement for delivery of a critical concentration and number of SSCs to the defect site, suggested as greater than 1000 CFU-F/ml, which when compared to the mean concentration in plain bone marrow aspirate (BMA) of approximately 600 CFU-F/ml, may explain the unpredictable outcomes of BMA used in clinical practice (Hernigou *et al.* 2005a;Ridgway *et al.* 2010). This concept has been extended to the application of allograft, whereby studies by Jones *et al* on impaction bone grafting, referenced in Chapter II, indicate that as cell seeding density on the allograft increases, so does the ability of the graft to resist shear and to support an implant (Jones *et al.* 2009).

Thus there appears to be a need for cell enrichment strategies from bone marrow for musculo-skeletal tissue engineering application. Concentrated SSCs have now been used in clinical practice and a number of groups have achieved significantly expanded cell numbers and concentration by *ex vivo* culture expansion (Vacanti *et al.* 2001;Quarto *et al.* 2001;Marcacci *et al.* 2007;Ohgushi *et al.* 2005;Morishita *et al.* 2006;Hibi *et al.* 2006;Kitoh *et al.* 2007). Whilst the generation of large numbers of SSCs is achievable, the process is 1) time consuming, 2) expensive, 3) subjects the patient to an extra procedure, 4) results in cells with altered phenotypic properties (including differentiation and proliferation capacity) and 5) carries inherent risk of *ex vivo* contamination (Banfi *et al.* 2000). Centrifuge-based devices are in clinical use (Giannini *et al.* 2009;Hernigou *et al.* 2006;Biomet Biologics Inc 2007), but also involve transfer of the aspirated marrow out of the sterile operating field for processing. Plasma, platelets and erythrocytes, along with their beneficial therapeutic properties (Muschler, Boehm, & Easley 1997) are lost in this process, and the costs of centrifuge, disposables and extra personnel are significant.

An alternative non-centrifuge device has been designed by Smith & Nephew (Ridgway *et al.* 2010) to eliminate some of these disadvantages. This point of care device has been designed with the following specifications: a) compact b) single use c) fully disposable d) entirely for use within the sterile operating field. The need for capital acquisition and maintenance of a large centrifuge system would therefore be eliminated, along with the contamination risk of passing material outside of the sterile field or during the laboratory process. In essence, a novel strategy of acoustic agitation and vacuum-assisted filtration has been employed for enrichment of the SSC cell fraction of BMA. The filtration process aims to retain the nucleated cell content whilst reducing plasma volume, erythrocytes and platelets. The product concept design is illustrated in **Fig.1A-B**, and the laboratory prototype that has been used in this study is shown in **Fig.1C**.

Preliminary testing of the device was performed by Smith & Nephew on BMA purchased from Lonza (Basel, Switzerland). BMA from 16 patients aged 18-25 years was processed and analysed. A mean 4.0 fold volume reduction was achieved, with corresponding 93.2% mean nucleated cell retention. CFU-F analysis showed a 4.8 fold increase in the processed aspirate with enrichment to in excess of 1000 CFU-F per millilitre (Ridgway *et al.* 2010). These samples were from healthy young individuals, however, in clinical practice, pathology that would benefit from biological augmentation is to be found largely in the elderly population. The aim of this study was to examine the efficacy of this device on bone marrow from typical elderly patients and to evaluate the isolated populations harvested, prior to planned clinical application.

Aspiration from the iliac crest carries associated morbidity, thus for this pre-clinical stage of the trial, waste bone marrow from the femoral canal harvested during total hip replacement (THR) surgery was used as an alternative. A robust and reproducible technique for bone marrow aspiration required development prior to analysis of the processed femoral canal BMA.

Figure 1A-B: Product concept of vacuum-assisted acoustic-filtration device, designed for single use within the sterile operating field. C: Prototype laboratory device used in this study for analysis of BMA from a cohort of elderly patients.

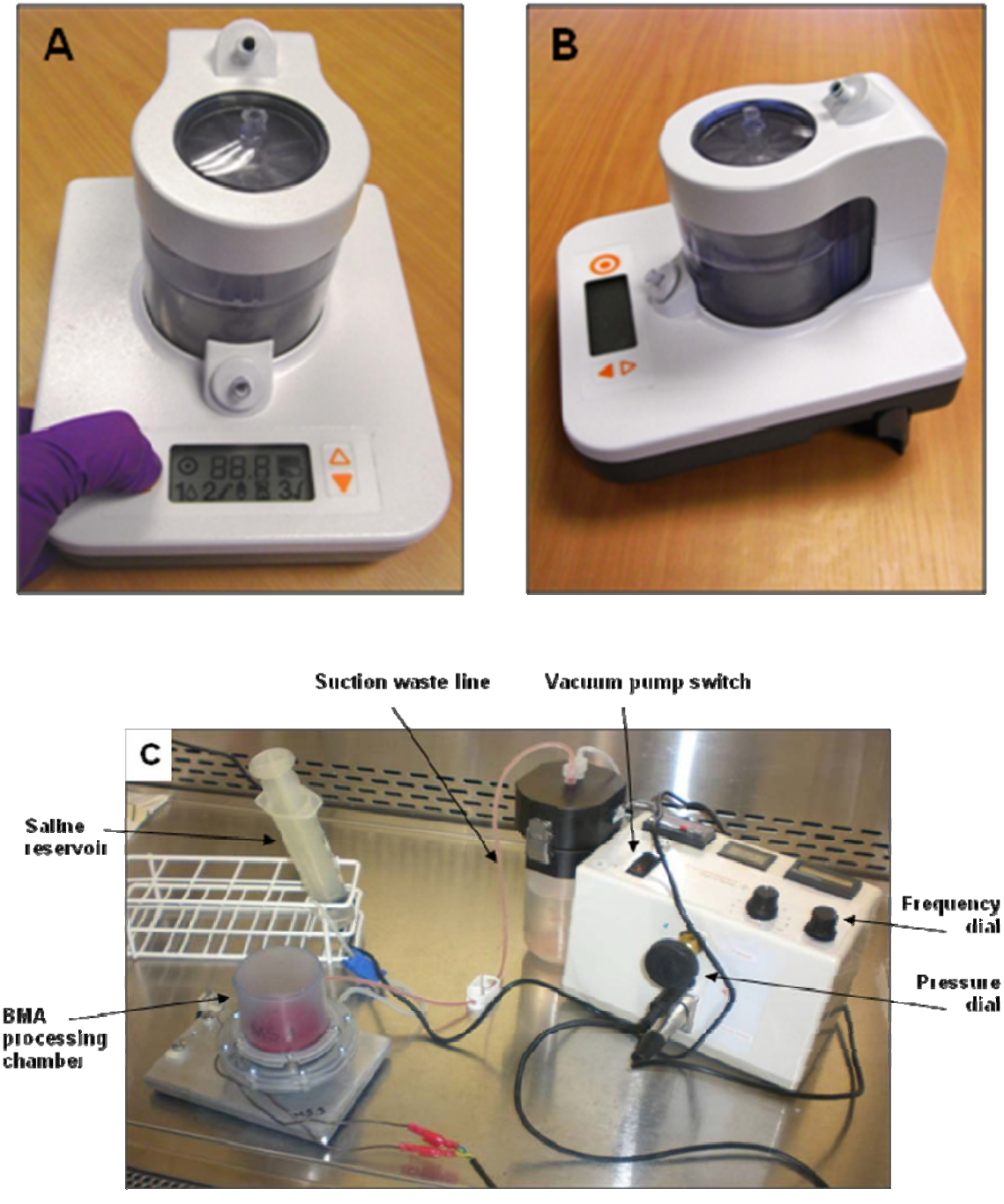

3.2 Aims

To evaluate and further develop a device that can be used intra-operatively to rapidly process bone marrow aspirate, to deliver a fluid fraction enriched in SSCs within an appropriate operating time for bone, cartilage or other skeletal repair.

Prior to analysis, a robust and reproducible technique for bone marrow harvest from the femoral canal needed to be developed.

3.3 Null Hypothesis

Skeletal stem cells cannot be enriched from human bone marrow aspirate from an elderly population, using a combination of acoustic vibration and vacuum-assisted filtration.

3.4 Materials & Methods

Patient selection

Volunteers from haematologically normal patients undergoing primary THR were selected. Exclusion criteria were history of Paget's disease of bone, malignancy, clotting disorders, osteogenesis imperfecta, rheumatoid arthritis, avascular necrosis of the femoral head, long term bisphosphonate or glucocorticoid therapy, known transmissible disease (e.g. hepatitis, HIV, malaria) or sickle cell disease, to avoid any confounding effects these conditions may have on cellular activity.

Patients provided fully informed consent after being provided with a lay summary of the trial, together with a verbal explanation and an opportunity for questioning. Ethical approval of the study was obtained locally (LREC194/99/1) and regionally (Research Ethics Committee 09/H0505/5). Medicines and Healthcare products Regulatory Agency (MHRA) registration was sought but unnecessary at this stage as the device was not being used for therapeutic intervention.

Operation of the device

2-5ml of fresh heparinised bone marrow aspirate (BMA) was set aside as unprocessed control (UC) for analysis of BMA prior to processing via acoustic agitation and vacuum-assisted filtration. The remaining volume was recorded and passed through a 70μm pore-size pre-filter to capture any adipocytes, magakaryocytes and particulate material (**Fig.2A**). The filtrate was then placed into the processing chamber on the second filter (3.5μm pore-

size, 20µm thick, $4x10^5$pores/cm^2) and a resonant frequency wave was passed through the saline reservoir, agitating the filter and BMA above it (**Fig.2B**). Filters were manufactured by a track etching process (it4ip s.a., Belgium). Application of acoustic vibration was by a voice-coil (model RM-ETNC0033K19C-2KOI, NXT Technology, Cambridge, UK) which produced a geometric standing waveform pattern on the aspirate fluid surface (**Fig.2B**). The frequency was manually adjusted as the volume reduced, in order to maintain a standing wave and cell agitation. Vacuum pressure was produced with a 6V miniature diaphragm pump (Kage KPV14A-GA, Taiwan).

Figure 2: A: Particulate material and fat captured on the 70µm pore-size pre-filter. B: Geometric standing wave created on BMA in the processing chamber, preventing clogging of the 3.5µm pores.

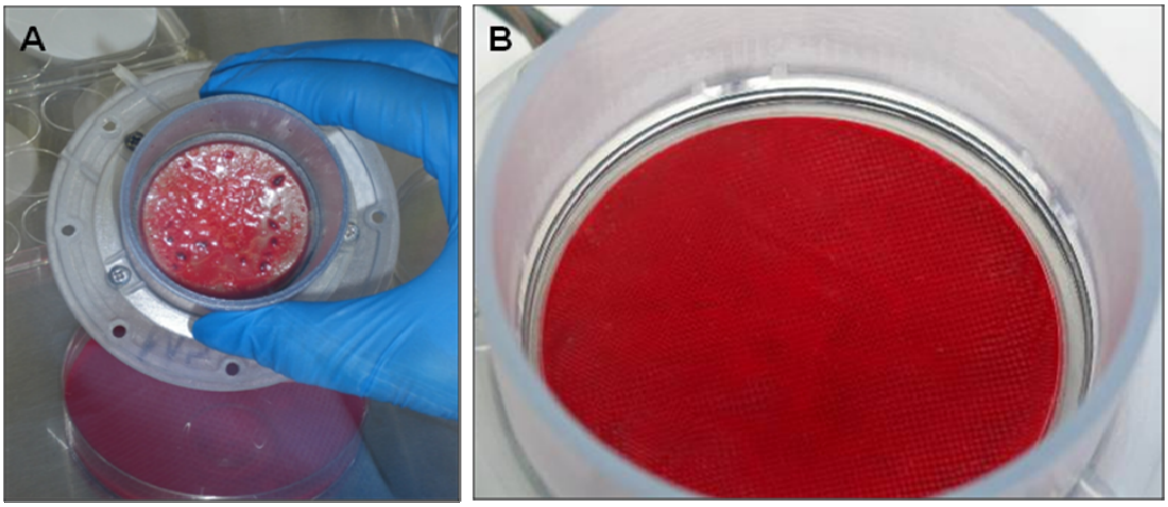

Filtration of BMA without acoustic vibration was observed to rapidly clog the filter pores due to the high cell concentration of BMA (Ridgway 10). A vacuum pressure (25psi) was applied from below the filter, with the aim of preferentially removing the smaller cells (erythrocytes (5-8µm) and platelets (1-3µm)), whilst retaining the nucleated cell fraction within the processing chamber. Following sufficient volume reduction, the final volume was recorded and removed as processed aspirate (PA). In clinical practice this could be seeded on scaffolds or allograft, but for this study both PA and UC were taken for analysis of cell number and viability, detailed below. The accousic-vibration and vacuum-assisted filtration process is illustrated schematically in **Figure 3**.

Figure 3: Schematic of processing stages of the device, followed by application of the concentrated nucleated cell fraction onto allograft. This can be viewed via the following web-link for a motion schematic: http://www.som.soton.ac.uk/research/dohad/groups/bone/awards.asp

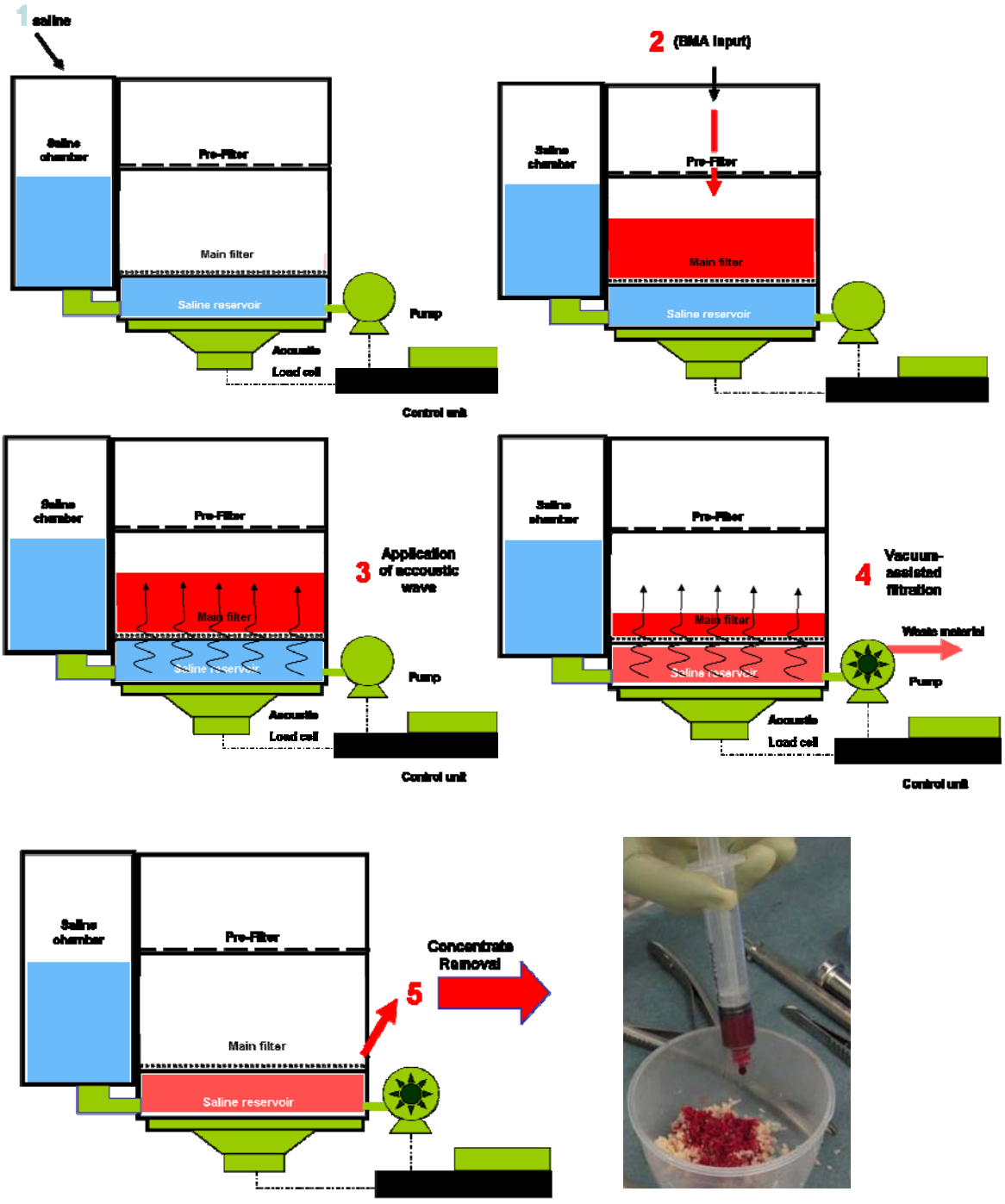

Processing time

Processing was stopped either after a 4.0 fold volume concentration was achieved, or when flow through the filter ceased. Start and end time-points were recorded for each sample processed.

Standard bone marrow harvest technique from the femoral canal

Isolation of skeletal stem cells from human bone marrow for *in vitro* experimentation can be performed by collection of waste material from the femoral canal during THR surgery. During THR surgery, the hip joint is dissected and a femoral neck osteotomy is performed (**Fig.4A-B**). The surgeon prepares the medullary canal of the femur for implantation of the femoral prosthesis. Cavitation of the canal is by box chisel, curettage and reaming in the standard fashion (**Fig.4C**) and the excavated tissue discarded. For consented patients, the waste tissue can be collected and placed into a sterile container containing 5,000IU heparin in 5ml normal saline.

Figure 4: A: Operating theatre set-up for a right THR. B: Oscillating sagittal saw used to perform a standard femoral neck osteotomy. C: Pin-reamer for cavitation of the femoral canal with waste tissue being collected with a spoon and placed into a sterile heparinised container. D: By comparison, percutaneous iliac crest bone marrow aspiration, produced a fluid blood-like marrow.

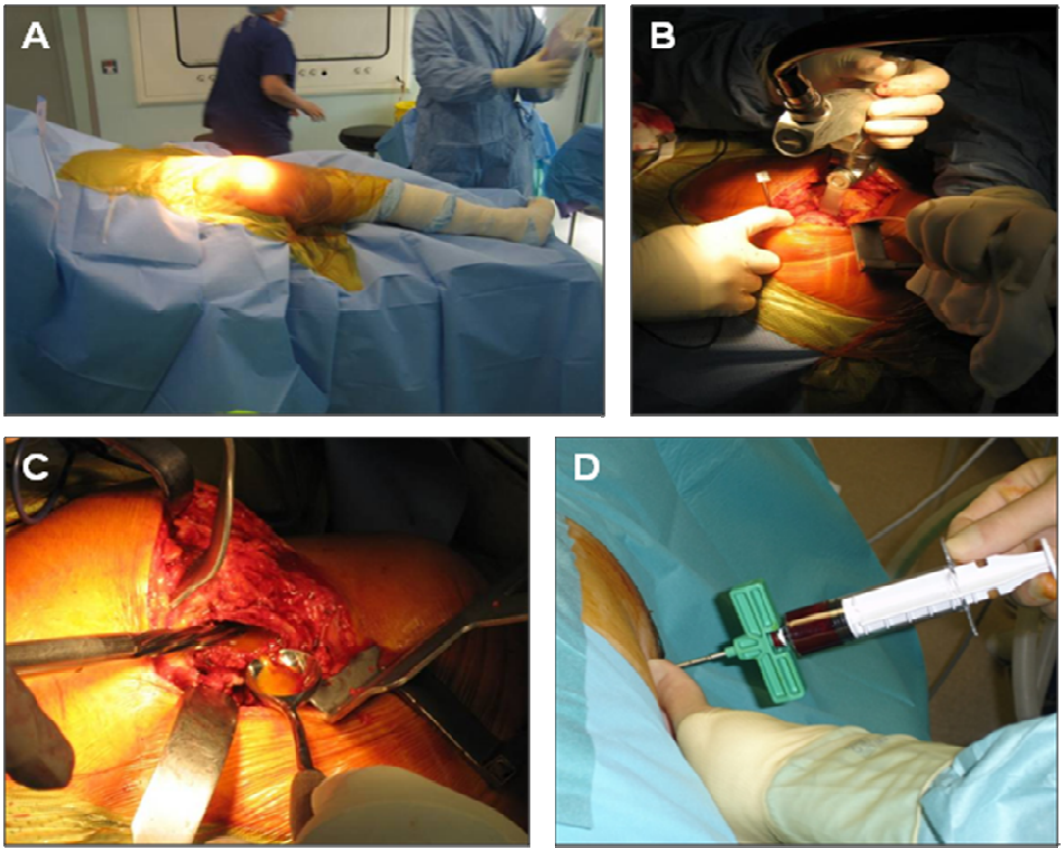

For analysis in this study and processing in the prototype device, the liquid component of the collected waste tissue was aspirated from the sterile container through a bone marrow aspiration needle. The fatty viscous bone marrow that was harvested by this technique (**Fig.4C**) had a distinctly different consistency to fresh bone marrow aspirated from the iliac crest (**Fig.4D**). It was predicted that processing problems may be encountered with this femoral canal tissue so alternative techniques were explored to harvest marrow from the femoral canal, within the confines of established ethical approval, yet mimicking iliac crest bone marrow aspiration.

Adapted techniques for bone marrow harvest from the femoral canal

Each technique was trialled from multiple patients to exclude individual patient variation as a factor.

a. Yankauer sucker: Suction of the femoral canal during THR is a standard technique to dry the medullary canal prior to cementing. A collection tube was attached to the Yankauer sucker (**Fig.5A**) to catch waste material in this fashion rather than via a spoon (**Fig.4C**).
b. Genos Boost needle aspiration from the femoral canal: a commercially available fenestrated bone marrow aspiration needle (Genos Boost needle, Smith & Nephew, UK) was used to aspirate directly from the open prepared femoral canal.
c. Aspiration prior to femoral canal preparation: the Genos Boost needle was inserted into the cancellous bone surface of the femoral neck osteotomy prior to any canal preparation (**Fig.5B**).
d. Aspiration prior to femoral neck osteotomy: the Genos Boost needle was placed through cortical bone of the femoral neck into the cancellous bone of the proximal femur (**Fig.5C**). The entry point was proximal to the level of the neck cut, therefore in waste tissue only.
e. Aspiration prior to soft tissue release from the femur: following dissection of fascia lata but prior to release of the small external rotators of the hip, the Genos Boost needle was passed through small external rotator muscles onto the femoral neck cortex, proximal to the pending neck osteotomy (**Fig.5D**).

Prior to aspiration of bone marrow through the Genos Boost needle, a 20ml Luer lock syringe containing 5000IU heparin in 5ml normal saline was prepared and the needle was flushed with heparin. Bone marrow was aspirated into the heparinised syringe then transferred to a sterile universal container for transport from the operating theatre to laboratory for processing. The marrow tissue that was harvested from each of these techniques, and the standard method of bone marrow waste tissue harvest, was trialled in the device. It was hypothesised that the viscous consistency may be a consequence of clot formation, so selected samples were fixed in formalin and stained for fibrin using trichrome stain MSB, along with a positive control (human placenta).

Figure 5: A: Intra-operative suction of femoral canal marrow through a Yankauer sucker. B: Aspiration from the osteotomised femoral neck. C: Needle puncture of cortical bone into femoral neck waste tissue, pre-osteotomy. D. Aspiration of liquid marrow from the proximal femur, with a consistency comparable to iliac crest BMA (D).

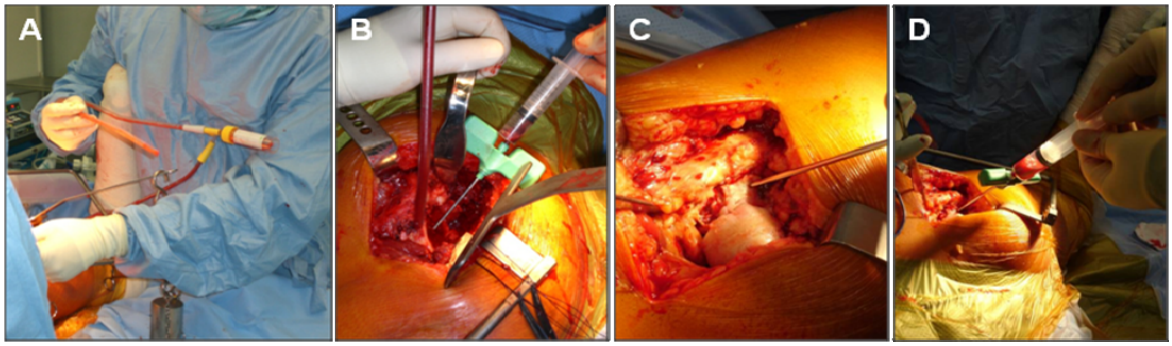

Analysis of cell viability

Upon successful development of a robust and reproducible method for harvest of marrow from the femoral canal that was comparable to iliac crest BMA, marrow was processed using the acoustic-vibration vacuum-assisted filtration technology. Cell viability analysis of UC and PA was performed using Guava Easycyte flow cytometry (Guava Technologies, Massachusets, USA) to measure any toxic effect that the processing technique may have.

Nucleated cell count and cell viability analysis

Nucleated cell counts of unprocessed control (UC) and processed aspirate (PA) were determined on 16 samples using Guava Easycyte flow cytometry and confirmed by manual count on a haemocytometer. Guava Viacount Reagent was used to differentiate live and dead cells, and the viable cell count value was used in all calculations. Statistical analysis was performed using Excel and SPSS Ver.18.

CFU-F analysis

Fibroblast colony forming unit (CFU-F) assay was used as an indicator of SSC number present in the aspirate pre- and post- processing through the device, and was performed on 9 samples. Following determination of viable nucleated cell count using Guava Easycyte flow cytometry, UC and PA samples were seeded in T25 culture flasks (n=3) according to the Friedenstein protocol for density independent growth (Bianco & Robey 2004). Briefly, aspirates were diluted in basal media to achieve clonal seeding densities of $1x10^4$ and $1x10^5$ nucleated cells/ml, and seeded at 25ml/cm^2. After three hours tissue culture, plates were washed twice with phosphate buffered saline (PBS) to remove non-adhered cells and returned to culture at 37˚C and 4% CO_2 for fourteen days. Following fixation in 95% ethanol, colony number was counted and the CFU-F/ml value for each aspirate was calculated by factoring in the dilution used to achieve the seeding density. Parallel assays of like-for-like volumes of UC and PA were also performed for illustration of the differences in CFU-F concentration.

Analysis of iliac crest BMA from a single patient

One patient undergoing primary THR (haematologically normal 78 year old) underwent therapeutic aspiration of bone marrow from the iliac crest to seed onto the uncemented acetabular cup (Ohgushi *et al.* 2005). Excess unused iliac crest BMA provided the opportunity to perform a direct comparison of the ability to process iliac crest BMA from an elderly patient to the iliac crest BMA that had been processed successfully from young healthy volunteers (Ridgway *et al.* 2010). This patient also consented to participate in the study, allowing comparison of iliac crest BMA and femoral canal BMA from the same patient (n=1). These samples were processed through the device and analysed as described above.

3.5 Results

Observations on consistency of bone marrow tissue

Bone marrow waste material harvested from the femoral canal, using the technique illustrated in **Figure 4C**, had variable consistency. Early attempts at processing through the device failed, due to an apparent viscous nature of the sample and the presence of bone fragments. Trichrome staining indicated negligible fibrin in the heparinised bone marrow sample (**Fig.6B**) in comparison to the positive control (**Fig.6A**). Multiple microscopic bone chips were visualised, but with an absence of clumping of cells. This result indicated that heparinisation was successful and that clotting was not a cause of the viscous consistency inhibiting filtration of the marrow samples.

Figure 6: A: Trichrome stain showed an abundance of fibrin in the human placenta positive control (A), but negligible evidence of fibrin in the heparinised marrow (B).

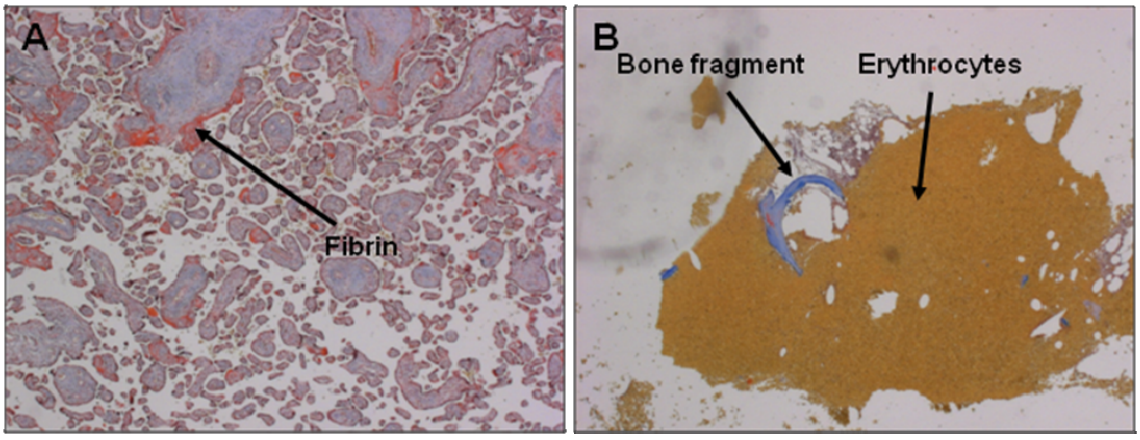

All attempts at aspiration of the liquid component from the sterile container (**Fig.7A**), or filtration through the 70μm pore-size pre-filter (**Fig.7B**), failed as a consequence of blockage with bone chips or the material being too viscous. Despite removal of all macroscopic bone fragments (**Fig.7C**), the sample remained highly viscous (**Fig.7D**) and unprocessable through the device. Initial efforts were therefore focused on resolving this difference, and adapting the harvest technique to mimic the sample produced by percutaneous iliac crest aspiration (**Fig.4D**).

Figure 7A: Attempted aspiration of the liquid component of marrow failed due to the high viscosity encountered. B: Passage through a 70µm cell strainer was not possible. C: Macroscopic bone chips and fragments removed from a marrow sample harvested from the femoral canal. D: The remaining liquid portion, revealing the gelatinous nature of the aspirate that prevented filtration.

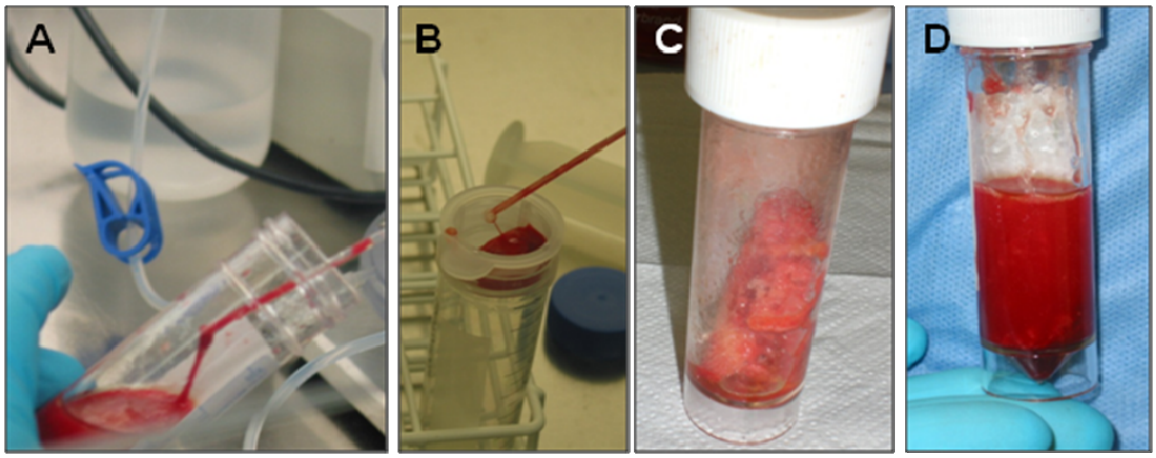

Adapted techniques for bone marrow harvest from the femoral canal

a. Yankauer sucker: due to the patulous opening of the sucker end, this yielded mostly air, low volumes of marrow and many loose bone chips.
b. Genos Boost needle aspiration from the femoral canal: whilst excluding the larger bone chips, this yielded low volumes of marrow, significant numbers of small bone chips and mostly air. The larger bone chips repeatedly blocked the end of the needle, preventing aspiration.
c. Aspiration prior to femoral canal preparation: there were no loose bone chips to obstruct or contaminate the aspirate, but this technique yielded mainly air which was sucked through the open porous trabecular bone from the surface of the femoral neck cut in preference to liquid bone marrow from the medulla.
d. Aspiration prior to femoral neck osteotomy: this technique produced liquid marrow but it was difficult to maintain a seal at the needle bone puncture site, allowing air to pass into the bone around the side of the needle and be aspirated preferentially to marrow.
e. Aspiration prior to soft tissue release from the femur: this technique closely mimicked percutaneous bone marrow aspiration, with the cortical bone puncture site covered by a soft tissue envelope. Liquid bone marrow aspirate with the consistency of blood was reliably and reproducibly harvested by this technique (**Fig.8**), and was able to be processed through the device in an identical fashion to iliac crest BMA.

Figure 8: Successful aspiration of bone marrow from the femoral neck prior to release of the small external rotators of the hip. This technique closely mimicked percutaneous bone marrow aspiration and reliably produced liquid bone marrow that could be processed through the filtration device.

In order to assess the utility of the prototype device for robust and rapid intra-operative processing of human BMA, samples from a range of donors were aspirated from femoral canals during THR surgery.

Analysis of unprocessed control (UC) and processed aspirate (PA)

16 samples aspirated using the technique of needle aspiration through the intact femoral neck, illustrated in **Figure 8**, were successfully processed through the device, after which further analysis was performed. These constituted 5 male and 11 female patients, with an average age of 72 years (range 55-89). All samples were analysed for cell number and viability, and nine samples were cultured for CFU-F analysis. No difference was observed between sexes.

A mean reduction in volume of 3.9 fold was achieved with an average processing time of 18.3 minutes (range 7-28 minutes). Corresponding viable nucleated cell count was increased by 3.1 fold from UC to PA. CFU-F analysis was performed on 9 of these samples (**Fig.9**). CFU-F numbers were enriched from a mean of 267 CFU-F/ml in UC to 920 CFU-F/ml in PA, with a mean 3.7 fold increase (**Table 1**).

Table 1: Fold concentration of processed BMA by volume, by nucleated cell count and by CFU-F are reported from 16 femoral canal BMA samples processed by the device. Corresponding viable cell percentage (%) is shown. Mean and standard deviations (S.D.) are recorded at the foot of the table.

Sample ID	Age / years	Fold conc by volume	Fold conc by nucleated cells	Fold conc by CFU-F	% viable cells in PA
1	82	4.63	4.19	n/a	87.9
2	69	2.18	1.98	n/a	97.9
3	61	2.00	1.96	n/a	97.5
4	67	3.00	2.57	n/a	90.6
5	59	4.57	4.27	n/a	93.4
6	78	2.55	1.72	n/a	76.0
7	55	4.00	3.95	n/a	92.3
8	70	5.16	3.50	3.52	94.4
9	77	2.40	1.99	1.99	93.4
10	78	4.30	2.53	1.87	97.8
11	71	4.66	3.35	3.79	94.7
12	75	5.50	4.37	5.39	97.9
13	89	6.00	3.89	4.30	97.5
14	78	4.00	4.64	3.48	97.7
15	82	4.00	2.09	5.28	98.4
16	68	4.00	3.33	3.86	99.6
Mean	**72**	**3.9**	**3.1**	**3.7**	**94.2**
S.D	**9.17**	**1.20**	**1.02**	**1.23**	**5.83**

Figure 9: CFU-F number was increased following processing, with multiple colonies visible in the culture of processed aspirate (top row) compared to unprocessed control (bottom row). Aspirates were seeded at comparable volumes for illustration, photographed here, but calculation of CFU-F number was performed from analysis of cultures at clonal seeding densities to exclude the effect of density dependent growth.

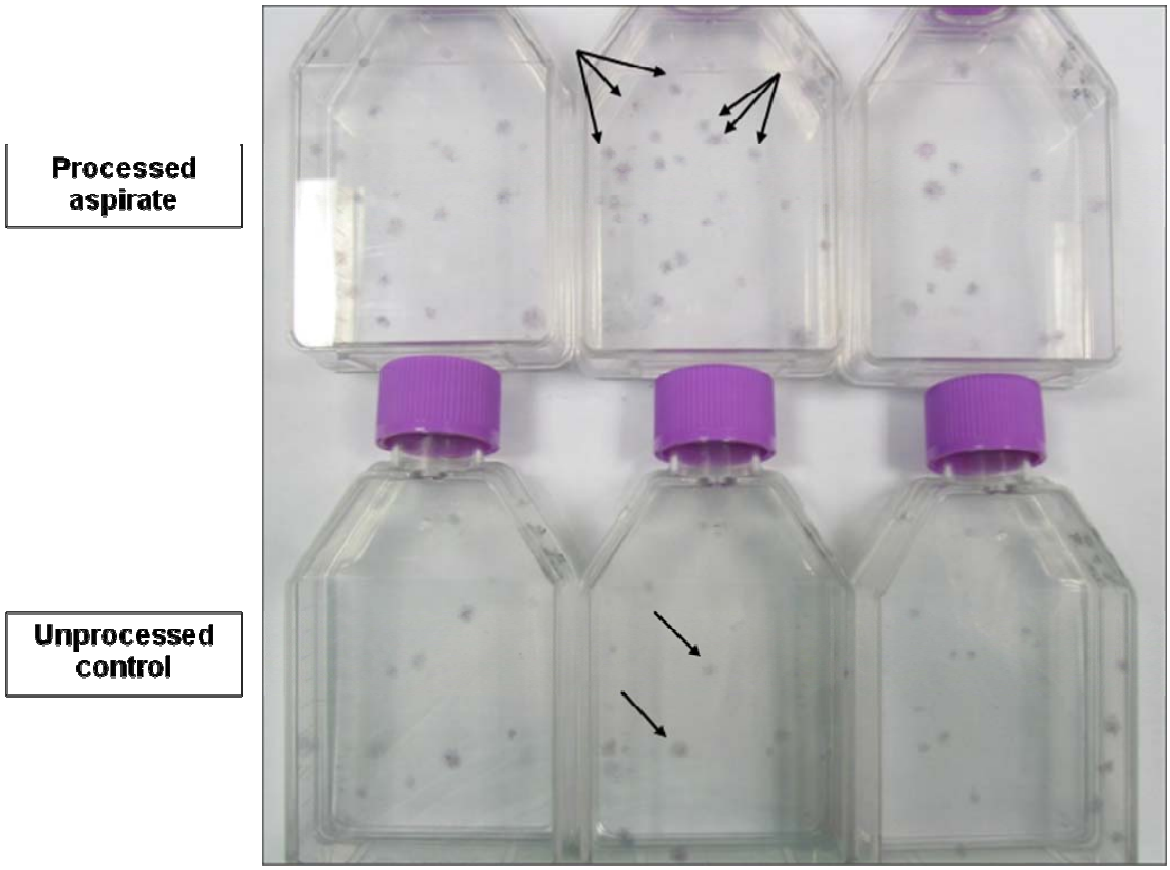

The scatter graph (**Fig.10**) illustrates the relationship between fold concentration by volume against nucleated cell count (blue) and CFU-F (purple), both of which show corresponding enrichment to volume reduction. Cell viability (red) demonstrated no loss of viable cell content with volume reduction during the vacuum-assisted accoustic-filtration enrichment process. Mean cell viability in PA was 94.2%, confirming the vacuum-assisted acoustic-filtration process did not result in damage of the nucleated cells.

Figure 10: Scatter graph of fold concentration by nucleated cells (blue) and CFU-F (purple), plotted against volume fold concentration. % cell viability (red) remained unaffected by the cell enrichment process.

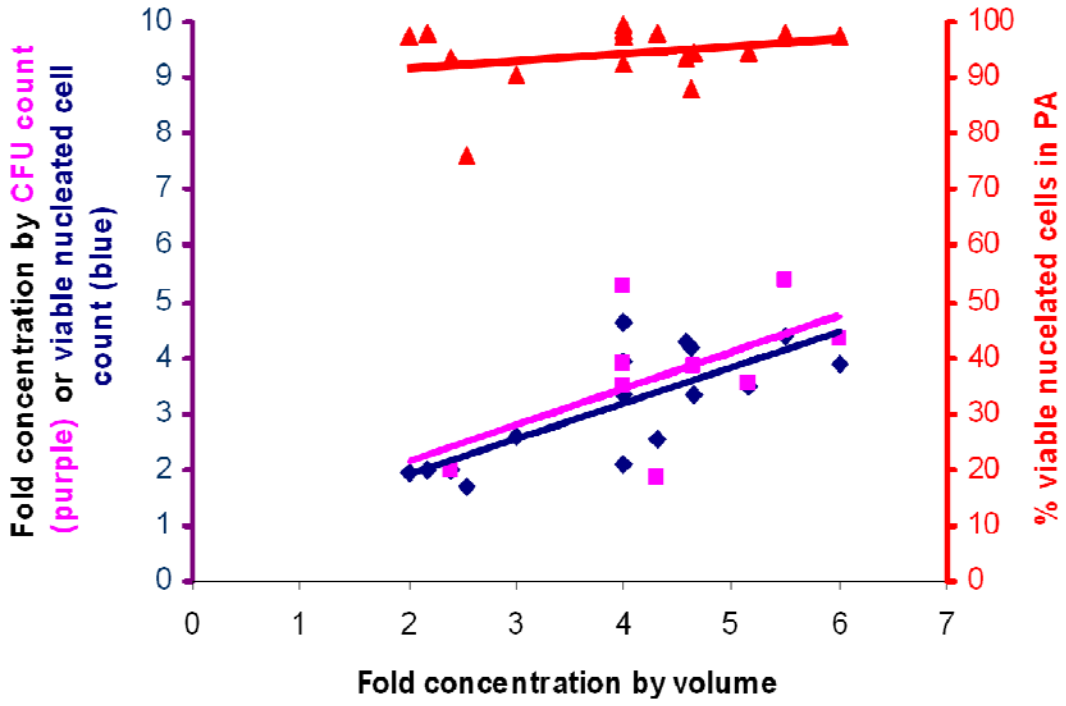

A large range in the CFU-F number in the unprocessed BMA was noted (40-826 CFU-F/ml), and whilst the highest CFU-F was found in a younger patient (Patient 16, 68 year old male), age had only a weak correlation with CFU-F (Pearson's correlation co-efficient r = 0.27). Age (range 55 to 89 years) did not correlate with any differences in ability for cell enrichment of the processed aspirate. Age to nucleated cell enrichment and to CFU-F enrichment provided low Pearson's correlation co-efficient values of r = -0.02 and r = 0.14 respectively.

Comparison of femoral canal v iliac crest BMA from a 78 year old patient

Iliac crest BMA from a 78 year old patient was successfully processed, with a 4.0 fold reduction in volume (14.0ml to 3.5ml) and cell enrichment (**Table 2**). Prior to this study, all previous samples that had been successfully processed were from individuals under 25 years of age obtained from commercial sources (Ridgway *et al.* 2010). Bone mineral content decreases with age and some authors believe this is related to decreased osteoblast numbers in bone marrow (Muschler *et al.* 2001). Concern that age-related effects on BMA

had been the cause of the difficulties in processing samples was alleviated by the successful processing and enrichment of this sample from the iliac crest of a 78 year old patient.

Direct comparison could be made on this iliac crest aspirate to bone marrow aspirated from the patient's proximal femur. Both samples were enriched to a four fold reduction in volume, with high viable cell counts following processing (**Table 2**).

Table 2: Comparison of fold concentration and viable cell percentage (%) from iliac crest and femoral canal BMA from the same patient, a 78 year old female.

	Fold conc. by volume	***Fold conc. by nucleated cell count***	***Fold conc. by CFU-F***	***% viable cells in PA***
Iliac crest	4.0	3.47	4.37	99.4
Femoral canal	4.3	2.53	1.86	97.8

The concentrating efficiency of cells appeared to be greater from the iliac crest BMA (4.37 fold for iliac *versus* 1.87 fold for femoral by CFU-F assay). However starting volumes of femoral canal BMA were greater than iliac crest BMA (28ml v 14ml respectively), so may have been contaminated with venous blood (Muschler, Boehm, & Easley 1997), restricting adherence of colony forming cells in the CFU-F culture from femoral BMA.

Therapeutic bone marrow aspiration resulting in excess iliac crest aspirate is a rare occurrence, so this comparison between femoral and iliac crest aspirate could only be performed on a single patient. Therefore results must be treated with caution. However the ability of femoral BMA to be processed by the device in a comparable way to iliac crest BMA has validated its use in this study, and is supported in the literature (Sagi *et al.* 2009;Cox *et al.* 2010).

3.6 Discussion

The aim of this chapter was to study the ability of a novel cell filtration technique to process and enrich BMA from a cohort of elderly patients, examining its suitability for clinical application. Given the demographics of an ageing population, there is a pressing need for additional reconstructive strategies and tissue engineering techniques to be translated to clinical practice. The preliminary work by Smith & Nephew UK (Ridgway *et al.* 2010) provided promising results on function of the device and cell enrichment, but all marrow samples used were from the iliac crest of young healthy volunteers. The technique of bone marrow aspiration from the iliac crest carries associated morbidity, thus for this pre-clinical phase of the trial in the elderly cohort of patients it was necessary to obtain bone marrow from an alternative source. Harvest of waste bone marrow from the femoral canal during THR provided an alternative benign source of aspirate, but the consistency was grossly different from iliac crest aspirates. Initial efforts therefore focused on defining a technique to harvest BMA from the femur that was comparable to the blood-like BMA from the iliac crest, such that it could be processed through the vacuum-assisted acoustic filtration technology. On successful development of the robust and reproducible technique, analysis of the processed femoral canal BMA was possible.

This study demonstrated effective volume reduction in BMA from the femoral canal of a cohort of elderly patients, achieving a mean volume reduction of 3.9 fold. Corresponding enrichment of SSC number was 3.1, as measured by viable nucleated cell count, and 3.7, as measured by CFU-F assay (**Table 1**), demonstrating this device to be effective in the intended function of SSC enrichment. Furthermore, the average processing time of 18 minutes proved the viability and practicality for intra-operative clinical application of the device.

Cell enrichment was assessed by two methods, nucleated cell count and CFU-F assay. The results correlated well with each other for all samples, with the exception of one outlier (Patient 15, 82 years old). The BMA from this patient showed discrepancy between fold concentration by CFU-F (5.28 fold) and by nucleated cell count (2.09 fold). This outlier may have been as a result of erythrocytes interfering with CFU-F culture of the unprocessed control (Stenderup 01), Guava Easycyte error, cell death or miscalculation in seeding volumes for CFU-F culture.

There was a wide variation of CFU-F/ml from the aspirated marrow of this cohort of patients (40-826 CFU-F/ml), though interestingly, a wide range was also seen in the young cohort previously tested (710-1440 CFU-F/ml, unpublished data). This may explain the variable outcomes seen in clinical practice, and why seven of Hernigou's tibial non-unions had low CFU-F counts even after concentration by centrifugation (Hernigou *et al.* 2005a). Initial SSC number in BMA from this cohort of elderly patients had a mean of 267 CFU-F/ml, which was significantly lower than the suggested therapeutic threshold of 1000 CFU-F/ml suggested by Hernigou and colleagues. Enrichment of CFU-F by 3.7 fold increased the mean value in processed aspirate (PA) to 920 CFU-F/ml.

CFU-F/ml values in BMA from the cohort of elderly patients in this study were lower than those found in the young cohort previously tested (267 v 600 CFU-F/ml) (Ridgway *et al.* 2010). A phenomenon of age-related decline in CFU-F number with age has been suggested by some authors (McLain *et al.* 2005;Muschler *et al.* 2001), though reported results have not been statistically significant. Other studies have demonstrated maintenance of SSC number and function with ageing, including in osteoarthritic and osteoporotic bone (D'Ippolito *et al.* 1999;Stenderup *et al.* 2001;Oreffo *et al.* 1998;Oreffo, Bord, & Triffitt 1998). Analysis in this study of age compared to nucleated cell count or CFU-F/ml of unprocessed BMA showed only a weak correlation in this group of 16 patients (r=0.27). The narrow age range and patient number limited the power of statistical correlation, and these results were from femoral canal BMA whilst the young patients' marrow was from iliac crest. Different skeletal sites may influence the composition of bone marrow (Stenderup *et al.* 2001;McLain *et al.* 2005) although comparable CFU-F numbers have been demonstrated within femoral canal and iliac crest marrow (Cox *et al.* 2010;Sagi *et al.* 2009). Nevertheless, clinical indication for this bone tissue engineering technology would be most applicable in the elderly population, and whilst questions remain regarding the effect of ageing on SSCs and bone marrow, it was necessary to trial the ability for processing and cell enrichment of marrow from a cohort of elderly patients.

The low CFU-F number found in this cohort of elderly patients highlights the need for cell enrichment strategies in clinical practice. This study has demonstrated that this novel technology has the capability to successfully enrich SSCs from aspirated bone marrow in elderly as well as young patients. The novel technology within this device is highly

differentiated from current leading technologies and could have a major role in clinical use, particularly as bone tissue engineering strategies become more commonplace.

Further work will involve the processing of BMA from more patients for exploration of SSC number and viability to empower the statistical analysis detailed in this chapter. Subsequent studies are planned regarding analysis of SSC surface markers (Stro-1, CD105, CD146) by Guava Easycyte flow cytometry, multi-lineage differentiation cultures, the osteogenic capacity of processed aspirates when seeded onto allograft and synthetic scaffolds, and *in vivo* small and large animal work.

Chapter IV
A Tale of Two Cysts

It was the best of times, it was the worst of times, it was the age of wisdom, it was the age of foolishness, it was the epoch of belief, it was the epoch of incredulity, it was the season of Light, it was the season of Darkness, it was the spring of hope, it was the winter of despair. From 'A Tale of Two Cities' by Charles Dickens (1812-1870).

PART 1: Retrieval analysis of tissue engineered bone within a non-ossifying fibroma of the femoral neck

The surgery was performed by Mr Douglas Dunlop, to whom I am grateful for harvesting the tissue and for fruitful discussions and guidance. Dr Stuart Lanham performed the μCT scans and analysis, the mechanical testing was performed with the assistance of Dr Adam Briscoe.

PART 2: Exploring the pathogenesis of unicameral bone cysts

With thanks to Mr Edward Gent and Miss Caroline Edwards, Southampton General Hospital Dept of Paediatric Orthopaedics, for providing the aspirated samples from unicameral bone cysts, Dr Paul Noakes for cytokine analysis and Dr Darren Fowler for analysis of the cyst lining. The production of the EM images and slide preparation of the cyst lining by Sue Cox, Electron Microscopist in the Biomedical Imaging Unit, is gratefully acknowledged.

PART I: Retrieval analysis of tissue engineered bone within a non-ossifying fibroma of the femoral neck

4.1.1 Introduction

Benign lesions of the proximal femur are common and treatments include curettage, void filling and mechanical stabilisation (Roposch, Saraph, & Linhart 2004). As a novel tissue engineering strategy for void filling, impaction bone grafting (IBG) can be combined with osteoprogenitor cells to produce a 3D living composite with significant mechanical and biological potential (Tilley *et al.* 2006).

IBG provides a solid mantle with which to fill a bone defect. It has been used as a void-filler in revision hip surgery for over forty years (Slooff *et al.* 1984) with some excellent long-term results (Schreurs *et al.* 2004;Halliday *et al.* 2003). Although remodelling of the impacted graft has been demonstrated on histological specimens from acetabular and femoral IBG, areas of non-incorporated graft with associated necrosis, fibrocartilage and fibrosis remain in all specimens (van Haaren *et al.* 2007;van der Donk *et al.* 2002;Ling, Timperley, & Linder 1993).

Skeletal stem cells (SSCs) can be combined with IBG to augment the biological and mechanical characteristics of the graft. The cells have been shown to survive the impaction process, proliferate and differentiate down the osteoblastic pathway (Bolland *et al.* 2006;Korda *et al.* 2006;Korda *et al.* 2008). Human bone marrow is a source of SSCs and the combination of these cells with IBG as a tissue engineering technique was used in the treatment of a proximal femoral cyst in 2006 (Tilley *et al.* 2006). Whilst this heralded translation of a bone tissue engineering technique to humans, it has subsequently been established that enhanced concentration of the SSC fraction is required in order for the aspirate to be therapeutic (Hernigou *et al.* 2005a). The patient has had recurrence of symptoms which has required a total hip replacement (THR). This has, however, afforded the rare opportunity for *ex vivo* analysis of clinically applied human tissue engineered bone.

Case history

A 62 year old male had a one year history of right hip pain attributable to a non-ossifying fibroma of his femoral neck **(Fig.1A)**. Due to progressive pain and the risk of impending fracture, surgical intervention was undertaken. As previously described (Tilley *et al.* 2006), milled allograft was prepared from fresh frozen femoral heads, bone marrow was aspirated from the iliac crest and the two were mixed. A channel was drilled into the femoral neck and cystic bone was removed by curettage. The bone marrow seeded milled allograft was impacted retrograde into the channel using a 12mm diameter Xchange tube saw (Stryker, Newbury, UK). Post-operatively the patient had complete resolution of symptoms. However, in time the cyst recurred **(Fig.1B)** and at four years following this surgery a THR was required **(Fig.1C)**.

Figure 1: A: Pre-operative radiograph of the well-circumscribed non-ossifying fibroma in the right femoral neck. B: Radiograph at 3 years post-operatively showing a channel of impacted bone but recurrence of the cyst. C: Radiograph following right THR.

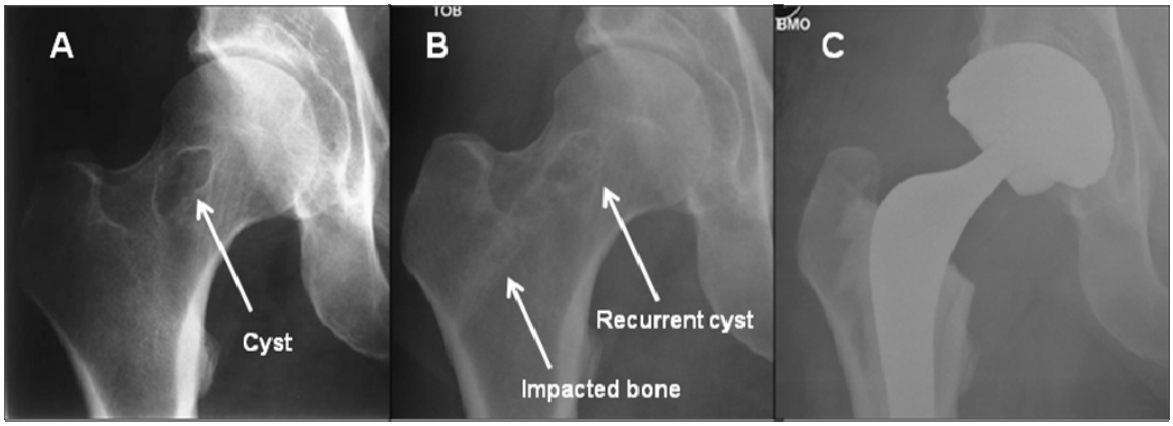

4.1.2 Materials & Methods

Retrieval of specimens

At THR, the femoral head was removed by standard neck osteotomy. A 15mm diameter cylinder incorporating the impacted channel of bone was excised from the inter-trochanteric region of the femur, distal to the surgical neck osteotomy, prior to preparation for the THR stem. A 1cm thick section of the mid-portion of the femoral head containing the proximal aspect of the cyst was retained for diagnostic purposes. The remaining head and neck specimens were retrieved, photographed and fixed in 4% paraformaldehyde (PFA) prior to further *ex vivo* analysis.

Micro computed tomography (μCT)

The retrieved femoral head sample was scanned using an Xtek Benchtop 160Xi scanner (Xtek Systems Ltd, Tring, UK) equipped with a Hamamatsu C7943 x-ray flat panel sensor (Hamamatsu Photonics, Welwyn Garden City, UK). Scan resolution was up to 74micron, at 150kV, 60μA using a molybdenum target with an exposure time of 534 ms and 4x digital gain. Reconstructed volume images and Grey Scale density were analysed using VGStudio Max 1.2.1 software (Volume Graphics GmbH, Heidelberg, Germany).

Histology

For histological analysis of impacted and normal trabecular bone, representative sections were taken from the femoral head neck, avoiding the residual cystic area **(Fig.2, Sections '1' and '3' respectively)**. Cyst tissue was excised and processed in an identical fashion **(Fig.2, Section '5')**. Specimens were de-calcified in 0.1M TRIS / 5%EDTA solution at pH7.3 and verified by Faxitron MX-20 micro X-ray (Faxitron X-ray, Wheeling, IL, USA). After wax embedding, mounting and processing through graded ethanols, 7μm thick sections were cut and stained with Alcian Blue / Sirius Red (A/S) or tartrate resistant acid phosphatase (TRAP). Microscope images were recorded using Carl Zeiss Axiovision software Ver 3.0 via an AxioCam HR digital camera on an Axiovert 200 inverted microscope (Carl Zeiss Ltd, Welwyn Garden City, UK), under white and polarised light.

Mechanical testing

Sections of trabecular, cortical and impacted bone were excised from each specimen for comparison of mechanical strength. As described above, these sections were taken from the femoral neck region to avoid incorporating residual cyst pathology **(Fig.2)**. There was sufficient material to harvest two representative sections of each tissue type. Bone cuboid sections (6x7x4mm) were prepared using a low-speed diamond-tipped wafering blade (Buehler, Coventry, UK) and tested to failure by compression with a hydraulic actuator (Instron Ltd, High Wycombe, UK). A compressive force was applied at a constant rate of 4.8mm over 60 seconds (0.08mm/s), from which stress-strain graphs were plotted and mechanical strength calculated. In order to represent the forces sustained *in vivo*, the direction of force applied was always in the orientation of the trabecular stress lines of the femoral neck. Statistical comparison of the six samples, two of each bone type, was performed using One-way ANOVA.

Figure 2: Schematic identifying the sections of the femur retrieved for analysis. A section of the femoral head was sent for diagnostic histology and the remaining retrieval tissue was fixed in 4%PFA and scanned by μCT. Sections were then excised and processed for histology and mechanical testing, as shown. 1 = impacted bone for histology; 2 = impacted bone for mechanical testing; 3 = normal trabecular bone for histology; 4 = normal trabecular bone for mechanical testing; 5 = cystic tissue for histology; 6 = normal cortical bone for mechanical testing.

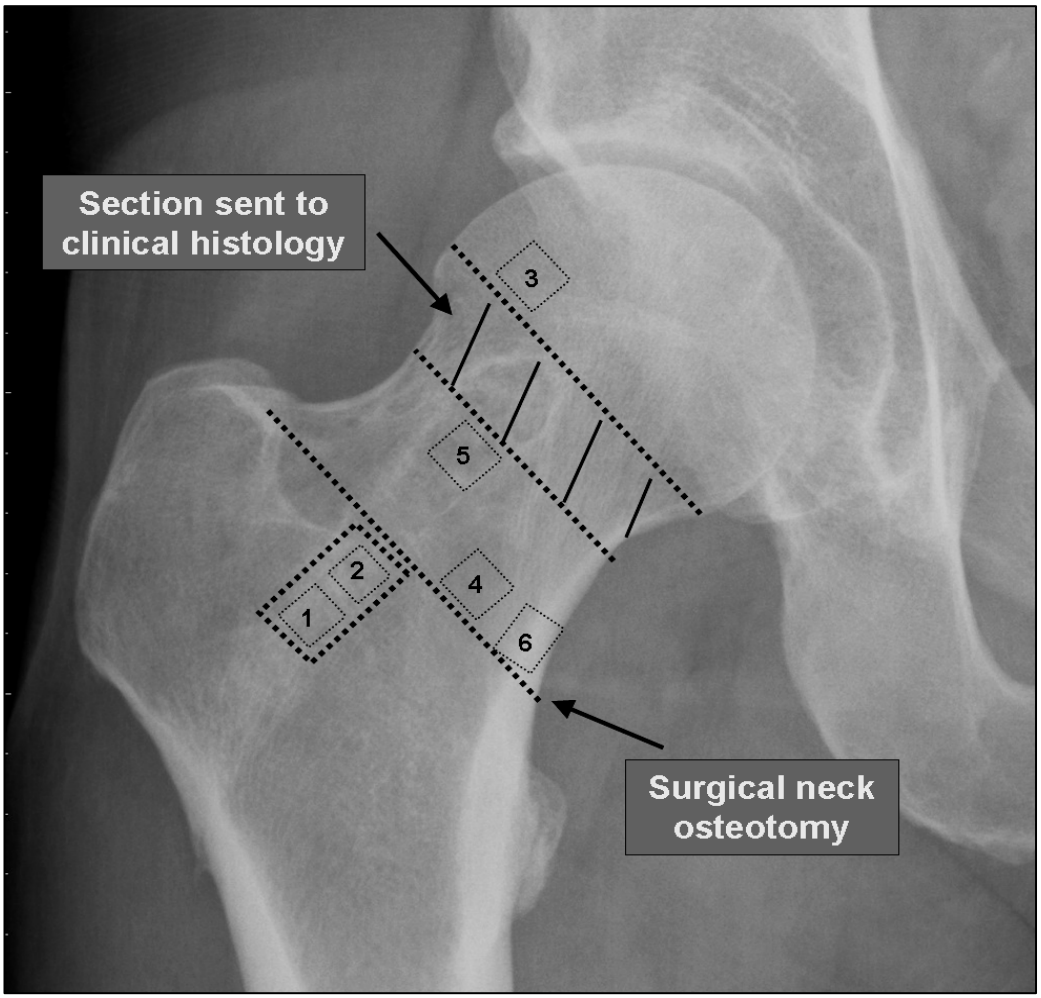

4.1.3 Results

Macroscopic analysis

Review of the cut surfaces of the femoral head and neck confirmed that the cyst had returned and migrated distally into the channel of impacted bone **(Fig.3A-B)**. However the segment of impacted bone retrieved from the inter-trochanteric region in the femur, distal to the surgical neck osteotomy, appeared to contain trabecular bone without cyst material **(Fig.3C)**.

Figure 3: A: Cranio-caudal view of the femoral head showed recurrence of the cyst. B: Caudo-cranial view of the surgical neck osteotomy showed penetration of the cyst to this level. C: Section taken from impacted channel of bone in the proximal femur (distal to the surgical neck osteotomy) showed compact trabecular bone without cyst material.

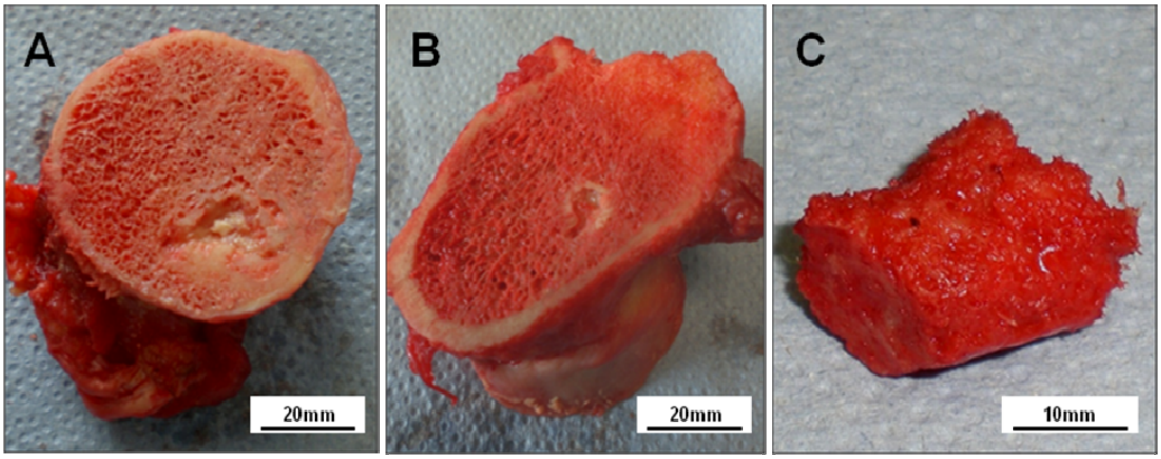

Micro computed tomography (µCT)

Analysis by µCT confirmed that the cyst had recurred and migrated, visualised clearly in 3D reconstruction **(Fig.4A)** and coronal section and axial slices through the neck **(Fig.4B-C)**. There was no calcified material nor remnant of allograft detected in this region, indicating an active resorptive process. However µCT analysis of the impacted bone distal to the cyst confirmed the macroscopic findings of a compact trabecular bone structure **(Fig.4D)**.

Figure 4: µCT images. A: 3D reconstruction, with 1cm section absent (sent to clinical histology). B: Coronal view of the femoral neck. C: Axial slice through the femoral head and proximal cyst. D: 3D reconstruction of cylinder of impacted bone taken from distal to the surgical neck osteotomy. Trabecular architecture is evident with the trabeculae in continuity.

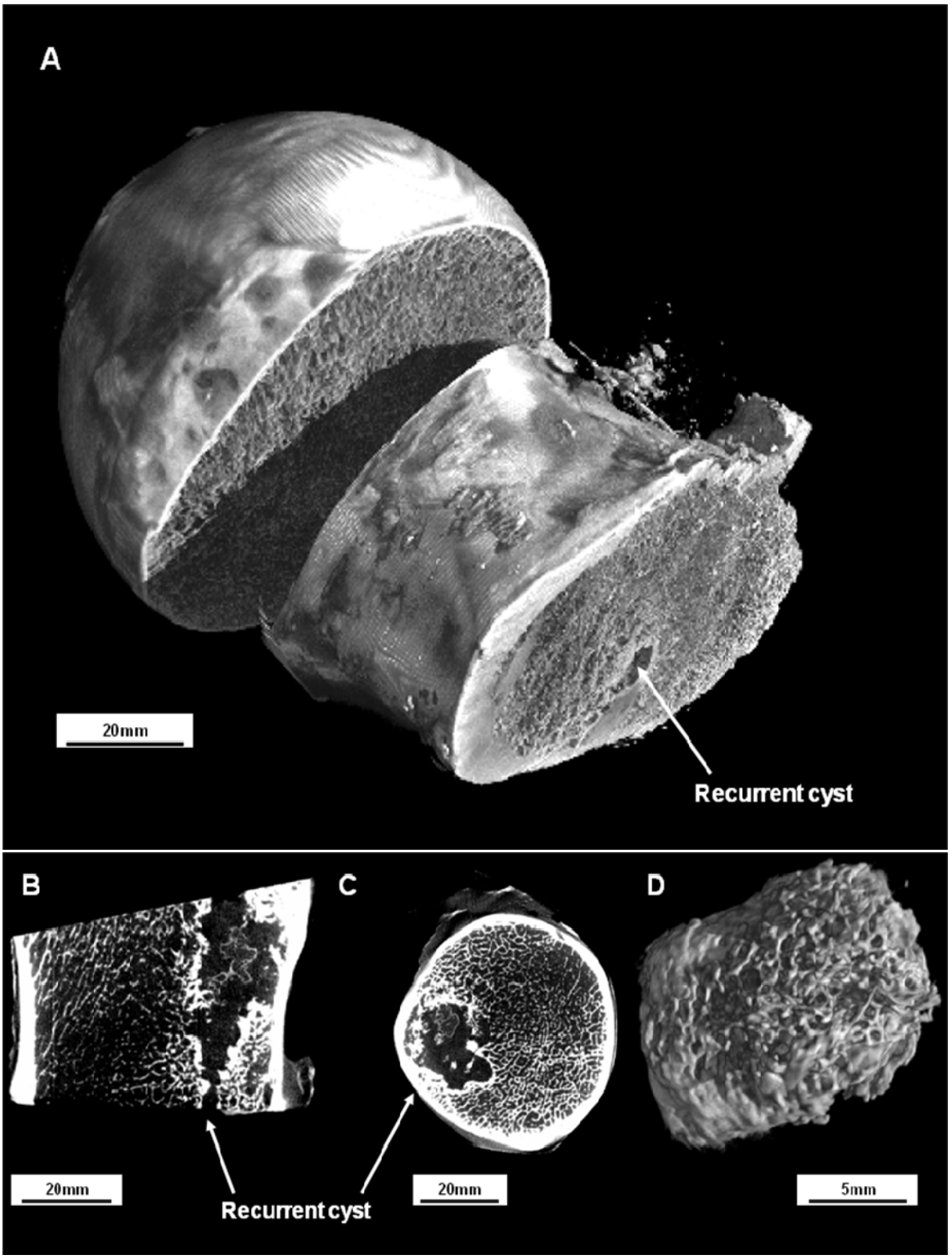

Apparent bone density for trabecular, cortical and impacted bone was determined by calculation of Grey Scale on μCT images **(Fig.5)**. As expected, density of cortical bone was greater than trabecular bone (3200 *versus* 1000 Grey Scale units). The density of the impacted channel of bone was bi-modal **(Fig.5B)**, with the main peak corresponding to trabecular bone (1200 units) and a second denser peak (2800 units) which could represent either the closely packed arrangement of trabecular bone (illustrated in **Figure 4D**), or non-incorporated cortical fragments from the original milled femoral head allograft, shown below in **Figure 6A**.

Histological analysis

Clinical diagnostic laboratory analysis confirmed this to be a benign lesion. A/S staining of tissue from the impacted channel of bone in the retrieved femoral head displayed some trabecular bone structure, osteocytes within lacunae and a lamellar micro-architecture **(Fig.6A)** comparable to that seen in normal trabecular bone **(Fig.6B)**. Birefringence confirmed the presence of mature organised bone structure within the impacted bone **(Fig.6D)**, comparable to normal trabecular bone **(Fig.6E).** However there were islands of non-incorporated allograft visible throughout the impacted bone **(Fig.6A, arrows)**, which under polarised light showed limited organisation of collagen fibres **(Fig.6D, arrows)**. This microscopic arrangement was grossly different from tissue within the recurrent cyst, which contained necrotic and fibrotic tissue within a mixture of cartilage, fibrous tissue and bone **(Fig.6C)**, with negligible evidence of organisation on birefringence **(Fig.6F)**. TRAP stain revealed osteoclasts concentrated on islands of non-incorporated graft in the impacted bone **(Fig.6G)**. No osteoclasts were observed on the sections of normal trabecular bone **(Fig.6H)** although this may be due to the limited sample size. The cystic tissue showed eroded bone and a high number of osteoclasts throughout **(Fig.6J)**.

Fig 5: Density analysis of µCT scans. A: Colour schematic. Yellow = 500-2000 Grey Scale units; Red = 2001-3500 units; Blue >3500 units. The corresponding graph (B) shows density peaks of trabecular (blue) and cortical (pink) bone at 1000 and 3200 units respectively, compared to the bimodal peaks of impacted bone (turquoise) at 1200 units with the smaller peak at 2800 units.

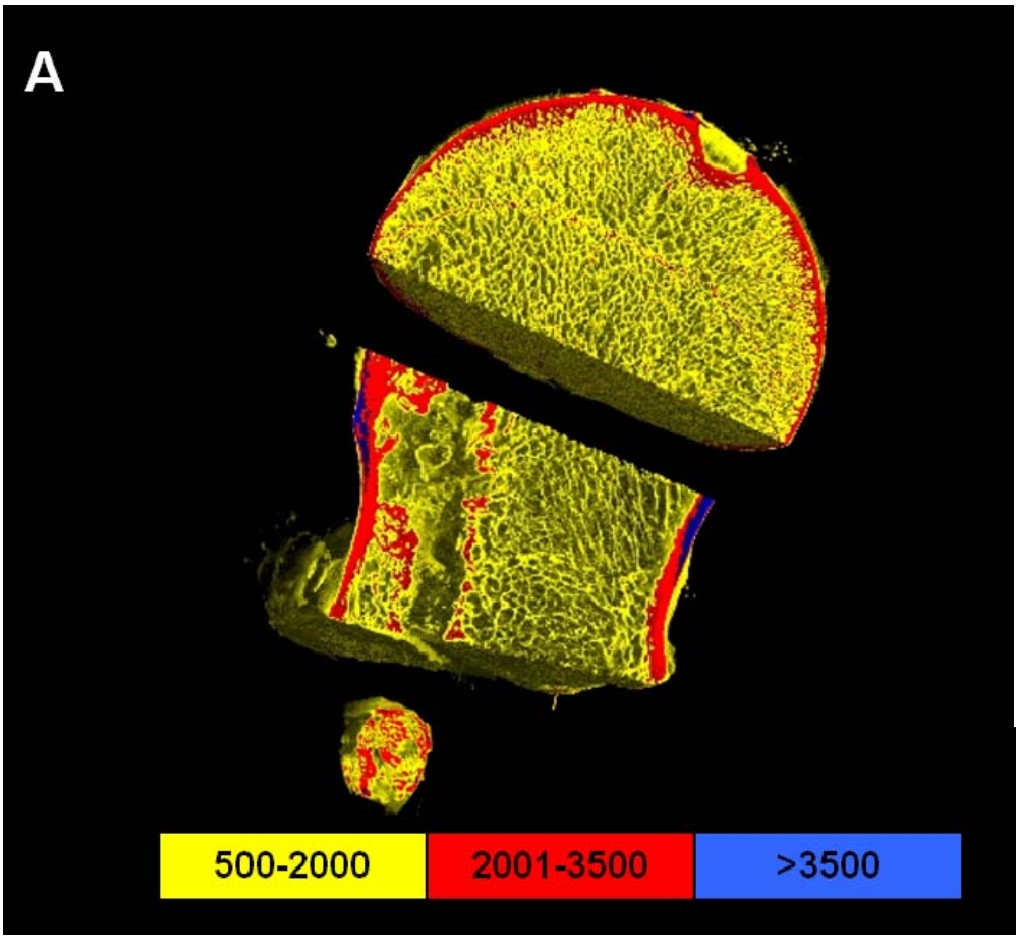

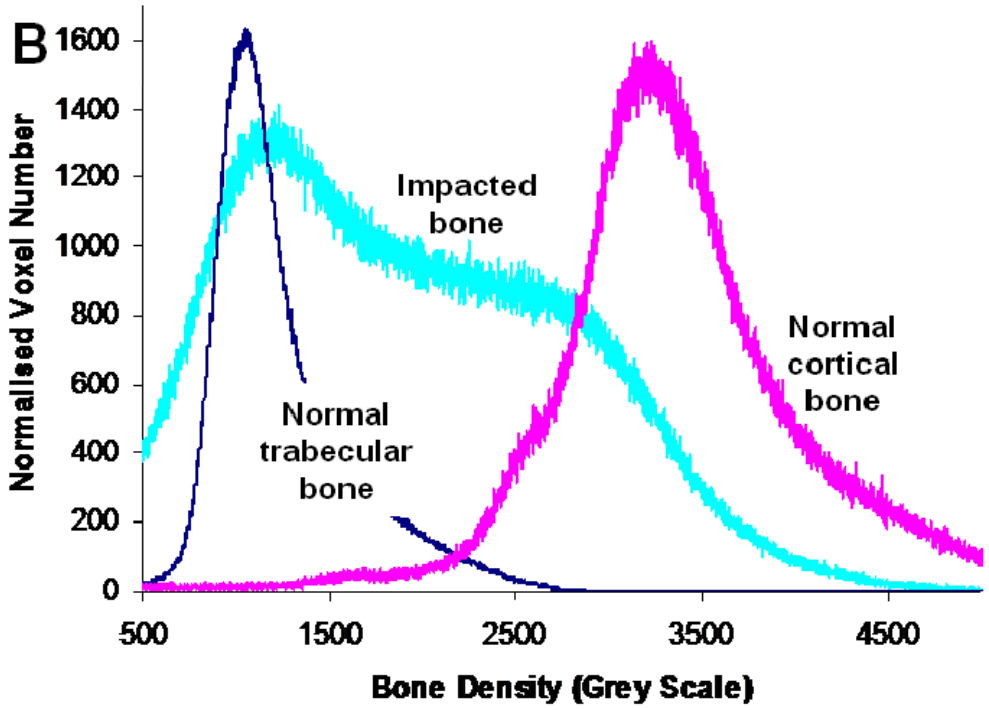

Figure 6: Histology; A/S stain revealed a mature bone structure in both impacted bone (A) and normal trabecular bone (B), however islands of non-incorporated graft were evident within the impacted bone (A, arrows). Necrosis, fibrosis and non-incorporated graft were present throughout the cystic tissue (C). Parallel birefringence showed organised collagen fibres in impacted (D) and normal trabecular bone (E), indicative of mature bone, but negligible evidence of organisation within the non-incorporated allograft (D, arrow) or cystic tissue (F). TRAP stain showed osteoclasts concentrated on the non-incorporated allograft within impacted bone (G, arrows). No osteoclasts were observed on normal trabecular bone surfaces (H), but were in higher concentration in cystic tissue (J). Scale bars: A,B,D,E = 200µm, C,F,G,H,J = 100µm.

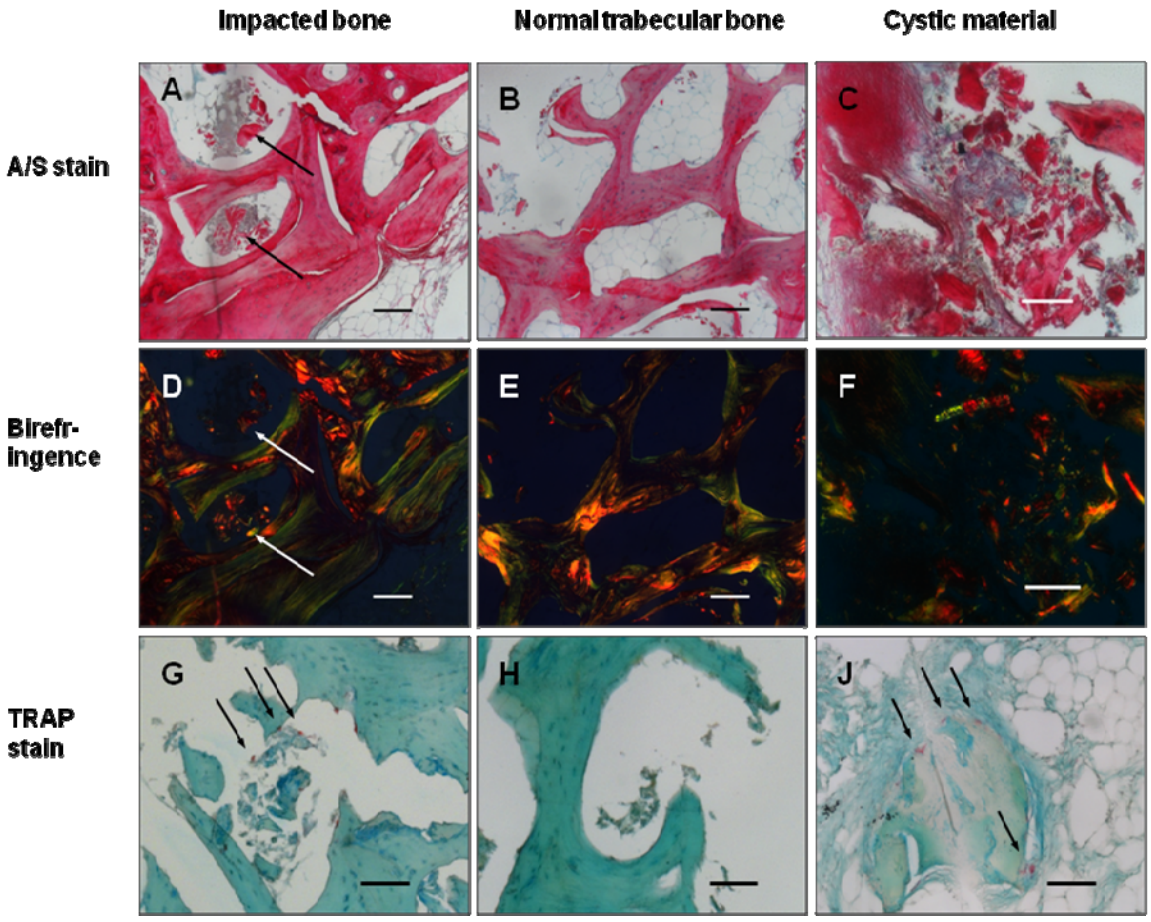

Mechanical testing

Cortical bone was stronger in axial compression than both trabecular and impacted bone. The six samples, two of each bone type, demonstrated statistical difference between the compressive strength of trabecular or impacted bone compared to cortical bone, using One-way ANOVA ($p<0.0001$) yet, critically, no statistical difference between the strengths of trabecular and impacted bone were observed ($p>0.05$). Significance was confirmed on Bonferroni Multiple Analysis ($p<0.05$) (**Fig.7**).

Figure 7: Bar chart demonstrating compressive strengths (MPa) of trabecular, impacted and cortical bone (n=2). One-way ANOVA test demonstrated statistical difference between trabecular and cortical bone ($p<0.0001$), but no statistical difference between trabecular and impacted bone. Error bars denote Standard Error of Mean, 'ns' = no statistical significance.

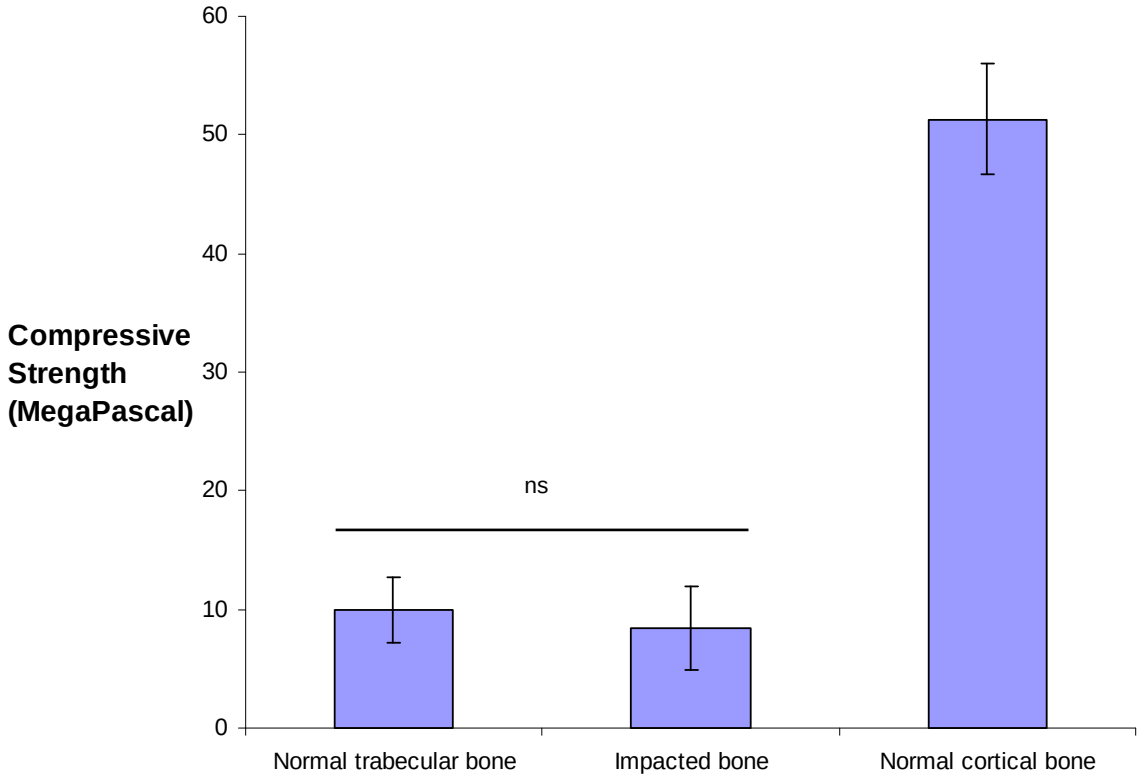

4.1.4 Discussion

This tissue engineered impaction bone graft construct retrieved from a human patient has provided a rare opportunity for *ex vivo* analysis. The trabecular architecture visualized within the impacted channel of bone on μCT **(Fig.4D)** combined with similar strength characteristics of impacted and trabecular bone demonstrated on mechanical testing **(Fig.7)** were evidence of some remodelling of the milled allograft. Histology provided further evidence of mature bone formation, but there were associated islands of non-incorporated allograft fragments **(Fig.6B,E)**. This is in keeping with previous histological studies performed on IBG specimens retrieved from acetabula and femora (van Haaren *et al.* 2007;van der Donk *et al.* 2002;Ling, Timperley, & Linder 1993), though these cases had not been supplemented with autologous bone marrow.

Work since the original studies has now established that osteoprogenitor cell number and concentration are important for augmentation of osteogenesis. It has been postulated that a threshold of 1000 osteoprogenitors / ml are required for bone marrow to be therapeutic (Hernigou *et al.* 2005a;Hernigou *et al.* 2005b). At the time of this patient's initial operation, the bone marrow aspirate yielded $4x10^5$ nucleated cells / ml, and parallel *in vitro* analysis revealed 2.18 CFU-F / 10^6 nucleated cells (Tilley *et al.* 2006). This approximates thirty CFU-F's within the 34ml of bone marrow that was applied, though erythrocytes in the marrow may have restricted adherence of colony forming cells giving a falsely low CFU-F count (Stenderup *et al.* 2001). While extensive *in vitro* and *in vivo* work has demonstrated that SSCs survive the impaction process and augment bone regeneration / osteogenesis (Bolland *et al.* 2006;Korda *et al.* 2006;Korda *et al.* 2008;Arthur, Zannettino, & Gronthos 2009), techniques to concentrate or culture-expand osteoprogenitor cells from fresh bone marrow aspirate will be important to achieve a therapeutic concentration (Hernigou *et al.* 2005a;Gronthos & Zannettino 2008;McCarty *et al.* 2009).

In the current study osteoprogenitor cell number appears to have been insufficient for biological augmentation of the graft, with islands of non-incorporated graft remaining (**Fig.6A**). Cyst recurrence may have been compounded by insufficient curettage of all cyst material, with subsequent osteoclast recruitment. The increased osteoclast numbers within the cyst tissue **(Fig.6J)**, combined with macroscopic and μCT findings of a paucity of calcified tissue in this region **(Fig.4A-C)** suggest an active resorptive / osteoclastic process associated with recurrence of cyst pathology.

The principles of tissue engineering have been successfully applied in this case, but concentration of autologous bone marrow now appears important for biological augmentation of allograft. Confidence can be drawn from the facile translation of this tissue engineering technique, and *ex vivo* analysis of this unique retrieval specimen has provided important lessons for bone tissue regeneration in clinical practice.

PART II: Exploring the pathogenesis of unicameral bone cysts

4.2.1 Introduction

Unicameral bone cysts (UBCs) are benign lesions of bone that are defined as minimally expansile lucent lesions consisting of a cavity filled with fluid and lined by a fibro-cellular membrane (Capanna, Campanacci, & Manfrini 1996). UBCs are typically found in the metaphyseal region of long bones of skeletally immature patients and resolve spontaneously with skeletal maturity. These cysts present with pain on weight bearing, pathological fracture or as an incidental finding on X-ray. Asymptomatic UBCs, judged to be low risk of fracture, can be treated conservatively. However due to the risk of pathological fracture, deformity, pain and long-term restriction from sporting activity until natural resolution at skeletal maturity, treatments to expedite the healing process are appealing.

Despite being recognised as a separate entity over a century ago (Bloodgood 1910) the pathogenesis of UBCs remains largely unknown. Theories presented in the literature include pressure effects from blockage of fluid drainage (COHEN 1960), local venous obstruction (Komiya *et al.* 2000;Chigira *et al.* 1983), increased lysosomal enzyme activity (Gerasimov *et al.* 1991), prostaglandins (Shindell *et al.* 1989), nitric oxide (Komiya *et al.* 2000), oxygen free radicals (Komiya *et al.* 1994), synovial origin (Mirra *et al.* 1978) and genetic causes (Vayego, De Conti, & Varella-Garcia 1996). As theories on the pathogenesis of UBCs have evolved, many treatments strategies have emerged. However theories have been based on analysis of single cases or small case series, thus targeted treatment remains difficult. Aspiration, curettage (COHEN 1977), autologous bone marrow injection (Docquier & Delloye 2003;Lokiec *et al.* 1996), steroid injections (Shindell *et al.* 1989;Scaglietti, Marchetti, & Bartolozzi 1979;Capanna *et al.* 1982), demineralised bone matrix (Rougraff & Kling 2002), grafting of synthetic materials, (Thawrani *et al.* 2009;Sponer & Urban 2004) and intramedullary fixation (Roposch, Saraph, & Linhart 2000;de Sanctis & Andreacchio 2006) are all used, though all have a high failure and /or recurrence rate of the cysts.

Much of the literature on the pathogenesis of UBCs has suggested a role for osteoclasts. Shindell et al have reported increased levels of PGE_2 in UBCs, and demonstrated a

reduction in levels following intra-lesional steroid injection associated with cyst resolution (Shindell *et al.* 1989). PGE_2 is a protein kinase A (PKA) mediated signal involved in the stimulation and proliferation of osetoclasts. Similarly, osteoclasts require lysosomal enzymes for bone resorption, and increased levels of these, together with collagen degradation products, have been demonstrated in UBCs, indicating on-going osteoclast-mediated bone destruction (Gerasimov *et al.* 1991). Increased acid phosphatase in UBCs, signifying increased osteoclast activity, has been demonstrated (Markovic, Cvijetic, & Karakasevic 1988) and osteoclast related bone resorptive factors have been demonstrated at increased levels in the cyst fluid and lining (Komiya *et al.* 2000). The presence of osteoclasts has been confirmed in the fibro-cellular lining of UBCs by histology (Komiya *et al.* 2000) and electron microscopy (Yu *et al.* 2005).

Complex signalling pathways exist between osteoclasts and osteoblasts, abnormalities of which result in a wide range of bone pathologies such as osteoporosis, osteopetrosis, Paget's disease, rheumatoid arthritis and peridontal disease (Suda *et al.* 1995;Kudo *et al.* 2003). Differentiation, fusion and activation of osteoclasts from macrophage-monocyte precursors is stimulated by factors derived from osteoblasts, notably RANK ligand (RANKL), so called because it binds to a receptor on osteoclast precursors called Receptor Activator of NFκB (RANK) (Oreffo *et al.* 2007). Cells expressing the osteoblast markers Stro-1 and RUNX-2 have been identified in the UBC fibro-cellular lining, and stromal cells within UBCs have been shown to induce osteoclastogenesis *in vitro* (Yu *et al.* 2005). Beyond this the role of osteoblasts in the pathogenesis of UBCs has not been explored. Furthermore, many of the abnormalities that have been identified in UBCs have been in the cyst fluid (Komiya *et al.* 1994;Komiya *et al.* 2000;Markovic, Cvijetic, & Karakasevic 1988;Gerasimov *et al.* 1991;Shindell *et al.* 1989), but any effect that the fluid itself contributes to UBC pathology has not been investigated.

4.2.2 Aims

This study aimed to explore the underlying pathophysiology of the unicameral bone cyst (UBC), focusing on the cyst fluid as a vehicle for formation or proliferation of the cyst, and specifically the effect of the fluid on osteogenesis.

4.2.3 Null Hypothesis

The fluid found within a unicameral bone cyst has no effect on skeletal stem cells nor osteogenesis.

4.2.4 Materials & Methods:

UBCs from two patients were analysed for this study. The use of human tissue was prospectively approved by the local regional ethics committee (LREC194/99/1) and full patient consent was obtained.

Case 1

A nine year old healthy male had a one year history of progressive pain in his right thigh and diagnosis of a UBC of the proximal femur was made on plain radiographs **(Fig.1A-B)**. Under general anaesthetic and fluoroscopic guidance, 20ml of straw coloured fluid was aspirated percutaneously from the cyst in the proximal femur (**Fig.1C**), prior to stabilisation with a flexible intra-medullary nail due to the risk of impending fracture **(Fig.1D)**.

Case 2

A six year old boy suffered a pathological fracture through a previously asymptomatic unicameral bone cyst of his proximal humerus. The fractured cortices progressed to bony union but the cyst remained, and required surgical stabilisation (**Fig.1E-F**). Intra-operatively 4ml of straw coloured fluid was aspirated percutaneously (**Fig.1G**), a window of bone and UBC membrane was excised from the medial wall, and the proximal humerus was stabilised with a flexible intra-medullary nail **(Fig.1H)**.

Figure 1: Radiographs of UBCs from Case 1 & 2: Pre-operative AP & lateral radiographs of Case 1 (A-B, proximal femur) and Case 2 (E-F, proximal humerus). Intra-operative fluoroscopy of percutaneous aspiration and cystogram, followed by stabilisation with flexible nailing of Case 1 (C-D) and Case 2 (G-H).

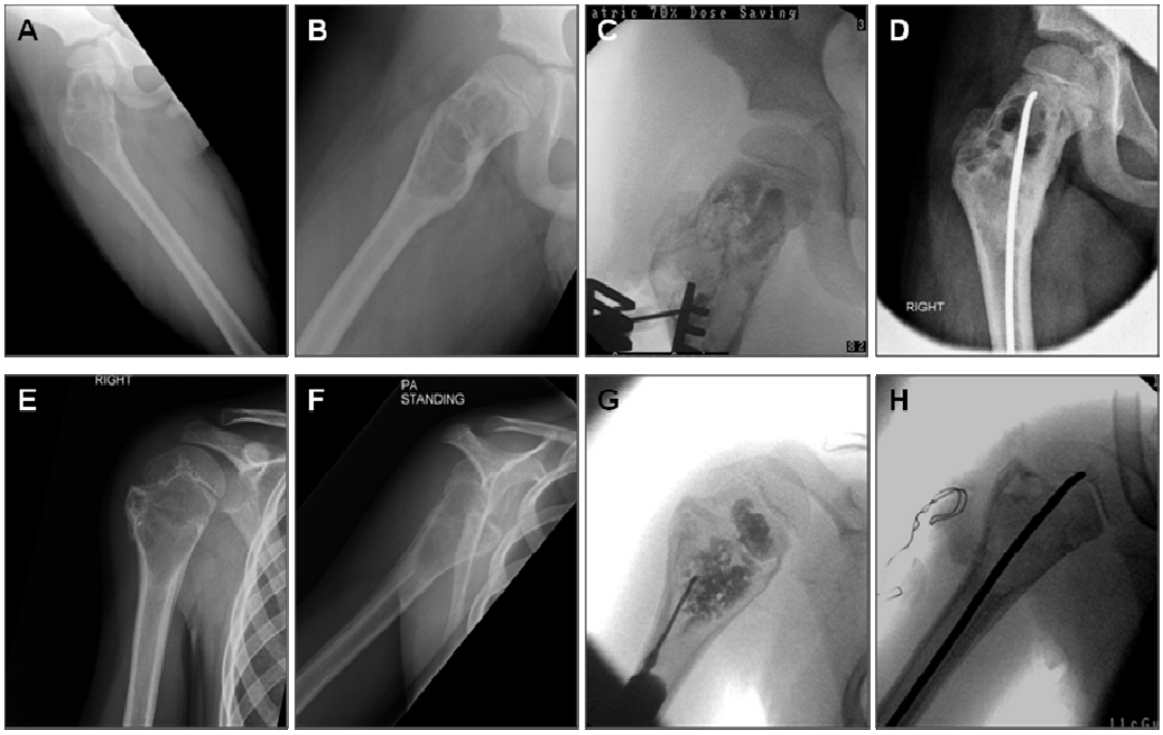

Scanning electron microscopy of fibro-cellular lining

Samples were fixed using 4% paraformaldehyde, and freeze dried. SEM analysis was performed using a JEOL JSM 6330F Scanning Electron Microscope (JEOL UK Ltd, Welwyn Garden city, UK) and an Oxford Instruments ISIS 300 system (Oxford Instruments, Abingdon, UK) was used to obtain Energy Dispersive X Ray Analysis (EDXA) data of the samples. Slides were dehydrated through graded ethanols, mounted in semi-thin sections and stained with toluidine blue for analysis of structural detail.

Cyst fluid separation

The aspirated samples were centrifuged at 1100rpm for four minutes at 21˚C to separate the cell pellet (**Fig.2A**). The supernatant was removed, providing the acellular fluid fraction which was used for further analysis (**Fig.2B**).

Analysis of protein, electrolytes, cytokines and pH of the cyst fluid

Cytokine levels in cyst fluid supernatant were assessed using a musculoskeletal Human Chemokine 6plex BMS813FF plate (Bender MedSystems, Vienna, Austria). This used

fluorescent bead immunoassay and flow cytometry to test for granulocyte colony stimulating factor (G-CSF), interferon-gamma (IFN-γ), interleukin (IL)-1β, IL-2, IL-4, IL-5, IL-6, IL-8, IL-10, IL-12p70, monocyte chemotactic protein (MCP)-1, monokine induced by gamma interferon (MIG), macrophage inflammatory protein (MIP)-1α, MIP-1β, tumour necrosis factor (TNF)-α and TNF-β. Protein and electrolyte levels were measured using a Beckman DXC Coulter Counter (Beckman Coulter Ltd, High Wycombe, UK) and pH was determined with a Microprocessor Bench pH Meter (Hanna Instruments, Bedfordshire, UK) and a pH indicator strip (VWR International Ltd, Poole, UK).

Skeletal stem cell culture in cyst fluid

Human bone marrow was obtained from haematologically normal adults undergoing routine total hip replacement surgery with the approval of the local ethics committee (LREC194/99/1). Adult skeletal stem cells (SSCs) were harvested by repeatedly washing the marrow in α-MEM, followed by centrifugation of the washed cell population. The cell pellet was resuspended in 10ml basal media, passed through a 70μm filter, plated onto tissue culture flasks and culture-expanded in basal media at 37ºC in 4% humidified CO_2. Every 3-4 days cells were washed in phosphate buffered saline (PBS) and the media changed. At 30% confluence the adult SSCs were released using trypsin in EDTA (ethylene diamine tetra-acetic acid), centrifuged, re-suspended in basal media and cell count was performed using a haemocytometer. The SSC solution was titrated to a concentration of $5x10^3$ SSCs per 100μl of basal media prior to seeding onto culture plates.

Graded concentrations of the acellular cyst fluid were prepared by mixing cyst fluid with α-MEM, as an inert control (**Fig.2C**). 100μl aliquots of graded cyst fluid / α-MEM mixes were added to 100μl aliquots of SSCs in basal media in culture wells of a 48 well plate. This provided 200μl of culture media / cyst fluid mixture containing $5x10^3$ SSCs for each well and cyst fluid concentrations of 0%, 25% and 50% (**Fig.4D**) (**Table 1**). Cultures were run for 72 hours in the central 24 wells of a 48 well plate, and 200μl of α-MEM was placed in all outer wells to prevent edge effects.

Figure 2: A: Centrifuged aspirate showing the separated cell pellet and supernatant. B: Acellular cyst fluid supernatant. C: Prepared aliquots of graded cyst fluid / α-MEM concentrations. D: 48 well culture plate containing graded cyst fluid / α-MEM mixes with basal media and $5x10^3$ SSCs in each well. The graded concentration are rows 2 to 4 progress from 0% cyst fluid to 25% and 50% cyst fluid – note the colour difference.

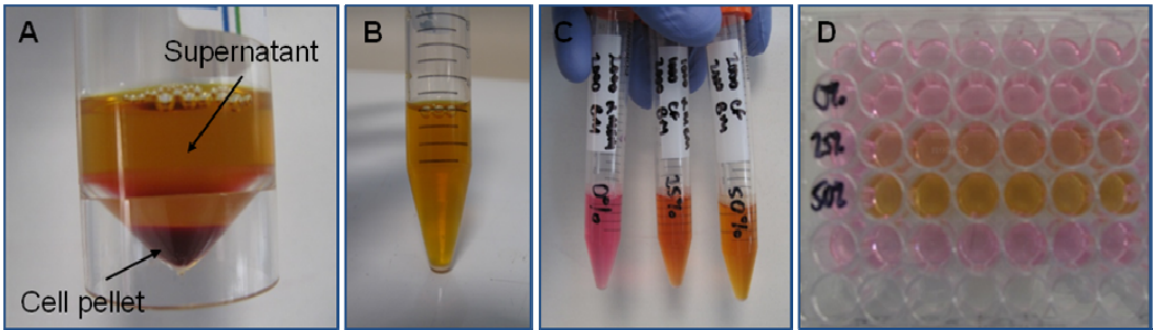

Table 1: The proportions of cyst fluid, α-MEM and basal media in each culture well, illustrating how the % value of cyst fluid was derived. For each category, n=12, and this was replicated for both cases.

% of cyst fluid in culture media	0%	25%	50%
Cell number	$5x10^3$	$5x10^3$	$5x10^3$
Cyst fluid volume / µl	0	50	100
α-MEM fluid volume / µl	100	50	0
Basal media volume / µl	100	100	100
Total media volume / µl	200	200	200

SSCs were cultured in 0-50% of cyst fluid / media concentrations from Patient 1 and 2 for 72 hours, as described above, with twelve identical wells prepared for each concentration of cyst fluid for each patient. Following 72 hours of culture, six wells of each fluid concentration from each case were fixed in 95% ethanol for 24 hours. The remaining six wells from each group had the cyst fluid removed at that time, cells were washed twice with phosphate buffered saline (PBS) to remove all traces of cyst fluid, then returned to culture with 200µl of plain basal media without cyst fluid. Cultures were run for a further five days until the SSCs reached confluence. At confluence cells were fixed in 95% ethanol for 24 hours, as described above, for analysis. The processing pathway is illustrated in **Figure 3**.

Figure 3: Flow diagram illustrating the processing and analysis of SSCs in graded cyst fluid concentrations. Cyst fluid from both patients was prepared identically, with three different concentrations of cyst fluid prepared, 0% (n=12), 25% (n=12) and 50% (n=12), for each patient. All culture wells contained $5x10^3$ SSCs and a total of 200µl of cyst fluid / culture media. Six wells from each group were fixed at 72 hours for analysis, and the remaining six had PBS washes, media changes and cultured in basal media without cyst fluid for a further five days.

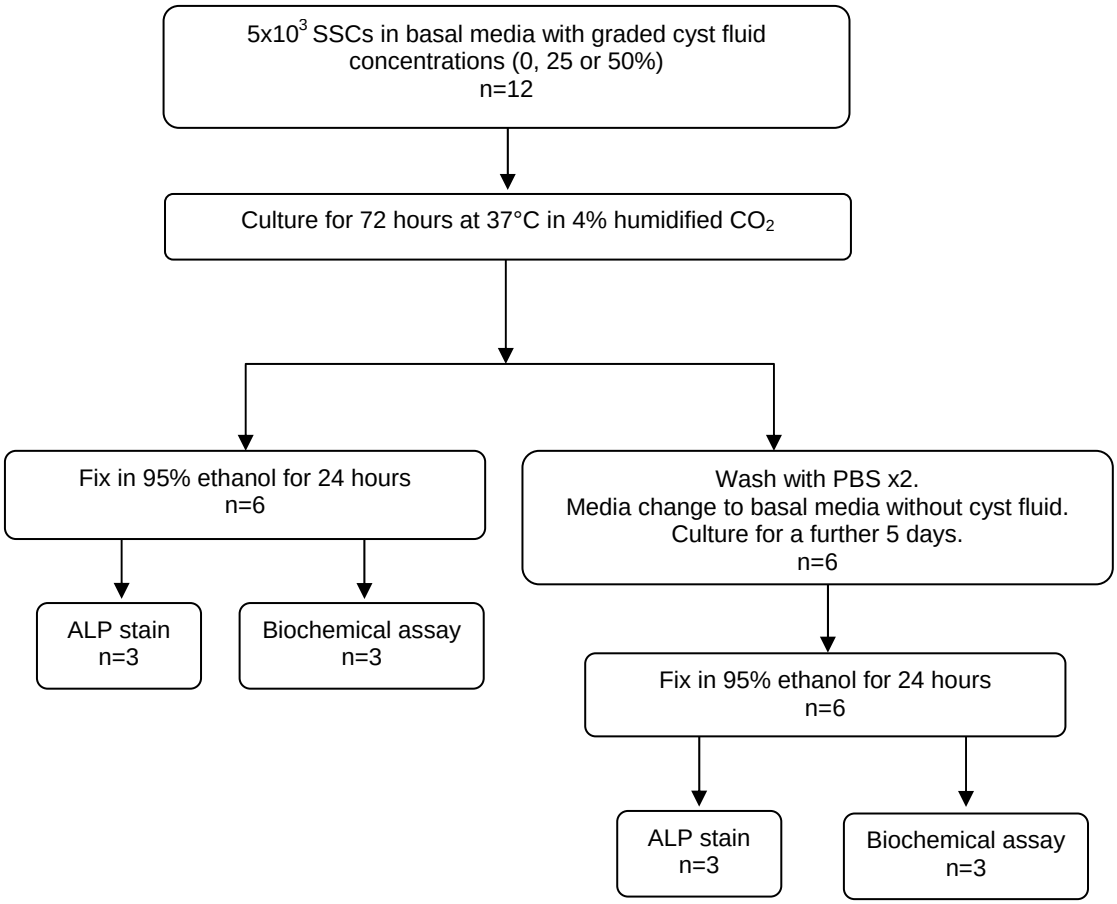

Alkaline phosphatase stain

Following fixation in 95% ethanol for 24 hours, SSCs were stained with Naphthos AS-MX and Fast Violet B Salts (Sigma-Aldrich, Poole, UK) for alkaline phosphatase (ALP). Microscope images were recorded using Carl Zeiss Axiovision software Ver 3.0 via an AxioCam HR digital camera on an Axiovert 200 inverted microscope (Carl Zeiss Ltd, Hertfordshire, UK).

Biochemical analysis

Culture wells were assessed by biochemical analysis for DNA content (as a measure of cell proliferation), and ALP activity (as a measure of osteogenic differentiation). Following fixation in 95% ethanol, cell lysates were obtained via three sequential freeze-thaw cycles in Triton X-100 (BDH Chemical Ltd, Poole, UK). ALP and DNA assays were then performed in a standard manner with 10µl of lysate run in triplicate for each concentration of cyst fluid on a plate against two standards and read on a BioTek KC4 and FLX-800 microplate fluorescent reader (BioTek, Potton, UK). Statistical analysis was performed by One-way ANOVA using GraphPad InStat version 3.00 (GraphPad Software, San Diego California USA).

4.2.5 Results

The aspiration of straw-coloured fluid confirmed the clinical and radiological diagnosis of UBC in Patient 1 & 2. Thus the differential diagnoses of aneurysmal bone cyst (ABC), which would be a bloody aspirate, and non-osteogenic fibroma, fibrous dysplasia and benign cartilage tumours, which are all solid, could be eliminated.

Protein and electrolyte levels and pH

Levels of sodium, potassium, bicarbonate and calcium in the cyst fluid were within the normal range for plasma, in keeping with previous analyses (COHEN 1960;Chigira *et al.* 1983). The protein content was 54g/l, defining the cyst fluid as an exudate, not transudate. Measurement of pH showed the cyst fluid to be alkaline, with fluid from Patient 1 having a pH of 8.4 and from Patient 2 having a pH of 8.5.

Fibro-cellular membrane

The fibro-cellular membrane that was excised from the cyst lining of Patient 2 was analysed histologically and by electron microscopy (E.M.). As reported by Komiya et al (2000) and Yu et al (2005), osteoclast-like giant cells with multiple nuclei and numerous mitochondria were seen on E.M. (**Fig.4A-B**) and histology (**Fig.4C**). Furthermore, toluidine blue staining demonstrated an abundance of osteoclasts in the paratrabecular bone region of the cyst lining, in far greater number than is seen in normal bone.

Figure 4: Electron micrographs (EM) and histological sections of the fibro-cellular lining of the UBC from Case 2. A: EM 1500x magnification, demonstrating large osteoclast-like cells with multiple nuclei (arrows). B: EM 3500x, illustrating the multiple nuclei and numerous mitochondria within the cell body. C: Toluidine blue staining of the lining confirmed the presence of osteoclast-like cells with multiple nuclei (arrows). D: Low power histology images of the cyst wall revealed multiple osteoclasts in the paratrabecular region, in far greater number than expected in normal remodelling bone (arrows).

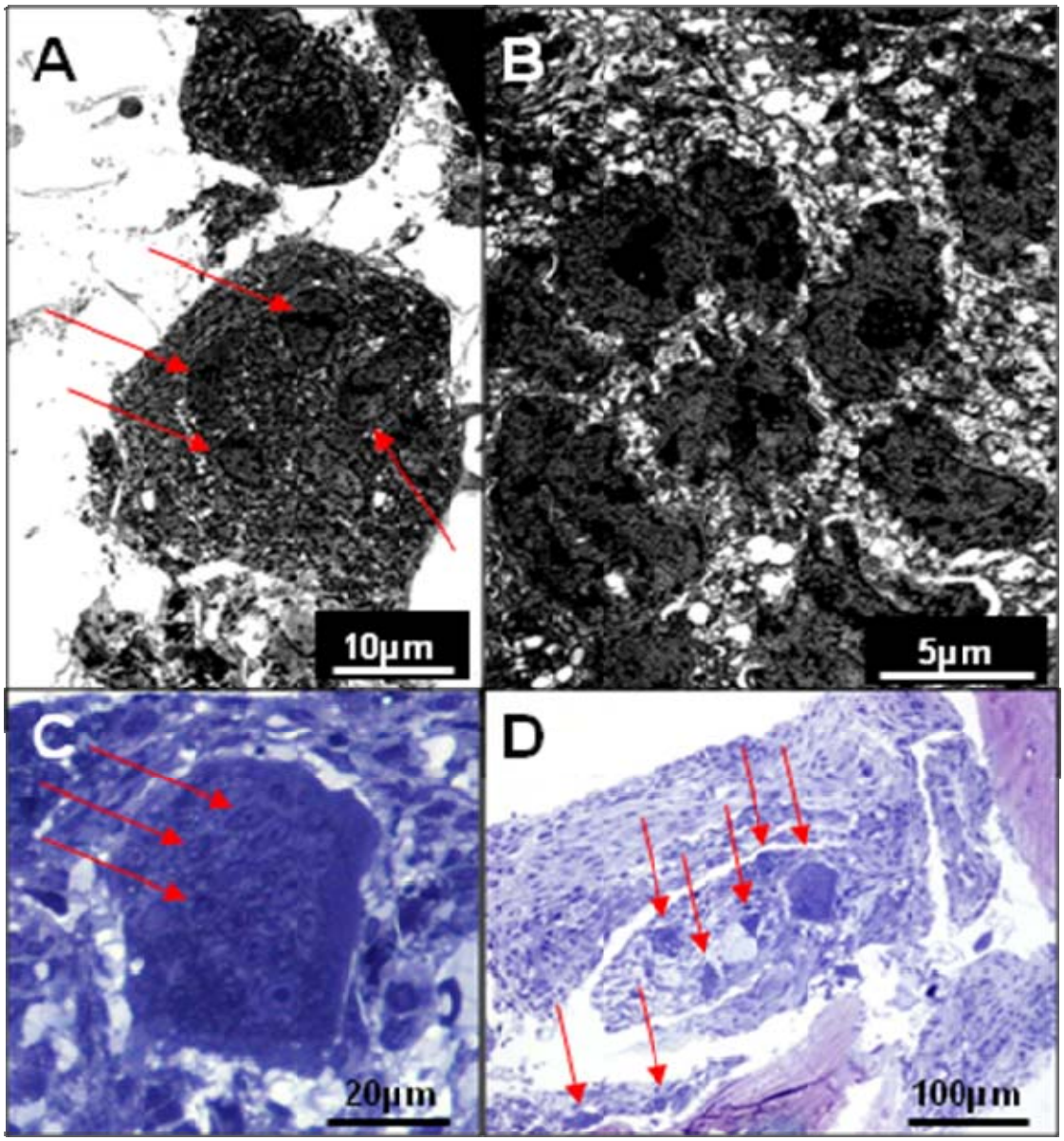

Cytokine levels

Elevated levels of three out of the fifteen musculoskeletal cytokines were recorded, illustrated in **Table 2**. IL-6, MIP-1α and MCP-1 levels were increased by 19, 31 and 35 times respectively compared against reference values found in the literature. This contrasted to all other cytokines tested, which were either below the level of detection by flow cytometry fluorescent bead immunoassay or below published reference values.

Table 2: High levels in the cyst fluid were recorded for three cytokines.

Cytokine	Level (pg/ml)	Reference level for serum (pg/ml)	Fold increase
IL-6	20.91	1.1 +/- 0.1[1]	19x
Macrophage inflammatory protein (MIP-1α)	400.7	13.0 (range 1.4-54)[2]	31x
Monocyte chemotactic protein (MCP-1)	1852	52.95 +/- 14.3[3]	35x

1. (Grey *et al.* 1996)
2. (Politou *et al.* 2004)
3. (Cai *et al.* 2009)

ALP staining of SSC culture with cyst fluid

Viewing of ALP stained SSCs after 72 hour culture (n=3 for each cyst fluid concentration) demonstrated increased cell proliferation with 25% and 50% cyst fluid compared to those cultured in basal media. Furthermore, greater ALP staining was demonstrated on the cells cultured in cyst fluid (**Fig.5A,C,E**). The control cells showed a steady increase in SSC number and ALP staining from 72 hours over the subsequent 5 days, as expected (n=3) (**Fig.5A-B**). By comparison, marked increases in cell proliferation and ALP staining were observed after the extended 5 day cultures, as a result of early exposure to cyst fluid (n=3). This was observed to be dose-dependent (**Fig.5B,D,F**).

Figure 5: Photo-microscope images of ALP stained SSC cultures in graded cyst fluid concentrations (0% (A-B), 25% (C-D), 50% (E-F)), showing increased cell proliferation and ALP staining with increased cyst fluid concentrations. The effect became more marked on extended culture in basal media (right hand column). Patient 1 and Patient 2 were comparable. Scale bars = 50µm.

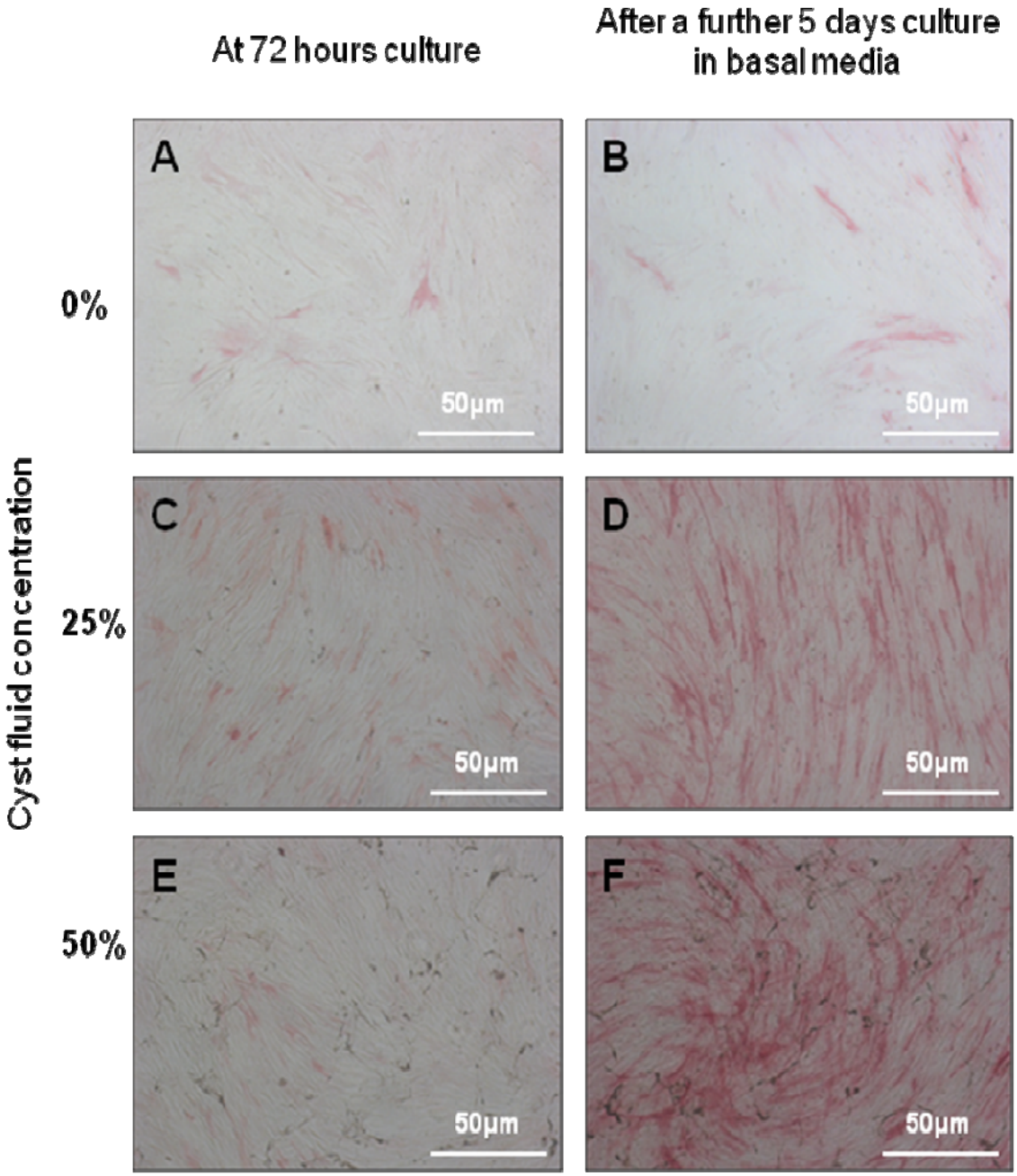

Biochemical analysis of SSC culture with cyst fluid

Biochemical analysis provided quantitative breakdown of the observations noted on ALP staining. This corroborated the marked increase in cell proliferation and ALP expression that was observed in a dose-dependent manner in the SSCs cultured in the presence of cyst fluid.

For both cases, following 72 hours of culture in graded cyst fluid / media concentrations, SSCs in cyst fluid showed increased ALP expression compared to those SSCs cultured in basal media only. These differences were significant between 0% and 50% cyst fluid (Case 1, $p<0.01$, Case 2, $p<0.001$), and the trend was reflected in the 25% cyst fluid concentrations, being statistically significant in Case 2 ($p<0.01$) (**Fig.6A-B**). Although DNA assays did not show significant differences between cyst fluid concentrations after 72 hours culture ($p>0.05$) (**Fig.6C-D**), ALP specific activity was increased with cyst fluid concentration for both cases ($p<0.01$ and $p<0.001$ respectively) (**Fig.6E-F**).

The differences in cell activity with graded cyst fluid concentrations were more marked when the cells were returned to culture in basal media for a further 5 days, despite the absence of exposure to cyst fluid. For both cases, comparisons between cells exposed to basal media only and those exposed to 50% cyst fluid showed significant increases in ALP expression ($p<0.001$), DNA activity ($p<0.001$) and ALP specific activity ($p<0.001$). This finding was observed to be dose-dependent with increasing cyst fluid concentration from 0 to 50% (**Fig.6A-F**), in keeping with the qualitative observations on histology.

Critically, in the cells cultured only in basal media, ALP specific activity remained unchanged over time ($p>0.05$), but was increased in those SSCs cultured with cyst fluid ($p<0.01$) (**Fig.6E-F**). This indicated that the cyst fluid promoted osteogenic differentiation, which, interestingly, continued beyond the initial exposure period.

Figure 6: Biochemical assays of SSCs cultured with graded concentrations of cyst fluid / culture media. The first three bars on each graph represent the values of the cells fixed at 72 hours. The next three bars represent those that were returned to culture in basal media for a further 5 days. The significance of all the results was more marked with extended culture, and differences were evident between SSCs cultured in basal media compared to those initially exposed to cyst fluid. Error bars denote standard deviation. *** = p<0.001, ** = p<0.01. Each assay was run in triplicate.

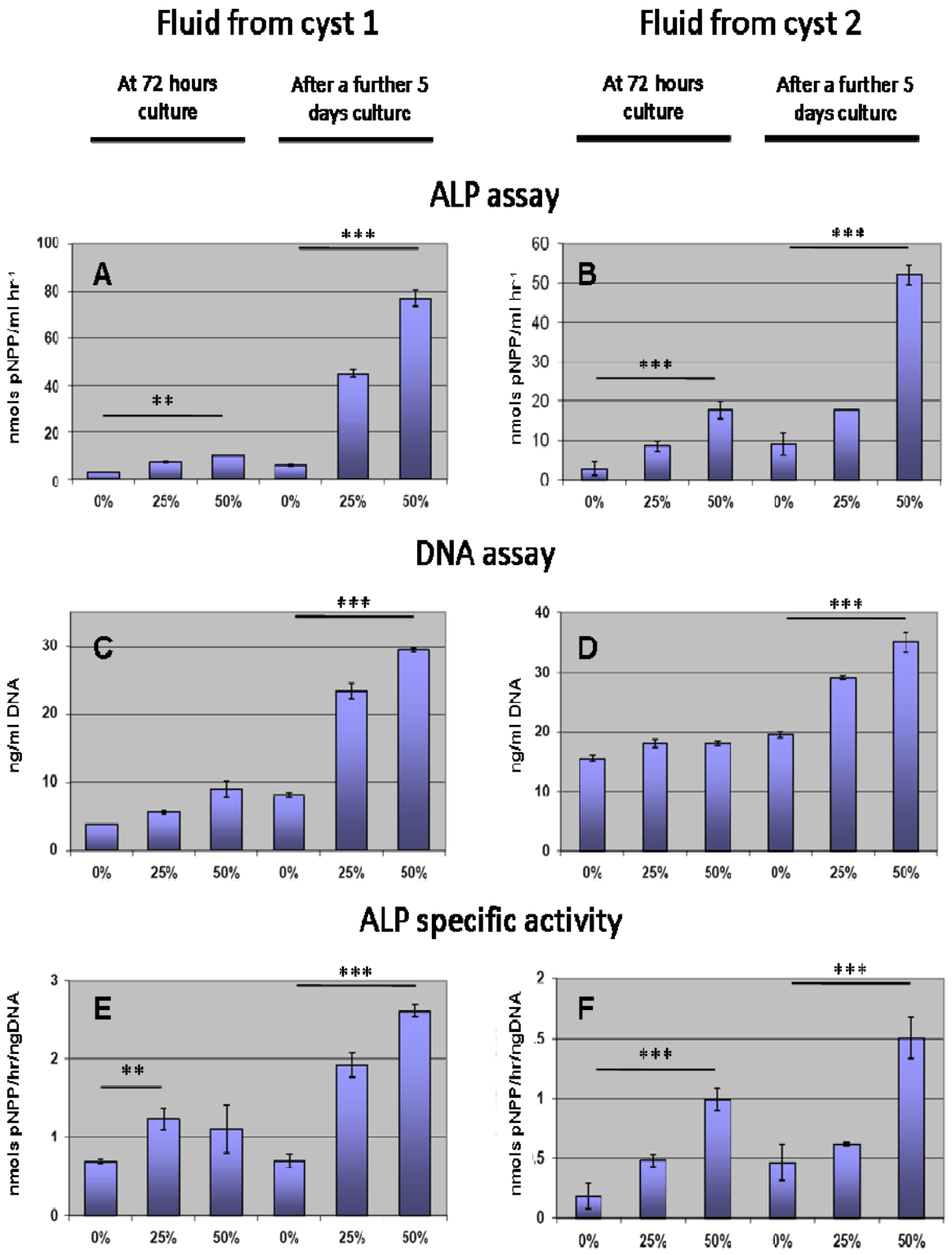

4.2.6 Discussion

A UBC is a radiographic diagnosis, but confirmation of the diagnosis in these two cases was made upon aspiration of straw-coloured fluid. This excluded the differentials of aneurysmal bone cyst, which contains blood, and non-osteogenic fibroma, fibrous dysplasia and benign cartilage tumours, which are all solid. The fluid was therefore retained for further analysis to explore the pathophysiology of this mysterious cyst.

The high protein levels detected in the cyst fluid (54g/l) indicated that the fluid was not a transudate formed passively by filtration, but an exudate, which is formed by an active process of synthesis or inflammation. Protein levels in UBC fluid have not previously been reported.

Typical radiographic appearances of UBCs demonstrate an eroded cyst cavity (**Fig.1**), and the role of osteoclasts in the formation of UBCs has previously been suggested (Markovic, Cvijetic, & Karakasevic 1988;Shindell *et al.* 1989;Gerasimov *et al.* 1991). Osteoclasts have been reported in the fibro-cellular lining of UBCs on histology (Komiya *et al.* 2000) and electron microscopy (Yu *et al.* 2005), and this study confirms their presence by direct visualisation by both these techniques (**Fig.4**). The histological sections revealed not only the presence of osteoclasts, but these multi-nucleated cells were observed in greater abundance than seen in normal bone, providing direct evidence of abnormal increased osteoclast activity in UBCs.

This study has demonstrated a number of new pro-osteoclast influences in the cyst fluid, in the up-regulation of osteoclast promoting cytokines IL-6, MCP-1 and MIP-1α. IL-6 is a key cytokine in the promotion of bone resorption by osteoclasts (Kudo *et al.* 2003;Tamura *et al.* 1993;Udagawa *et al.* 1995;Lowik *et al.* 1989;Ishimi *et al.* 1990), acting via Gp130 signalling of osteoblasts to induce RANKL. Normal physiological levels of IL-6 in the circulation are below the level of detection (Suda *et al.* 1995), but were grossly elevated in the cyst fluid. Notably, IL-6 acts via a different signalling pathway to the PKA mediated promotion of RANKL by PGE_2, which has also been shown to be elevated in cyst fluid (Shindell *et al.* 1989). Up-regulation of IL-6 has been implicated in the up-regulation of osteoclastogenesis causing osteoporosis (Manolagas 1995;Ancey *et al.* 2003), and is associated with pathological bone resorption in multiple myeloma (Ancey *et al.* 2003;Feng *et al.* 2006;Klein *et al.* 1991) and Paget's disease of bone (Roodman & Windle 2005).

Increased levels in UBC fluid have been reported once previously (Komiya *et al.* 2000), though the authors made negligible comment on this finding.

Monocyte chemotactic protein-1 (MCP-1), also called chemokine ligand 2 (CCL2), is induced by RANKL to promote osteoclast differentiation from monocyte precursors. A positive feedback loop exists, as MCP-1 is released by osteoclasts upon differentiation (Kim, Day, & Morrison 2005;Kim *et al.* 2006). MCP-1 activity has been linked to oseteoclastogenesis and osteoclastic activity of bone resorbing lesions of metastatic breast, lung and prostate carcinoma (Bussard, Venzon, & Mastro 2010;Craig & Loberg 2006;Cai *et al.* 2009).

Macrophage inflammatory protein-1α (MIP-1α), also called chemokine ligand 3 (CCL3), is potently stimulated by RANKL to promote chemotaxis of human osteoclast precursors and differentiation to mature osteoclasts (Votta *et al.* 2000;Kim *et al.* 2006). MIP-1α mediated osteoclast formation has been implicated in osteolysis caused by multiple myeloma (Oyajobi *et al.* 2003). An MCP-1 / MIP-1α / RANKL autocrine loop has been described (Kim *et al.* 2006), and, interestingly, this mechanism was hypothesised to cause pathology when chemokines are abundant (Kim, Day, & Morrison 2005). The increased levels of MCP-1, MIP-1α and IL-6 observed in the cyst fluid provide a mechanism by which to explain the enhanced osteoclast activity observed on histology sections and the macroscopic appearances of bone erosion seen on radiographs of UBCs.

The effect of cyst fluid on osteoblast function was also examined. Increases in cell growth and osteogenic differentiation of SSCs were seen *in vitro* when cultured with cyst fluid compared to plain basal media (**Fig.6A-F**), which indicates a pro-osteoblast influence on SSCs by the cyst fluid. This finding can not be attributed to pH differences between cyst fluid (pH 8.4-8.5) and basal media (pH 7.0-7.6) as although alkaline pH promotes osteoblast function, it does not affect proliferation (Brandao-Burch *et al.* 2005). Furthermore, the extended cultures in basal media with equal pH demonstrated more marked differences in cell proliferation and osteogenic differentiation, all of which were highly significant ($p<0.001$). Thus the positive influence of cyst fluid on SSC growth and differentiation continued beyond any exposure to the cyst fluid.

UBCs demonstrate bone erosion (**Fig.1**), thus the finding that the fluid promoted osteoblastic proliferation and differentiation may appear paradoxical. On the basis of these biochemical findings, increased osteogenesis might be the expected pathology rather than the eroded bone appearance seen. However complex signalling pathways exist between osteoblasts and osteoclasts (Suda *et al.* 1995;Kudo *et al.* 2003;Arnett 2008). During the normal bone remodelling process, osteoclasts discontinue resorption of bone and disappear from the resorption site before osteoblasts are able to lay down new bone at sites of prior resorption (Mundy *et al.* 1995). The continued action of osteoclasts demonstrated in UBCs would therefore prevent osteogenesis, despite increased SSC proliferation and ALP expression. Critically, osteoblasts are required for osteoclast activation via the RANKL signalling pathway. IL-6, a key cytokine in up-regulation of RANKL (Manolagas 1995;Udagawa *et al.* 1995) and MCP-1 and MIP-1α, stimulated by RANKL to promote osteoclast formation, have been demonstrated in this study to be highly elevated in cyst fluid. Thus increased osteoblast activity provides further evidence of up-regulation of the RANKL signalling pathway, and may hold the key to the pathogenesis of UBCs.

Presented with evidence in the literature and in this thesis that osteoclasts are active in UBCs (Komiya *et al.* 2000;Yu *et al.* 2005;Gerasimov *et al.* 1991;Markovic, Cvijetic, & Karakasevic 1988;Shindell *et al.* 1989), the finding that the fluid is alkaline is paradoxical. Osteoclasts are activated in an acidic environment, and increasing the pH has been demonstrated, *in vitro* and *in vivo*, to neutralise their activity (Arnett & Dempster 1986;Arnett 2008). Thus the marked osteoclast activity demonstrated in the cyst lining of Patient 2 **(Fig.4**), despite the alkaline environment of the cyst cavity, would appear contrary to the *in vitro* and *in vivo* observations of Arnett *et al*. Although the pH of cyst fluid has been measured previously (Markovic, Cvijetic, & Karakasevic 1988;Chigira *et al.* 1983), actual pH values have never been reported. Markovic et al, who demonstrated raised acid phosphatase activity in UBCs, commented on the pH that "the fluid within the cyst does not show a marked acidosis". Chigira et al noted that the fluid pH "was not significantly different from arterial or venous blood" which ranges from 7.35-7.45, and is alkaline. Neither author expanded on these observations, but two theories on the cause of alkalinity of the cyst fluid are offered here. Firstly, the alkalinity of the fluid could be a result of the bone mineral, hydroxyapatite. In keeping with ongoing bone erosion, dissolution of this alkaline mineral could raise the pH of the fluid (Arnett 2008). Secondly, osteoclast intra-cellular homeostasis could explain cyst fluid alkalinity. To generate the

low pH of approximately 4.5 on the osteoclast ruffled border (Vigorita, Ghelman, & Mintz 2007), the formation of H^+ and HCO_3^- is catalysed by carbonic anhydrase within the osteoclast cell body. Protons are actively transported into the sealed micro-environment of the ruffled border and HCO_3^- is passed out of the cell body the other way, through HCO_3^- / Cl^- exchange channels, which would be into the cyst cavity.

This study has demonstrated an effect of cyst fluid on both osteoclast and osteoblast activity, therefore the Null Hypothesis that "The fluid found within a unicameral bone cyst has no effect on skeletal stem cells nor osteogenesis" can be rejected. More patients requiring surgery for this uncommon pathology are awaited in order to build on these findings. On subsequent patients, investigation into the effect of cyst fluid on SSC proliferation and differentiation could focus on cultures using Stro-1+ cells. This would specify the effect of cyst fluid on selected osteoblasts as well as generic SSCs.

The elevated levels of certain pro-osteoclast cytokines found within the fluid of this UBC can guide a more focused investigation of the cytokine profile. RANKL and macrophage colony stimulating factor (M-CSF) are produced by osteoblasts and directly stimulate osteoclast proliferation and differentiation (Suda *et al.* 1995;Oreffo *et al.* 2007) thus investigation of levels of these proteins would be indicated. As the elevated cytokines were suggestive of abnormal osteoclast stimulation via RANKL, notable cytokines of further interest would include those, like IL-6, that are mediated by the Gp130 signalling pathway for RANKL stimulation. These include IL-11, oncostatin M and leukaemia inhibitory factor. Other cytokines for focused investigation are the PKA-mediated promoters of RANKL, like PGE_2 that Shindell et al found in elevated levels in UBC fluid (Shindell *et al.* 1989). These include parathyroid hormone related peptide (PTHrP) and IL-1. Down-regulation of osteoclast inhibitors such as transforming growth factor (TGF)-β (Oreffo *et al.* 1989;Mundy *et al.* 1995) and osteoprotegerin (OPG), an inhibitor of RANKL signalling (Oreffo *et al.* 2007;Trouvin & Goeb 2010), may play a role in the autocrine loop for up-regulation of osteoclast activity. Following further assays of cytokine levels, knockout cultures of SSCs with selected cytokines would quantify any observed effects.

This study has demonstrated the stimulation of osteoblast differentiation and proliferation by the fluid of UBCs. Together with a number of osteoclast activating factors closely related to osteoblasts and RANKL (IL-6, MIP-1α and MCP-1) and evidence of increased

osteoclast activity, these findings indicate that there is an abnormality in the regulatory process between osteoblasts and osteoclasts that underlies the pathogenesis of UBCs. Treatments of UBCs may therefore need to be directed at down-regulation of the pro-osteoclast cytokines or localised bisphosphonate therapy.

Chapter V

A novel tissue engineering strategy for the treatment of avascular necrosis of the femoral head, with analysis of retrieval specimens

The surgical procedures were performed by Mr Douglas Dunlop, and parallel *in vitro* cultures by Mr Andrew Jones. μCT and bone density analysis was performed by Dr Stuart Lanham and I am grateful to Dr Adam Briscoe for his help with compression testing.

5.1 Introduction

Clinical imperatives to replace bone lost as a consequence of age or disease has led to the need for novel therapies to generate bone for skeletal applications. Tissue regeneration promises to deliver specifiable replacement tissues and the prospect of efficacious alternative therapies for orthopaedic applications is enormous. Yet despite extensive *in vitro* and *in vivo* work there is a gap in translation to the clinic, the so called 'Valley of Death' (Hollister 2009). Consequently bone tissue engineering treatments in patients are restricted to case reports and small case series (Tare *et al.* 2010). This chapter describes the translation of a bone tissue engineering strategy to the clinic, for the treatment of bone defects in the femoral head associated with avascular necrosis (AVN), and subsequent unique *ex vivo* analysis of retrieved human tissue engineered material.

AVN of the femoral head usually affects young adults, progressing to bone collapse and osteoarthritis in over 80% of untreated patients (Mont, Carbone, & Fairbank 1996). Progression occurs even in 59% of asymptomatic patients (Mont *et al.* 2010). Most cases are idiopathic but other causes include steroid therapy, chemotherapy, alcohol and sickle cell disease, whilst the chance of developing AVN after a traumatic dislocation of the native hip may be as high as 40% (McKee *et al.* 1998).

The pathology of AVN has been described as passing through four distinct phases (Ficat 1985). Stage I is death without structural change, Stage II is repair via a resorption front, Stage III is major structural failure leading to stage IV where collapse causes degeneration of the cartilage. Staging of AVN is problematical as evidenced by the number of different staging systems, with the most common, described above, being the Ficat & Arlet Classification (Ficat 1985). The Steinberg (Steinberg, Hayken, & Steinberg 1984), Association Research Circulation Osseous (ARCO) (Sugano *et al.* 2002), Japanese Investigation Committee (Ono 1986) and Mitchell Classifications (Mitchell *et al.* 1989) are also used. The most important predictor remains progression from an intact bony architecture (Ficat & Arlet Stage I or II) to loss of normal bone structure and involvement of articular cartilage (Ficat & Arlet Stage III or IV). Such changes indicate arthritic change which may require arthroplasty. Position and distribution of the necrotic bone in the femoral head has a bearing on prognosis, with widespread necrosis or focused laterally, in

the weight bearing region of the femoral head, more likely to collapse (Mitchell *et al.* 1989;Mont *et al.* 2010).

In the 1970's and 80's, early studies showed that the rate of progression for the untreated disease was high. Merle d'Aubigné et al found symptomatic and radiological progression of the disease in 75% of 90 conservatively treated patients (Merle *et al.* 1965). Furthermore, a meta-analysis of over 800 hips in 21 studies showed that only 22.7% of patients had a satisfactory outcome (defined as not requiring subsequent arthroplasty) with non-operative treatment (Mont, Carbone, & Fairbank 1996). A systematic review of asymptomatic AVN (usually being diagnosed in the contralateral hip of a symptomatic one) has shown a 59% progression to symptoms and collapse (Mont *et al.* 2010). Untreated cases therefore, even in the early and asymptomatic stages, have a high probability of requiring a THR. In the young patient, typically the case with AVN, an implant is unlikely to last the lifetime of a patient, therefore committing him / her to at least one revision hip operation. Joint preserving therapies are therefore advocated by most authorities to prevent the progression to collapse. These include core decompression (Mont, Carbone, & Fairbank 1996), electrical stimulation (Steinberg *et al.* 1984), tantalum trabecular metal rods (Veillette *et al.* 2006), vascularised fibular grafts (Korompilias *et al.* 2009), fibular or tibial strut grafts (Keizer *et al.* 2006), concentrated autologous bone marrow (Hernigou & Beaujean 2002) or hydroxyapatite rods coated with skeletal stem cells (Yamasaki *et al.* 2010).

Hernigou was the first to describe the use of skeletal stem cells (SSCs) for the treatment of avascular necrosis (Hernigou & Beaujean 2002), and has generated encouraging long term results by combining SSCs with core decompression (Hernigou *et al.* 2009). While the osteogenic characteristics of the SSCs within bone marrow may stimulate repair and regeneration of the necrotic segment of bone, this treatment does not provide any structural support for the overlying cartilage.

Impaction bone grafting (IBG) provides mechanical support and has been used as a void-filler in revision hip surgery for over forty years (Slooff *et al.* 1984) with some recorded excellent long-term results (Schreurs *et al.* 2004;Halliday *et al.* 2003). IBG provides a solid mantle to support the hip prosthesis and has now also been used in the treatment of AVN (Wang *et al.* 2010). Whilst remodelling has been demonstrated on histological specimens

from IBG in acetabula and femora, areas of non-incorporated graft with associated necrosis, fibrocartilage and fibrosis remain in all specimens (van Haaren *et al.* 2007;van der Donk *et al.* 2002;Ling, Timperley, & Linder 1993).

Studies from Bolland et al and Korda et al have shown that SSCs can be combined with IBG to augment the biological and mechanical characteristics of the graft. The SSCs have been shown to survive the impaction process, proliferate and differentiate down an osteoblastic pathway (Bolland *et al.* 2006;Korda *et al.* 2006;Korda *et al.* 2008;Bolland *et al.* 2008).

This novel technique was translated to two clinical cases, reported in 2006 (Tilley *et al.* 2006), and has been translated to the treatment of early stage AVN in five hips in 4 patients (Aarvold *et al.* 2011). Three patients remain asymptomatic at up to 44 month follow-up. Two femoral heads collapsed, both in the same patient, thought to be due to widespread head involvement. This has provided the unique opportunity to retrieve the specimens and analyse the human tissue engineered impacted bone. We report this case series and the findings from *ex vivo* analysis of the two collapsed femoral heads.

5.2 Aims

1. To evaluate a tissue engineering strategy for the treatment of AVN
2. To analyse retrieved tissue engineered bone from those cases that subsequently required THR

5.3 Null Hypothesis

The addition of skeletal stem cells to impaction bone graft has no demonstrable effect on bone formation in clinical translation.

5.4 Materials & Methods

Patient Cohort

Four patients, all with bilateral AVN of their femoral heads, were treated at Southampton General Hospital for their disease. Pre-operative imaging of two patients is illustrated in **Figure 1**. Three patients presented with advanced disease in one hip (Ficat & Arlet stage III or IV), requiring total hip replacement (THR). Early stage disease was treated with SSCs and IBG, which was bilateral in one patient **(Table 1)**.

Figure 1: A: Patient 1 pre-operatively with Stage IV AVN on the right and Stage II AVN on the left. B: MRI scan of Patient 3 pre-operatively with Stage III AVN on the right and Stage II AVN on the left.

Table 1: Patient details and aetiology of AVN

Patient	*Age*	*Attributed Cause*	*Right hip stage**	*Right hip treatment*	*Left hip stage**	*Left hip treatment*
1	42	Systemic steroids for sub-arachnoid haemorrhage	IV	THR	II	SSC/IBG
2	40	Alcohol	III	THR	II	SSC/IBG
3	31	Idiopathic	III	THR	II	SSC/IBG
4	32	Systemic steroids for testicular carcinoma	II	SSC/IBG	II	SSC/IBG

*Ficat & Arlet Stage (Ficat 1985), which is used throughout the chapter unless otherwise stated.

Surgical technique

Milled allograft was prepared from fresh frozen femoral heads according to standard clinical practice (Halliday *et al.* 2003). Briefly, cartilage and soft tissue was removed with bone nibblers and an oscillating sagittal bone saw (Stryker UK), the femoral head was ground through a bone mill (Noviomagus Bone Mill, Stryker UK), de-fatted with H_2O_2 and washed extensively with saline pulse lavage. With the patient positioned laterally on the operating table, bone marrow was aspirated from the posterior iliac crest **(Fig.2A)**, rotating and re-angling the needle regularly to minimise contamination with venous blood, as described by Hernigou (Hernigou *et al.* 2006). The marrow was concentrated by calibrated centrifugation (Marrowstim, Biomet, Swindon, UK) and the nucleated cell fraction was removed and mixed with the prepared allograft **(Fig.2B)**.

The patient was then placed supine on the operating table to allow guidance of instrumentation up the femoral neck into the necrotic area of the femoral head, under fluoroscopic control on antero-posterior and frog lateral views. Through a 2cm incision in the lateral thigh, a channel was drilled over a guidewire into the sub-chondral bone and the necrotic bone was removed by curettage. The cell-seeded milled allograft was impacted retrograde into the channel using a 12mm diameter Xchange tube saw (Stryker, Newbury, UK) **(Fig.3A-F)**. Patients maintained protected weight bearing for 6 weeks post-operatively and follow-up was by serial radiological and clinical examination.

Figure 2: Surgical technique; A: aspiration of iliac crest bone marrow. B: Mixing of concentrated SSCs with milled allograft.

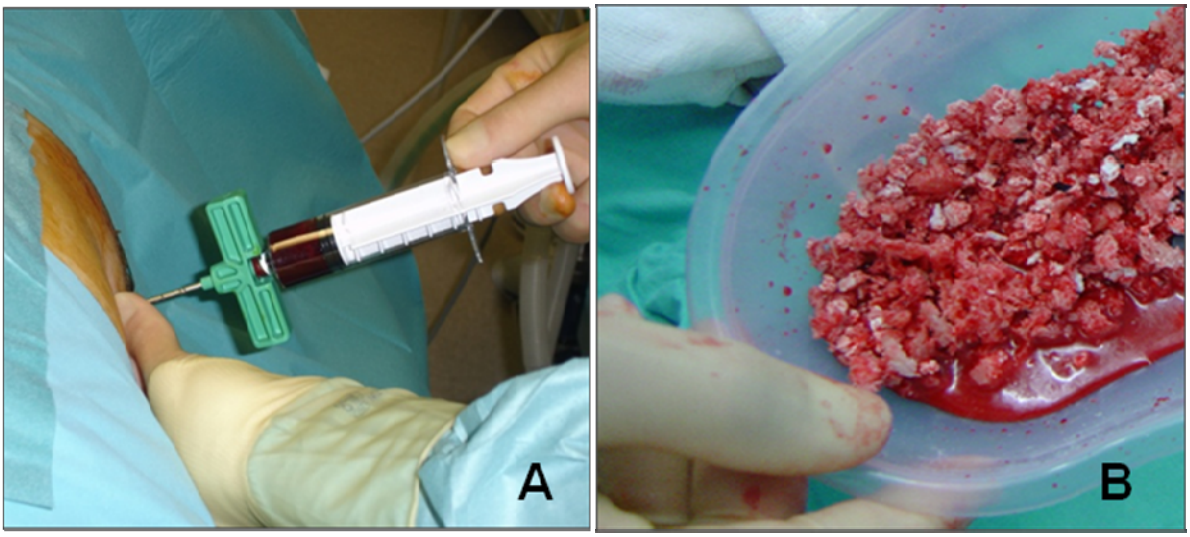

Figure 3: Surgical technique; A: Optimal guidewire placement. B: Drilling into sub-chondral necrotic bone. C: Radio-lucent empty channel is visible. D: Curettage of necrotic bone. E: Retrograde impaction of SSC-seeded milled allograft. F: Radio-dense channel of impacted bone clearly visible.

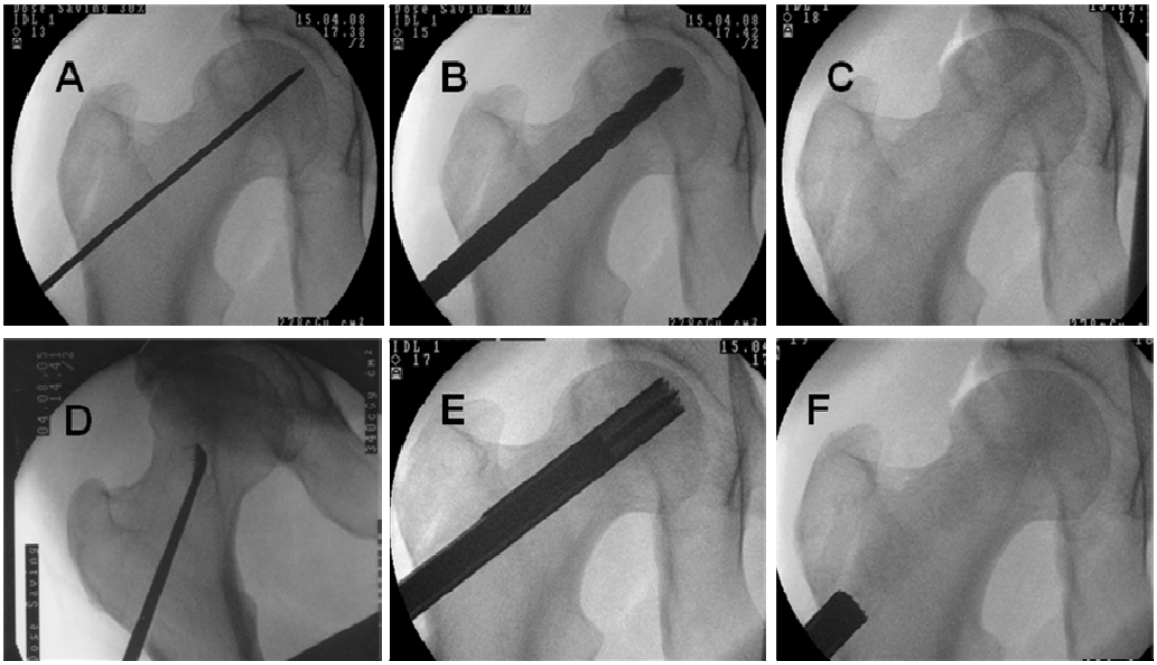

Parallel in vitro assessment

Samples of combined allograft and SSC mix were retained prior to implantation into each patient, to confirm cell viability. These samples were cultured in basal media for 14, 28 and 42 days, with twice weekly media changes, prior to staining with CellTracker Green and ethidium homodimer ((CTG-EH), Sigma-Aldrich Ltd, Gillingham, UK). Microscope images were recorded using Carl Zeiss Axiovision software Ver 3.0 via an AxioCam HR digital camera on an Axiovert 200 inverted microscope (Carl Zeiss Ltd, Welwyn Garden City, UK) under fluorescent light.

Equal volumes (0.5ml) of concentrated versus un-concentrated aspirated bone marrow were also cultured in monolayer in basal medium (αMEM, 10%FCS) for two weeks (n=3), fixed in 95% ethanol and stained with Naphthos AS-MX and Fast Violet B Salts for alkaline phosphatase (Sigma-Aldrich Ltd, Gillingham, UK).

Retrieval of specimens

In Patient 4, both femoral heads progressed to collapse and the patient required bilateral THR, on the right after 13 months and on the left after 19 months. Reasons for failure are discussed below in the results. At each operation the collapsed femoral head was retrieved with patient consent and prior ethical approval (LREC194/99/1), photographed and fixed in 4% paraformaldehyde (PFA) prior to further analysis.

Micro computed tomography (μCT)

All samples were scanned using an Xtek Benchtop 160Xi scanner (Xtek Systems Ltd, Tring, UK) equipped with a Hamamatsu C7943 x-ray flat panel sensor (Hamamatsu Photonics, Welwyn Garden City, UK). Scan resolution was up to 31micron, at 150kV, 60μA using a molybdenum target with an exposure time of 534 ms and 4x digital gain. Reconstructed volume images were analysed using VGStudio Max 1.2.1 software (Volume Graphics GmbH, Heidelberg, Germany).

Histology

For histological analysis of normal trabecular and impacted bone, representative sections were excised from the femoral neck **(Fig.4, Sections '1' and '2' respectively)**, avoiding areas of collapse as these represented osteonecrotic bone with pathology that was residual from pre-procedure. Sections of the collapsed necrotic tissue were excised and processed in an identical fashion **(Fig.4, Section '3')**. Cortical bone was not included due to the associated difficulty of decalcification and sectioning.

Figure 4: Schematic identifying the sections processed for histology

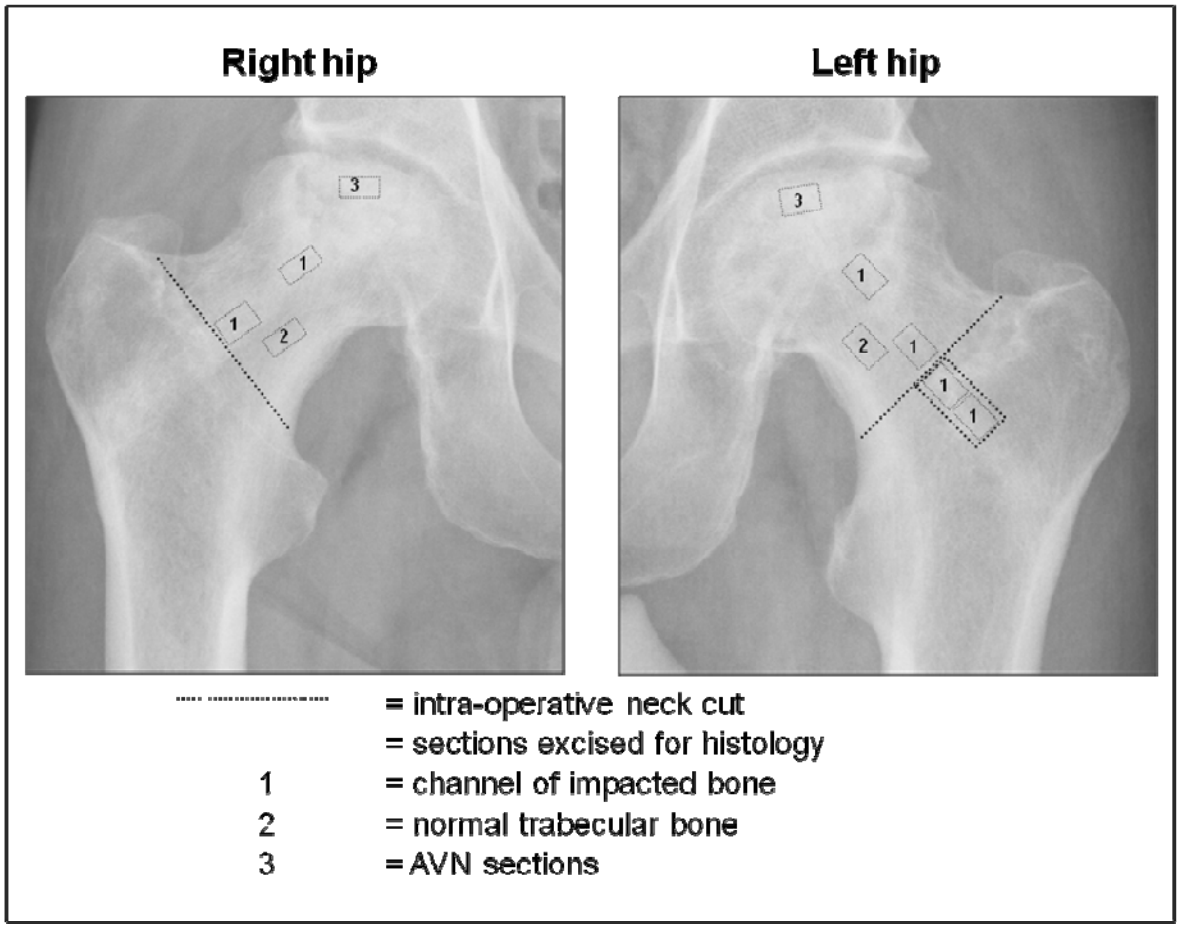

Specimens were decalcified using 0.1M TRIS / 5%EDTA solution at pH7.3 which was changed weekly. Decalcification was verified by Faxitron MX-20 micro X-ray (Faxitron X-ray, Wheeling, IL, USA). Once decalcified, the specimens were embedded in wax, mounted, serially dehydrated in histoclear and graded ethanols, and sectioned to 7μm thickness. Slides were stained with Alcian Blue / Sirius Red (A/S) and tartrate resistant acid phosphatase (TRAP). Microscope images were recorded as described above for CTG-EH stains, under white and polarised light.

Mechanical testing

Sections of trabecular, cortical and impacted bone were excised from each specimen for comparison of mechanical strength. As described above, these sections were taken from the femoral neck region to avoid incorporating residual pathology **(Fig.5)**. There was sufficient tissue to harvest two representative sections of each tissue type from each femoral head, providing four samples of each in total. Bone sections were the trimmed to equal sized cuboids (6x7x4mm) using a low-speed diamond-tipped wafering blade (Buehler, Coventry, UK) **(Fig.6A)** and tested to failure by compression with a hydraulic actuator (Instron Ltd, High Wycombe, UK) **(Fig.6B)**. A compressive force was applied at a constant rate of 4.8mm over 60 seconds (0.08mm/s), from which stress-strain graphs were plotted and mechanical strength calculated. In order to represent the forces sustained *in vivo*, the direction of force applied was always in the orientation of the trabecular lines of the femoral neck. Statistical significance was determined by One-way ANOVA test of the three independent bone types.

Figure 5: Schematic identifying the sections excised for mechanical testing

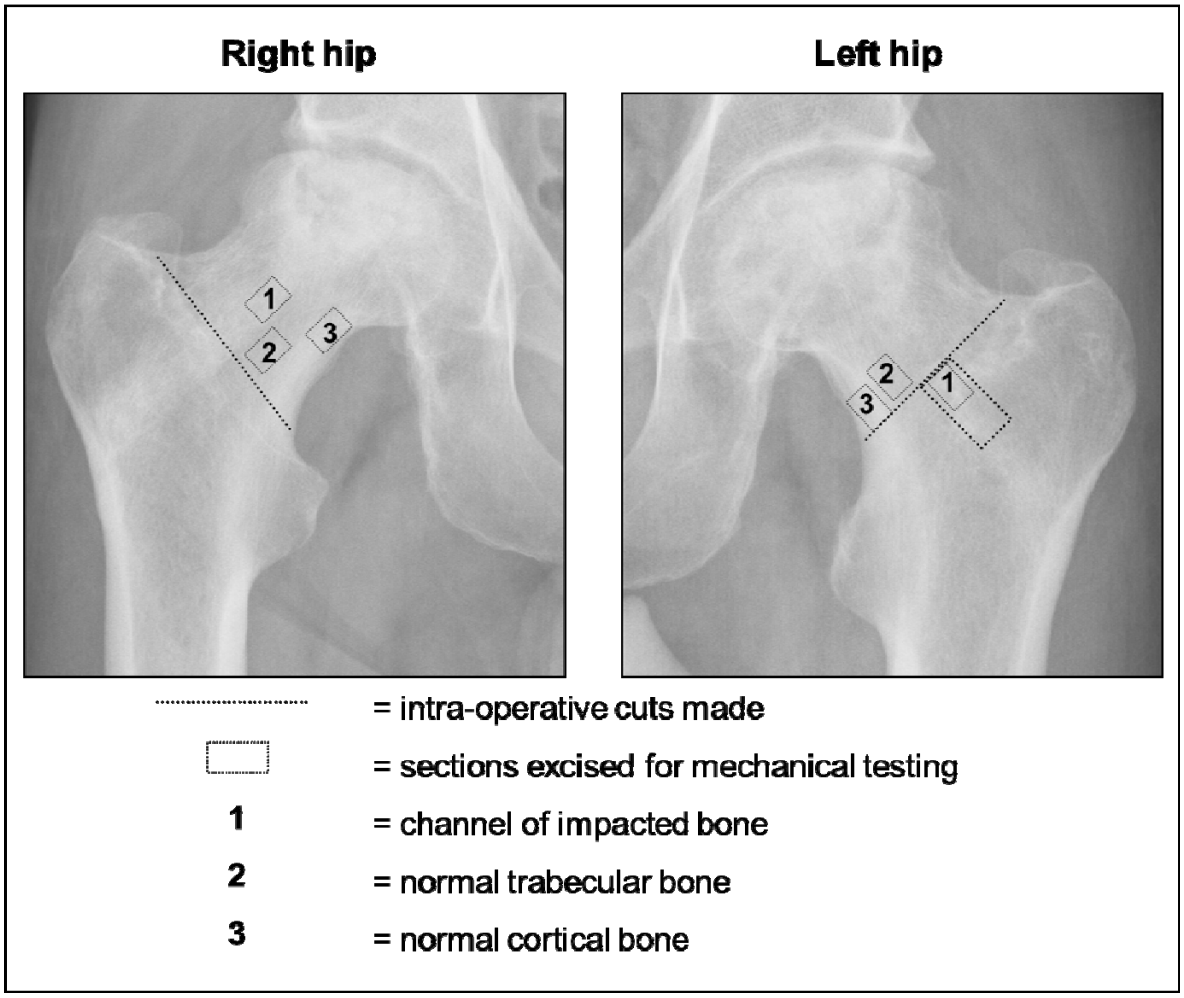

Figure 6: A: Buehler diamond tipped wafering blade for trimming bone sections to equal sized cuboids. B: Hydraulic actuator set to apply a constant rate of compression

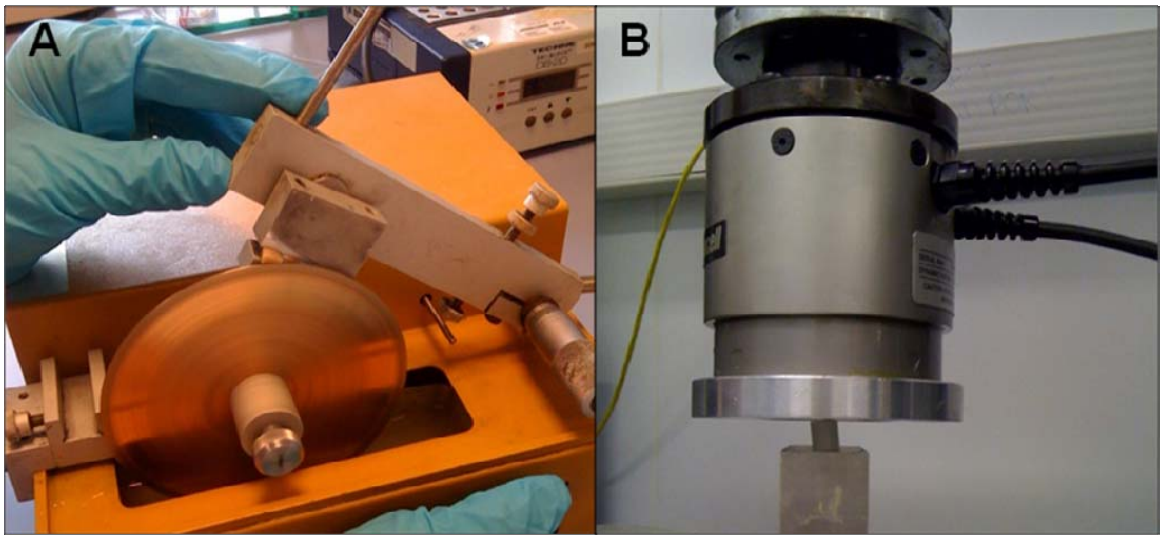

5.5 Results

Clinical follow-up

Three patients remain, to date, asymptomatic at 23-45 month follow-up, with no radiological evidence of collapse **(Fig.7A)**. One patient progressed to bilateral collapse requiring THR **(Fig.7B-C)**, reasons for which are discussed below. This has, however, afforded the unique opportunity to retrieve tissue engineered impacted bone from a human case for *ex-vivo* analysis.

Figure 7: A: Patient 1 at 44 months post-operatively with a right THR (for Stage IV AVN) and a left radio-dense channel of impacted bone, with no collapse. B: CT scan of Patient 4, three days post bilateral IBG & SSC procedure. C: Patient 4, twelve months post-operatively, with bilateral femoral head collapse.

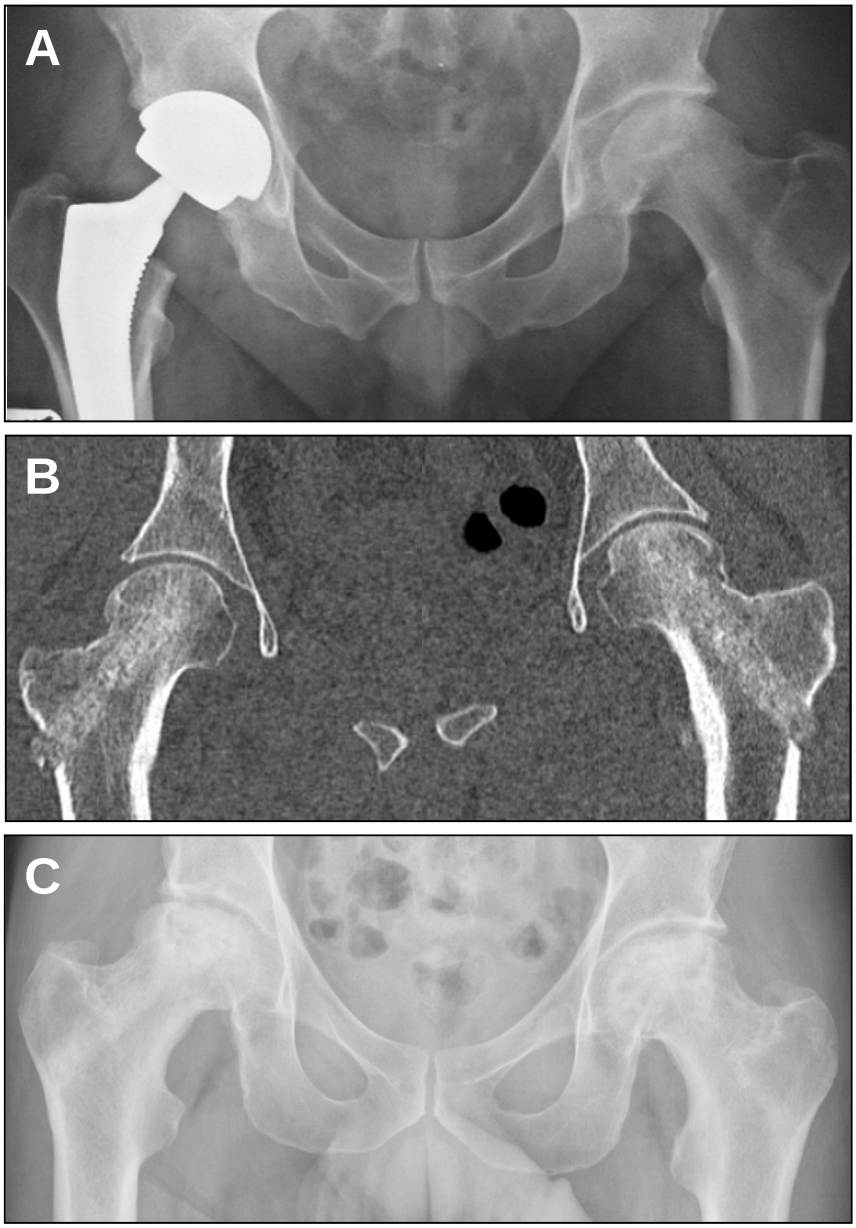

Parallel in vitro assessment

In vitro culture of SSCs on allograft demonstrated sustained cell viability and proliferation on CTG-EH stain **(Fig.8A-C)**.

Figure 8: CTG-EH stain demonstrated enduring cell viability and proliferation on *in vitro* cell-seeded milled allograft. A: 2 weeks culture. B: 4 weeks culture. C: 6 weeks culture.
Scale bar = 200µm.

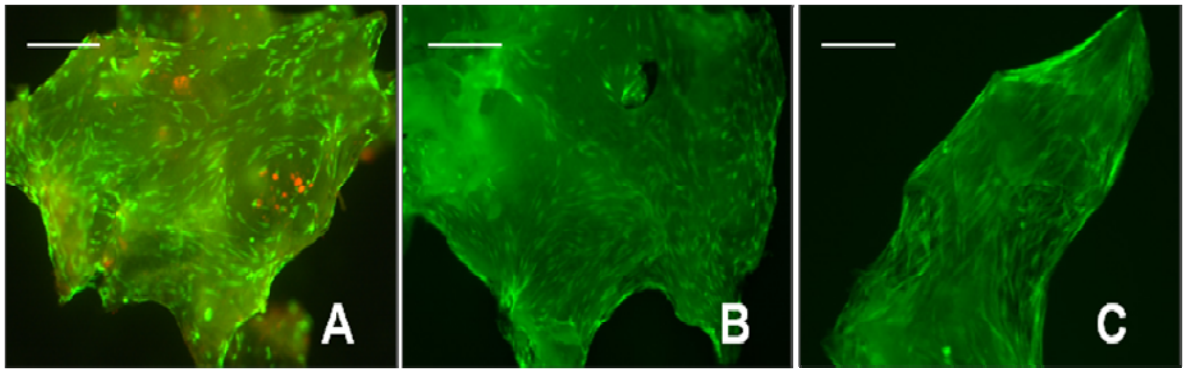

ALP staining identified 148 osteoblastic colonies in 0.5ml of concentrated marrow culture versus 41 osteoblastic colonies in 0.5ml of unconcentrated marrow **(Fig.9)**.

Figure 9: Equal volumes (0.5ml) of unconcentrated marrow versus concentrated marrow from Patient 1, indicating the difference in osteoblast colony number (n=3). Arrows highlight colonies.

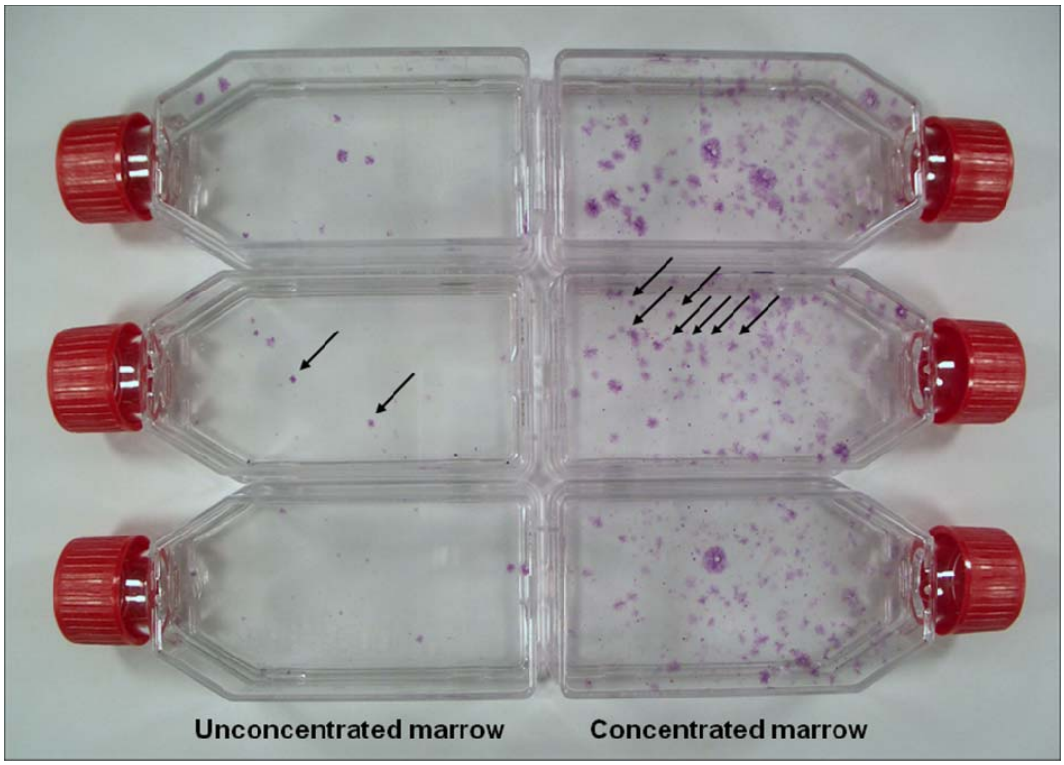

Reasons for collapse of femoral heads of Patient 4

At diagnosis, the necrotic area in the right hip was widespread across the sub-chondral bone **(Fig.10A)**. MRI analysis confirmed a high Mitchell score (Mitchell *et al.* 1989), suggestive of more widespread necrosis than was initially suspected, and predictive of increased technical difficulty in effective curettage of the whole area. Such disease may therefore not have been conducive to treatment by such a percutaneous technique. For the left hip of Patient 4, despite maintenance of femoral head architecture on pre-operative radiographs, high signal could be identified on MRI **(Fig.10B)**. Diagnosis on CT scan of a cyst **(Fig.10C)** confirmed degenerative change that may have been unsalvageable. The collapse that occurred in both femoral heads was focused laterally to the impacted channel of bone, in Mitchell Zone C as illustrated in **Figure 7C**, most likely due to residual necrotic bone beyond the reach of the curette.

Figure 10: Pre-operative images of Patient 4; A: Coronal MRI scan of right hip showing diffuse disease. B: Axial MRI scan showing a focus of high signal density in the left femoral head (circled). C: Axial CT scan identifying this as a cyst in the femoral head (circled).

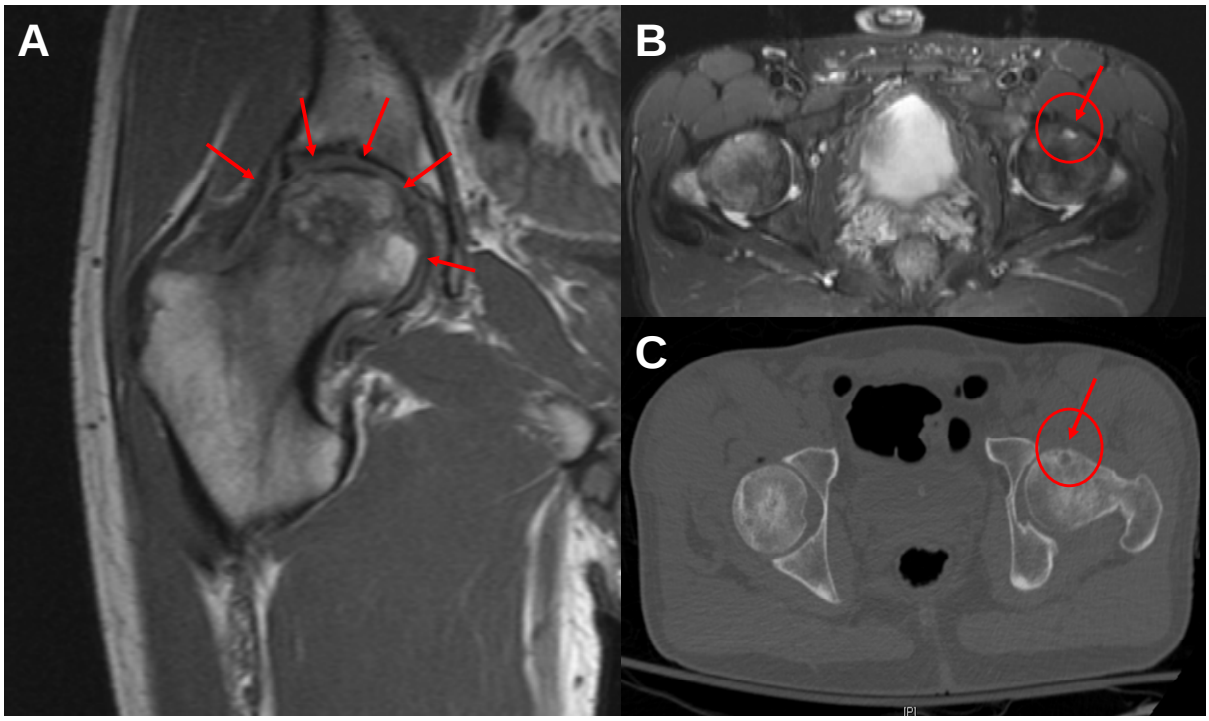

Macroscopic analysis of retrieved femoral heads

Review of the cut surface of the femoral neck identified a demarcated dense central channel of bone, which continued through the femoral head up to the collapsed sub-chondral bone **(Fig.11)**.

Figure 11: Base of right femoral head of Patient 4 seen after surgical neck cut, showing a clearly demarcated dense central channel of remodelled impacted bone.

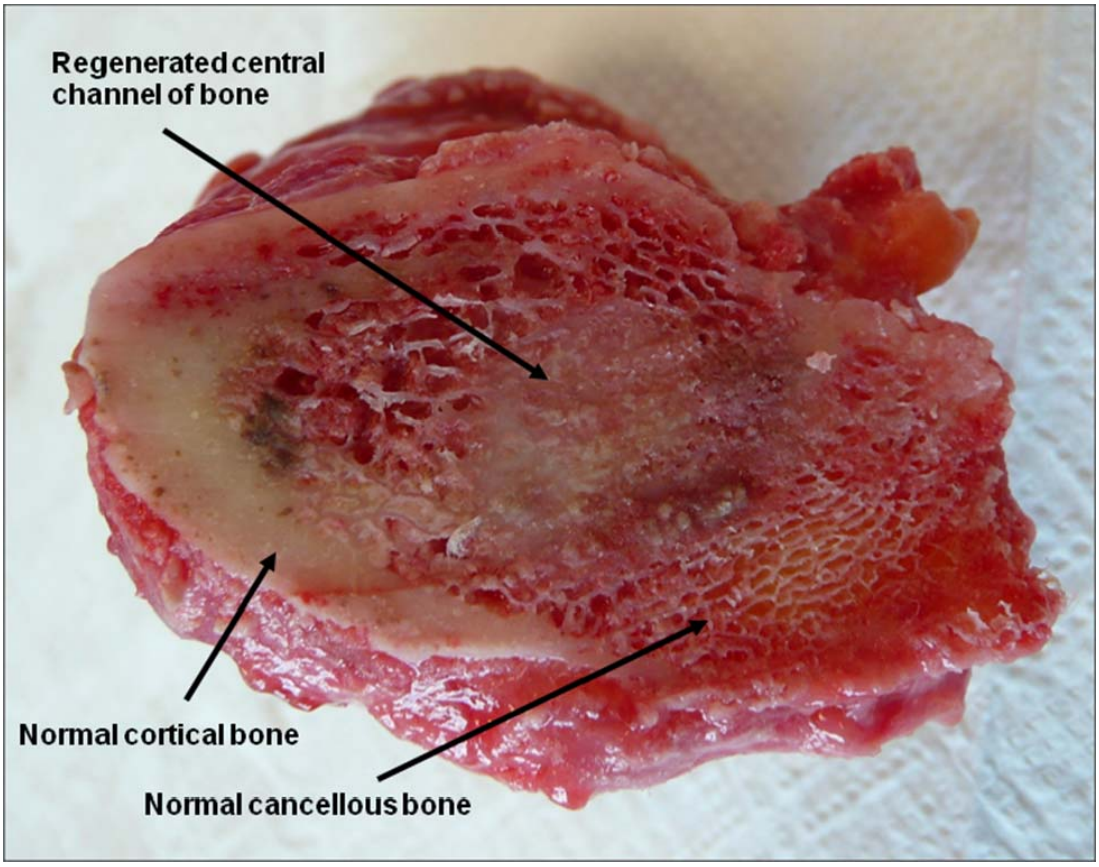

Micro computed tomography (μCT) 3 dimensional reconstruction

Analysis by μCT revealed the dense central channel with a mature uniform trabecular structure visualised in cross section along its length **(Fig.12A-B)**. With the exception of collapsed necrotic sub-chondral tissue, the trabecular micro-architecture was maintained, and observed to be in continuity throughout the impacted channel of bone **(Fig.12D)**. Critically, in contrast to all previous analysis performed on IBG retrieval specimens without SSCs, which show areas of necrosis, fibrosis and non-incorporated graft (van Haaren *et al.* 2007;van der Donk *et al.* 2002;Ling, Timperley, & Linder 1993), no islands of necrotic bone were seen. Furthermore, the trabecular stress lines visualised in cross-

section (**Fig.12B**) cross from normal trabecular to impacted bone, indicating that remodelling has occurred in accordance with Wolff's Law.

Bone density analysis µCT

The apparent bone density for trabecular, cortical and impacted bone was determined by Grey Scale on µCT images. As expected, bone densities in the right and left femoral heads were comparable to each other. Cortical bone was denser than trabecular bone, with a Grey Scale Density of 1800 versus 1200 units. The density of the right and left impacted channels of bone were also comparable to each other, and greater than trabecular bone, with a Grey scale density of 1400 units, illustrated by false-colour coding **(Fig.12C)** and graphically **(Fig.12E)**.

Figure 12: A: µCT 3D reconstruction of retrieved right femoral head from Patient 4 at 70 micron resolution. B: Coronal section revealed a dense channel of impacted bone up to the collapsed area, with trabecular stress lines crossing into the remodelled central channel. C: False-colour scheme of density analysis - Yellow ≤1400 Grey Scale units, Red = 1400-1800 units, Blue ≥1800 units. D: Impacted bone from the left femoral head at 31 micron resolution demonstrated trabeculae in continuity. E: Graph of density analysis corresponding to Fig.13C, with peaks of trabecular, impacted and cortical bone seen at 1200, 1400 and 1800 units respectively.

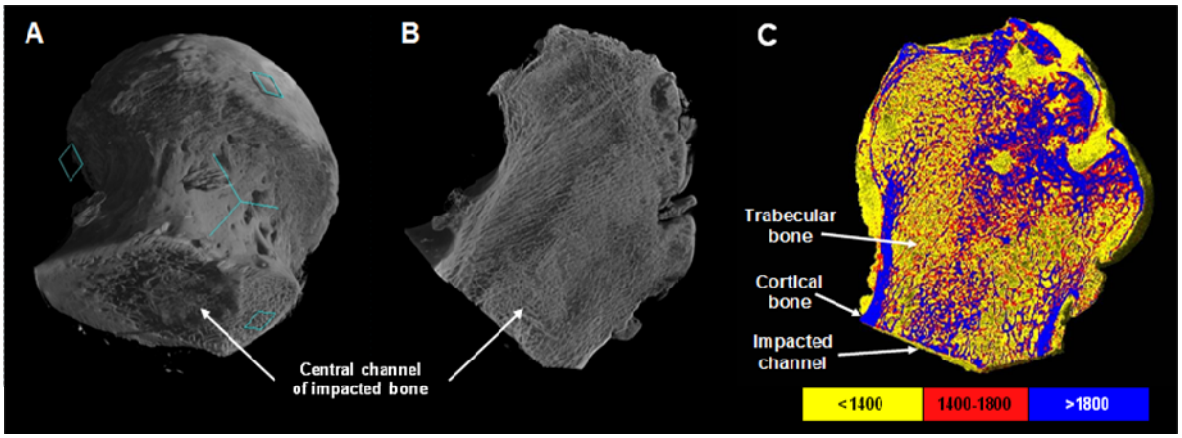

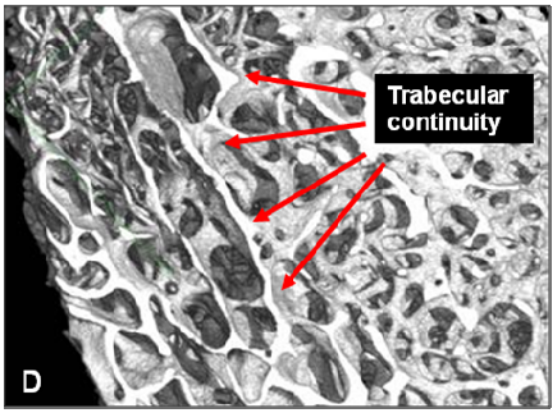

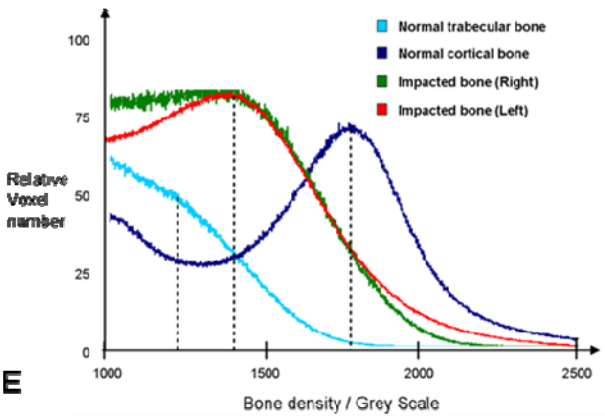

Microscopic analysis by histology

A/S staining of tissue from the impacted channels of retrieved femoral bone showed histology consistent with normal trabecular bone. Osteocytes within lacunae were visible surrounded by a lamellar structure **(Fig.13A)**, which was confirmed as mature organised bone when viewed under polarised light **(Fig.13D)**. The micro-architecture of the impacted bone was observed to be histologically identical to the patient's normal trabecular bone **(Fig.13B,E).** Low power images of impacted bone confirmed the presence of a trabecular structure, incorporating marrow **(Fig 13A inset)**, though macroscopically and on μCT trabeculae were more densely arranged (**Fig.12**). TRAP stain revealed osteoclasts and Howship's lacunae on the bone surfaces of impacted bone **(Fig13G)** and normal trabecular bone **(Fig.13H)**. This microscopic arrangement was grossly different from tissue in the necrotic area which showed a high concentration of osteoclasts, eroded bone **(Fig.13J)**, and a disordered mixture of cartilage, fibrous tissue and bone **(Fig.13C)**. There was negligible evidence of organisation on birefringence **(Fig.13F)**.

Mechanical testing

Comparable values in compressive strength of the cortical, trabecular and impacted bone were found between right and left femoral heads **(Fig.14)**. One-way ANOVA test demonstrated statistical difference between the compressive strength of trabecular and cortical bone, which was confirmed on Bonferroni Multiple Analysis ($n=4$, $p<0.05$). Critically there was no statistical difference in the strengths of trabecular and impacted bone ($p>0.05$).

Figure 13: Histology; A/S stain of impacted bone revealed a trabecular structure (A, inset), with lamellae and cells in lacunae (arrows) (A), comparable to trabecular bone (B); Parallel birefringence confirmed a mature lamellar structure of both (D-E); This contrasts the necrotic tissue which demonstrated a disordered mixture of cartilage, fibrous tissue and bone (C), with negligible evidence of organisation when viewed under polarised light (F); TRAP staining demonstrated normal osteoclasts and Howship's lacunae in impacted bone (G) and trabecular bone (H) but a high concentration of osteoclasts seen in the necrotic bone (J). Arrows in G-J indicate osteoclasts. Scale bars: A,B,D,E = 100µm; A inset,C,F = 200µm; G,H,J = 50µm.

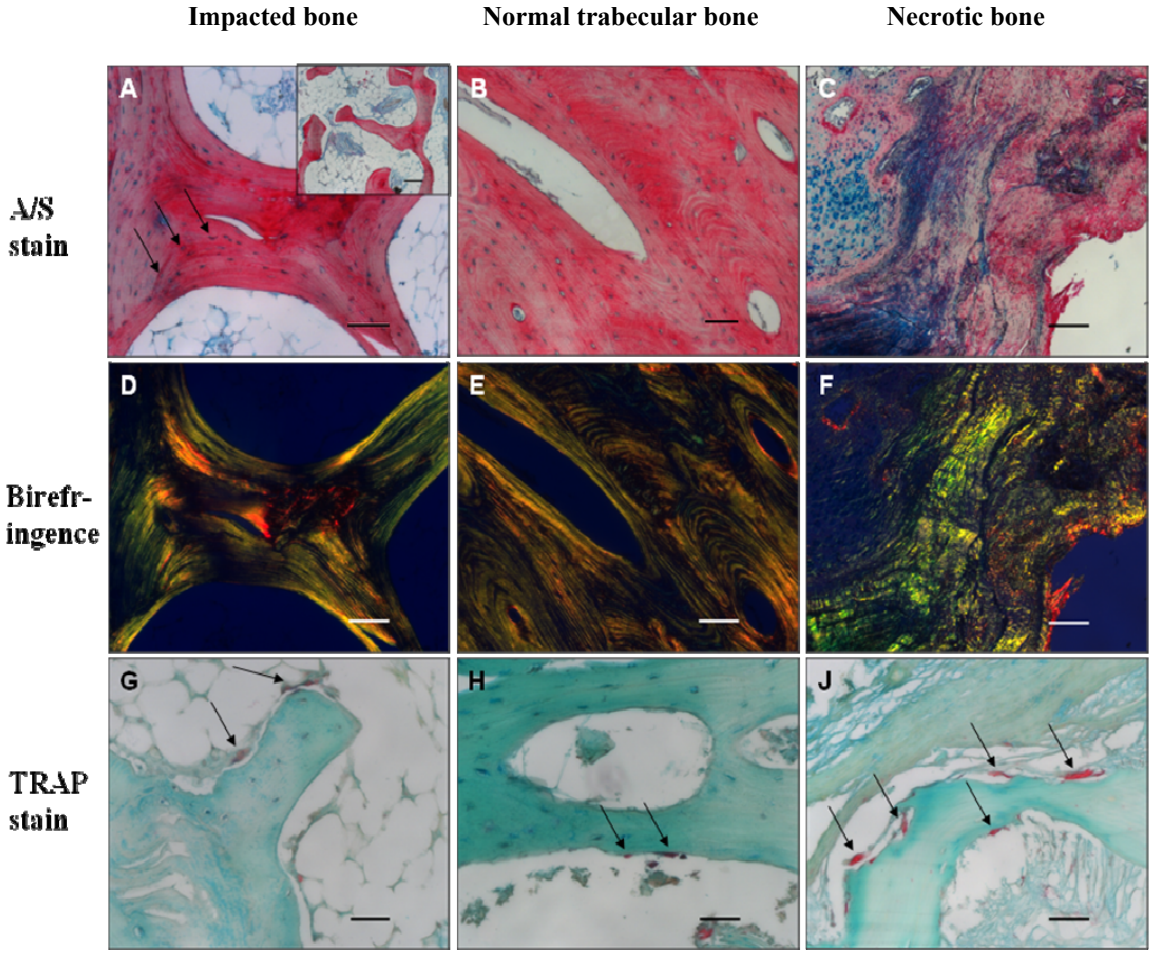

Figure 14: Bar chart demonstrating compressive strengths / MegaPascals of trabecular, impacted and cortical bone of both hips of Patient 4 (n=4). One-way ANOVA test demonstrated statistical difference between trabecular and cortical bone ($p<0.0001$), but no statistical difference between trabecular and impacted bone. Error bars denote Standard Error of Mean, 'ns' = no statistical significance.

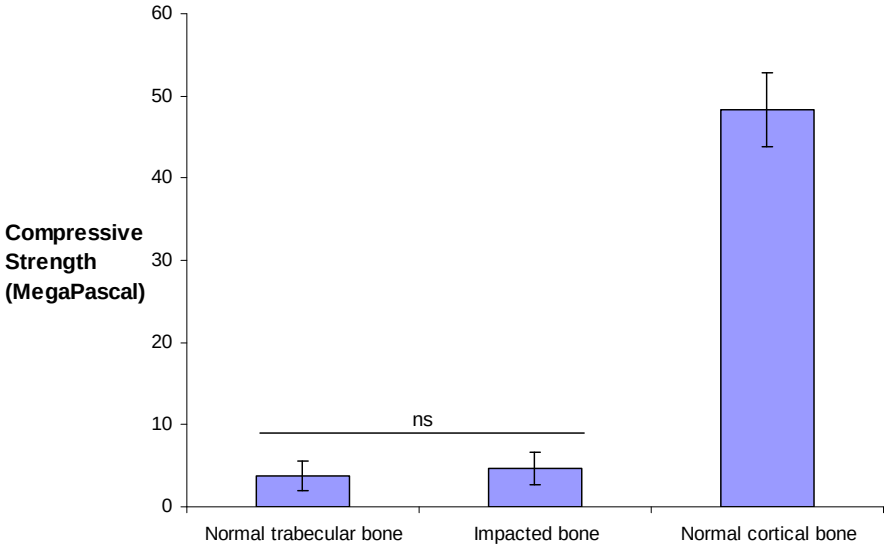

5.6 Discussion

Retrieval of this tissue-engineered impaction bone graft construct has provided the opportunity for *ex vivo* analysis of this novel clinically translated bone regeneration technique. Although collapse occurred in these retrieved specimens at the pathological area due to residual osteonecrotic tissue, analysis of the impacted channel of tissue engineered bone away from this area is revealing: Analysis of architecture, density and mechanical strength indicated the regeneration of a living bony construct in the lines of force.

The continuous trabecular architecture throughout the impacted channel of bone observed by μCT **(Fig.12A,B,D)** provided evidence of remodelling of the milled allograft, to form mature living bone. With the exception of retained pathology in the sub-chondral bone, critically, no necrotic / fibrotic tissue was observed within the impacted channel, indicating all impacted fragments had been integrated, resorbed or remodelled.

Histological analysis confirmed the presence of a mature trabecular bone structure **(Fig.13A,inset)**. Osteoclasts and Howship's lacunae were indicative of normal remodelling **(Fig.13G)** and the lamellar micro-architecture of the impacted bone, with osteocytes in lacunae, was observed to be histologically identical to normal trabecular bone **(Fig.13A,B,D,E)**. These results indicated that SSCs together with the impacted milled allograft resulted in formation of a bone composite that underwent remodelling and incorporation into host bone. This must be contrasted with previous histological analysis performed on retrieval specimens of IBG without supplementation with SSCs (Ling, Timperley, & Linder 1993;van Haaren *et al.* 2007;van der Donk *et al.* 2002). Whilst remodelling has been demonstrated in biopsies from IBG in acetabula and femora, islands of non-incorporated graft with associated necrosis, fibrocartilage and fibrosis remained in all specimens.

Compression testing demonstrated that the regenerated bone was of comparable strength in compression to normal ipsilateral trabecular bone. An aggregate of milled allograft, as originally impacted into the patient, would crumble under minimal loading without lateral constraints *in vitro*. The test segments of impacted bone failed only in compression (not shear despite no lateral constraints), indicating a significant increase in inter-particulate cohesion of the milled fragments. μCT scans confirmed that the fragments were conjoined, which together with the compression testing accounted for the structural integrity.

The Null Hypothesis, that the addition of skeletal stem cells to impaction bone graft has no demonstrable effect on bone formation in clinical translation, can be rejected.

This paper describes a technique which appears to be effective for the treatment of AVN of the femoral head. It supplements each of the current therapies of core decompression (Steinberg 1995), SSCs (Hernigou *et al.* 2009) and IBG (Wang *et al.* 2010) by providing both a biological stimulus for osteogenesis as well as mechanical support for the sub-chondral bone. Three patients remain asymptomatic at medium term follow-up. Furthermore, parallel *in vitro* analysis confirmed cell viability in the implanted tissue, and the *ex vivo* analysis of the two collapsed femoral heads has demonstrated the regeneration of structurally and functionally normal bone in humans. There are, as yet, only a small number of clinical cases compared to the papers of Hernigou (534 hips) (Hernigou *et al.* 2009), Steinberg (300 hips) (Steinberg 1995), Wang (138 hips) (Wang *et al.* 2010) or Yamasaki (30 hips) (Yamasaki *et al.* 2010) and continuation of this clinical trial is necessary. However, the following authors have performed extensive *in vitro* and *in vivo* studies on SSC augmentation of bone regeneration on IBG: (Bolland *et al.* 2007;Bolland *et al.* 2008;Korda *et al.* 2008;Korda *et al.* 2006;Burwell 1964;Arthur, Zannettino, & Gronthos 2009;Hernigou *et al.* 2005b).

While clinical translation of tissue engineering strategies remains rare (Tare *et al.* 2010;Reichert *et al.* 2009), the analysis of this tissue engineering construct from bench to clinic and back has confirmed the potential of SSC constructs for bone regeneration in humans. This technique offers significant potential for treatment of the broader spectrum of bone defects, such as bone loss following trauma, infection or tumour.

Chapter VI

Conclusions and future perspectives

6.1 Conclusions

The experimental strategies and clinical application detailed in this thesis have allowed us to refute the Major Null Hypothesis that 'Skeletal stem cells cannot be used to augment bone formation'. Thus, as Phoenix rose from the ashes, regenerated anew to live again (**Fig.1**), this tissue engineering technology offers potential for translation from the bench to the clinic for regeneration of bone tissue.

Figure 1: The sacred firebird Phoenix, depicted in 'Bilderbuch fur Kinder' c 1790 by Friedrich Johann Justin Bertuch (1747-1822).

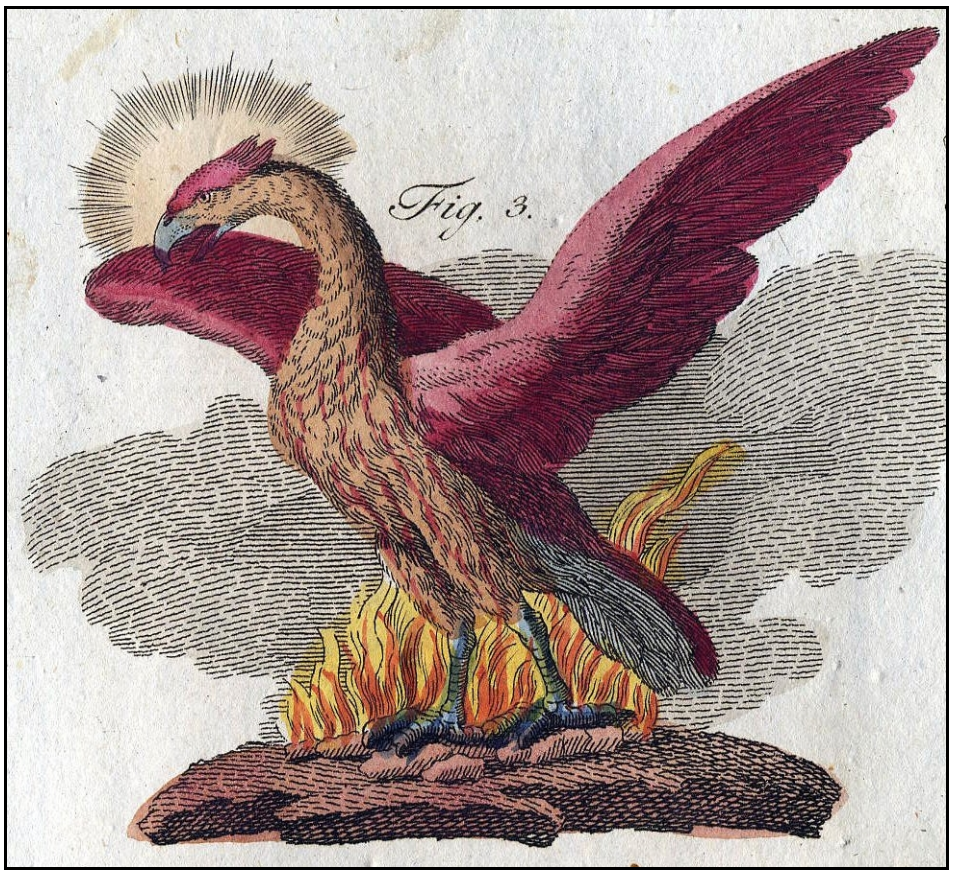

The conclusions from the experimental strategies and clinical application detailed in this thesis are summarised below:

Effect of Skeletal Stem Cells and Human Fibronectin on the Biomechanical Properties of Impacted Bone after Impaction Bone Grafting

The combination of coating human fibronectin onto milled allograft and seeding with skeletal stem cells was shown to improve the mechanical properties of the impaction bone graft construct. Further work should focus on the seeding density of SSCs and parameters for optimising HFN coating of allograft.

The Effect of Scaffold Porosity on Skeletal Stem Cell Growth and Differentiation

A novel technique for fabrication of ceramic scaffolds has enabled control of porosity and pore size in an HA/TCP porous scaffold. *In vivo* culture of SSCs on scaffolds of two determined porosities showed increased SSC proliferation, osteogenic differentiation and osteoid formation on the more porous 45ppi scaffold, as measured by SEM, μCT and biochemical analysis.

The enrichment of skeletal stem cells from human bone marrow to enhance skeletal repair

The skeletal stem cell fraction from aspirated autologous bone marrow of an elderly cohort of patients was successfully enriched to a therapeutic concentration using a novel acoustic-vibration vacuum-assisted filtration technique. This novel technology is rapid, single use and fully disposable, so is ideally placed for intra-operative clinical use for regeneration of bone defects.

Retrieval analysis of tissue engineered bone within a non-ossifying fibroma of the femoral neck

This tissue engineered impaction bone graft construct retrieved from a human patient has provided a rare opportunity for *ex vivo* analysis. Histology and μCT demonstrated some mature bone formation but with associated necrosis, fibrosis and islands of non-incorporated graft. The bone marrow aspirate that had been seeded onto the milled allograft had a low SSC yield, which has subsequently been demonstrated to be sub-therapeutic for musculoskeletal application.

Exploring the pathogenesis of unicameral bone cysts

Fluid aspirated from the unicameral bone cysts (UBCs) of two patients was shown to stimulate SSC proliferation and osteoblastic differentiation *in vitro*. A high concentration of osteoclasts was identified in the cyst lining and the pro-osteoclast cytokines IL-6, MCP-1 and MIP-1α were found in grossly elevated levels in the cyst fluid. These results indicated a RANKL mediated signalling abnormality to be the underlying pathophysiological cause of UBCs. Further exploration of the cytokine profile of UBC cyst fluid is planned.

A novel tissue engineering strategy for the treatment of avascular necrosis of the femoral head, with analysis of retrieval specimens

This study describes a technique which appears to be effective for the treatment of AVN of the femoral head, by providing both a biological stimulus for osteogenesis as well as mechanical support for the sub-chondral bone. Three patients remain asymptomatic at up to 4 year follow-up. The analysis of this tissue engineering construct from bench to clinic and back has confirmed the potential of SSC constructs for bone regeneration in humans. This technique offers significant potential for treatment of the broader spectrum of bone defects, such as bone loss following trauma, infection or tumour.

6.2 Future Perspectives

Current strategies for the treatment of lost bone stock have inherent disadvantages and in view of ever increasing demand, there is a pressing need for novel treatment modalities. The possibilities of tissue regeneration have been proposed since the time of Prometheus, but only in the last ten years has the field of skeletal stem cells and tissue regeneration changed dramatically, with the generation of induced pluripotent stem cells, culture strategies for adult and foetal and embryonic stem cells and tissue specific application (Takahashi & Yamanaka 2006). Skeletal cell-based strategies auger well for future orthopaedic use and suggest that the combination of a patient's enriched skeletal stem cells added to an appropriate synthetic scaffold or allograft is a promising technique for bone tissue regeneration. The ideal scaffold would be biocompatible and have structural integrity, yet be appropriately bioresorpable, acting as a temporary framework until new bone is generated. This thesis goes some way to answering questions on this emerging technology, upon which foundation the complexities of bone tissue regeneration can continue to be explored.

The continuing basic science breakthroughs for novel bone tissue engineering techniques has afforded the opportunity to push the boundaries of tissue engineering strategies in clinical practice, where other treatment modalities have failed. The gathering tide of robust *in vitro* evidence is finally beginning to produce tangible clinical results as the first steps to cross the translational gap to patient application are taken. However there remains a scarcity of clinical translation from bench to clinic. The absence of reliable controls in the few case series reported in the literature prohibit the routine clinical use of many of these strategies until large scale randomised double blind clinical trials have been performed. In addition, development and manufacture will require continued financial input, which may become harder to find in the current fiscal climate until greater numbers of translated therapies reach the market.

In the field of orthopaedics, the next decade will see intense focus on not only autologous stem cell but allogeneic skeletal stem cell application to regenerate the patient's bone. Enrichment of SSCs from autologous bone marrow will move to research programmes to derive and apply stem cells derived from allogeneic ("universal donor stem cell") and in time, patient specific induced pluripotent cell populations, providing new practical paths to clinical translation. The wealth of basic science in the bone tissue engineering arena and

emerging translational cases, indicates the application of skeletal stem cells will reach routine patient benefit over the coming decade.

The research and development of tissue engineering technology for orthopaedic applications clearly requires close co-ordination within a multidisciplinary framework involving surgeons, physicians, patients, mathematicians, cell scientists and biomedical engineers (Watt & Driskell). As described in 1999 regarding the Bone & Joint Decade: "The Decade aims to promote partnership with patient, professional and scientific organisations, research bodies, scientific journals, health-care providers, governments and non-governmental organisations in all countries and regions. The vital need for adequate funding for orthopaedic research must be made clear and continual attention will be drawn to this throughout the Decade." (Horan *et al.* 1999). The goals and strategies of tissue engineering are similar to those of The Bone and Joint Decade and these new evolving techniques in bone regeneration may offer a solution for the growing burden of musculoskeletal pathology. As we reach the end of the Bone and Joint Decade, perhaps these new developments have heralded the start of 'The Regenerative Medicine Decade'.

Reference List

1. AARVOLD A, JONES AMH, NEW AM, DUNLOP DG, & OREFFO RO. The Treatment of Avascular Necrosis of the Femoral Head Using Impaction Bone Grafting and Skeletal Stem Cells. J Bone Joint Surg Br In Press, British Orthopaedic Research Society 2010[Supplement]. 2011.

2. ABED YY, BELTRAMI G, CAMPANACCI DA *et al.* (2009) Biological Reconstruction After Resection of Bone Tumours Around the Knee: Long-Term Follow-Up. *J.Bone Joint Surg.Br.* 91, 1366-1372.

3. AHLMANN E, PATZAKIS M, ROIDIS N, SHEPHERD L, & HOLTOM P (2002) Comparison of Anterior and Posterior Iliac Crest Bone Grafts in Terms of Harvest-Site Morbidity and Functional Outcomes. *J.Bone Joint Surg.Am.* 84-A, 716-720.

4. ALDEGHERI R (1999) Distraction Osteogenesis for Lengthening of the Tibia in Patients Who Have Limb-Length Discrepancy or Short Stature. *J.Bone Joint Surg.Am.* 81, 624-634.

5. ALSOUSOU J, THOMPSON M, HULLEY P, NOBLE A, & WILLETT K (2009) The Biology of Platelet-Rich Plasma and Its Application in Trauma and Orthopaedic Surgery: a Review of the Literature. *J.Bone Joint Surg.Br.* 91, 987-996.

6. ANCEY C, KUSTER A, HAAN S *et al.* (2003) A Fusion Protein of the Gp130 and Interleukin-6Ralpha Ligand-Binding Domains Acts As a Potent Interleukin-6 Inhibitor. *J.Biol.Chem.* 278, 16968-16972.

7. ARNETT TR (2008) Extracellular PH Regulates Bone Cell Function. *J.Nutr.* 138, 415S-418S.

8. ARNETT TR & DEMPSTER DW (1986) Effect of PH on Bone Resorption by Rat Osteoclasts in Vitro. *Endocrinology* 119, 119-124.

9. ARONSON J (1997) Limb-Lengthening, Skeletal Reconstruction, and Bone Transport With the Ilizarov Method. *J.Bone Joint Surg.Am.* 79, 1243-1258.

10. ARTHUR A, ZANNETTINO A, & GRONTHOS S (2009) The Therapeutic Applications of Multipotential Mesenchymal/Stromal Stem Cells in Skeletal Tissue Repair. *J Cell Physiol* 218, 237-245.

11. BAAS J (2008) Adjuvant Therapies of Bone Graft Around Non-Cemented Experimental Orthopedic Implants Stereological Methods and Experiments in Dogs. *Acta Orthop.Suppl* 79, 1-43.

12. BANFI A, MURAGLIA A, DOZIN B *et al.* (2000) Proliferation Kinetics and Differentiation Potential of Ex Vivo Expanded Human Bone Marrow Stromal Cells: Implications for Their Use in Cell Therapy. *Exp.Hematol.* 28, 707-715.

13. BIANCO P & ROBEY PG (2001) Stem Cells in Tissue Engineering. *Nature* 414, 118-121.

14. BIANCO P & ROBEY PG (2004) Skeletal Stem Cells. In: *Handbook of stem cells* (eds. L Robert, G John, H Brigid *et al.*), 415-424. Burlington Academic Press.

15. BIOMET BIOLOGICS INC. Marrowstim Concentration System. 2007.

16. BLOODGOOD JC (1910) I. Benign Bone Cysts, Ostitis Fibrosa, Giant-Cell Sarcoma and Bone Aneurism of the Long Pipe Bones: A Clinical and Pathological Study With the Conclusion That Conservative Treatment Is Justifiable. *Ann.Surg.* 52, 145-185.

17. BOBYN JD, POGGIE RA, KRYGIER JJ *et al.* (2004) Clinical Validation of a Structural Porous Tantalum Biomaterial for Adult Reconstruction. *J.Bone Joint Surg.Am.* 86-A Suppl 2, 123-129.

18. BOLLAND BJ, KANCZLER JM, GINTY PJ *et al.* (2008) The Application of Human Bone Marrow Stromal Cells and Poly(Dl-Lactic Acid) As a Biological Bone Graft Extender in Impaction Bone Grafting. *Biomaterials* 29, 3221-3227.

19. BOLLAND BJ, PARTRIDGE K, TILLEY S *et al.* (2006) Biological and Mechanical Enhancement of Impacted Allograft Seeded With Human Bone Marrow Stromal Cells: Potential Clinical Role in Impaction Bone Grafting. *Regen.Med.* 1, 457-467.

20. BOLLAND BJ, TILLEY S, NEW AM, DUNLOP DG, & OREFFO RO (2007) Adult Mesenchymal Stem Cells and Impaction Grafting: a New Clinical Paradigm Shift. *Expert.Rev.Med.Devices* 4, 393-404.

21. BRANDAO-BURCH A, UTTING JC, ORRISS IR, & ARNETT TR (2005) Acidosis Inhibits Bone Formation by Osteoblasts in Vitro by Preventing Mineralization. *Calcif.Tissue Int.* 77, 167-174.

22. BROWN JS & SHAW RJ (2010) Reconstruction of the Maxilla and Midface: Introducing a New Classification. *The Lancet Oncology* 11, 1001-1008.

23. BULLENS PH, SCHREUDER HW, MALEFIJT MC, VERDONSCHOT N, & BUMA P (2009) The Presence of Periosteum Is Essential for the Healing of Large Diaphyseal Segmental Bone Defects Reconstructed With Trabecular Metal: A Study in the Femur of Goats. *J.Biomed.Mater.Res.B Appl.Biomater.* 92B, 24-31.

24. BURWELL RG (1964) Studies in the Transplantation of Bone. VII. The Frsh Composite Homograft-Autocraft of Cancellous Bone; an Anlysis of Factors Leading to Osteogenesis in Marrow Transplants and in Marrow-Continaing Bone Grafts. *J Bone Joint Surg.Br.* 46, 110-140.

25. BUSSARD KM, VENZON DJ, & MASTRO AM (2010) Osteoblasts Are a Major Source of Inflammatory Cytokines in the Tumor Microenvironment of Bone Metastatic Breast Cancer. *J.Cell Biochem.* 111, 1138-1148.

26. CAHILL KS, CHI JH, DAY A, & CLAUS EB (2009) Prevalence, Complications, and Hospital Charges Associated With Use of Bone-Morphogenetic Proteins in Spinal Fusion Procedures. *JAMA* 302, 58-66.

27. CAI Z, CHEN Q, CHEN J *et al.* (2009) Monocyte Chemotactic Protein 1 Promotes Lung Cancer-Induced Bone Resorptive Lesions in Vivo. *Neoplasia.* 11, 228-236.

28. CAPANNA R, CAMPANACCI DA, BELOT N *et al.* (2007) A New Reconstructive Technique for Intercalary Defects of Long Bones: the Association of Massive Allograft With Vascularized Fibular Autograft. Long-Term Results and Comparison With Alternative Techniques. *Orthop.Clin.North Am.* 38, 51-60, vi.

29. CAPANNA R, CAMPANACCI DA, & MANFRINI M (1996) Unicameral and Aneurysmal Bone Cysts. *Orthop.Clin.North Am.* 27, 605-614.

30. CAPANNA R, DAL MA, GITELIS S, & CAMPANACCI M (1982) The Natural History of Unicameral Bone Cyst After Steroid Injection. *Clin.Orthop.Relat Res.* 204-211.

31. CENNI E, SAVARINO L, PERUT F *et al.* (2009) Background and Rationale of Platelet Gel in Orthopaedic Surgery. *Musculoskelet.Surg.*

32. CHIGIRA M, MAEHARA S, ARITA S, & UDAGAWA E (1983) The Aetiology and Treatment of Simple Bone Cysts. *J.Bone Joint Surg.Br.* 65, 633-637.

33. CODIVILLA A (2008) The Classic: On the Means of Lengthening, in the Lower Limbs, the Muscles and Tissues Which Are Shortened Through Deformity. 1905. *Clin.Orthop.Relat Res.* 466, 2903-2909.

34. COHEN J (1960) Simple Bone Cysts. Studies of Cyst Fluid in Six Cases With a Theory of Pathogenesis. *J.Bone Joint Surg.Am.* 42-A, 609-616.

35. COHEN J (1977) Unicameral Bone Cysts. a Current Synthesis of Reported Cases. *Orthop.Clin.North Am.* 8, 715-736.

36. CONNOLLY JF, GUSE R, TIEDEMAN J, & DEHNE R (1991) Autologous Marrow Injection As a Substitute for Operative Grafting of Tibial Nonunions. *Clin.Orthop.Relat Res.* 259-270.

37. COOL SM & NURCOMBE V (2005) Substrate Induction of Osteogenesis From Marrow-Derived Mesenchymal Precursors. *Stem Cells Dev.* 14, 632-642.

38. COX G, GIANNOUDIS P, BOXALL S *et al.* (2010) The investigation of the abundance of mesenchymal stem cells within the intra-medullary cavities of long bones.

39. CRAIG MJ & LOBERG RD (2006) CCL2 (Monocyte Chemoattractant Protein-1) in Cancer Bone Metastases. *Cancer Metastasis Rev.* 25, 611-619.

40. D'IPPOLITO G, SCHILLER PC, RICORDI C, ROOS BA, & HOWARD GA (1999) Age-Related Osteogenic Potential of Mesenchymal Stromal Stem Cells From Human Vertebral Bone Marrow. *J.Bone Miner.Res.* 14, 1115-1122.

41. DAHABREH Z, DIMITRIOU R, & GIANNOUDIS PV (2007) Health Economics: a Cost Analysis of Treatment of Persistent Fracture Non-Unions Using Bone Morphogenetic Protein-7. *Injury* 38, 371-377.

42. DE SANCTIS N & ANDREACCHIO A (2006) Elastic Stable Intramedullary Nailing Is the Best Treatment of Unicameral Bone Cysts of the Long Bones in Children?: Prospective Long-Term Follow-Up Study. *J.Pediatr.Orthop.* 26, 520-525.

43. DELLOYE C, CORNU O, DRUEZ V, & BARBIER O (2007) Bone Allografts: What They Can Offer and What They Cannot. *J.Bone Joint Surg.Br.* 89, 574-579.

44. DOCQUIER PL & DELLOYE C (2003) Treatment of Simple Bone Cysts With Aspiration and a Single Bone Marrow Injection. *J.Pediatr.Orthop.* 23, 766-773.

45. DUNLOP DG, BREWSTER NT, MADABHUSHI SP *et al.* (2003) Techniques to Improve the Shear Strength of Impacted Bone Graft: the Effect of Particle Size and Washing of the Graft. *J.Bone Joint Surg.Am.* 85-A, 639-646.

46. ELDRIDGE JD, SMITH EJ, HUBBLE MJ, WHITEHOUSE SL, & LEARMONTH ID (1997) Massive Early Subsidence Following Femoral Impaction Grafting. *J.Arthroplasty* 12, 535-540.

47. EMMS NW, BUCKLEY SC, STOCKLEY I, HAMER AJ, & KERRY RM (2009) Mid- to Long-Term Results of Irradiated Allograft in Acetabular Reconstruction: a Follow-Up Report. *J.Bone Joint Surg.Br.* 91, 1419-1423.

48. EWARD WC, KONTOGEORGAKOS V, LEVIN LS, & BRIGMAN BE (2009) Free Vascularized Fibular Graft Reconstruction of Large Skeletal Defects After Tumor Resection. *Clin.Orthop.Relat Res.*

49. FELLAH BH, GAUTHIER O, WEISS P, CHAPPARD D, & LAYROLLE P (2008) Osteogenicity of Biphasic Calcium Phosphate Ceramics and Bone Autograft in a Goat Model. *Biomaterials* 29, 1177-1188.

50. FENG J, YANG Z, LI Y *et al.* (2006) The Rational Designed Antagonist Derived From the Complex Structure of Interleukin-6 and Its Receptor Affectively Blocking Interleukin-6 Might Be a Promising Treatment in Multiple Myeloma. *Biochimie* 88, 1265-1273.

51. FICAT RP (1985) Idiopathic Bone Necrosis of the Femoral Head. Early Diagnosis and Treatment. *J Bone Joint Surg.Br.* 67, 3-9.

52. FINDLAY DM, WELLDON K, ATKINS GJ *et al.* (2004) The Proliferation and Phenotypic Expression of Human Osteoblasts on Tantalum Metal. *Biomaterials* 25, 2215-2227.

53. FLECHER X, SPORER S, & PAPROSKY W (2008) Management of Severe Bone Loss in Acetabular Revision Using a Trabecular Metal Shell. *J.Arthroplasty* 23, 949-955.

54. FRIEDENSTEIN AJ (1976) Precursor Cells of Mechanocytes. *Int.Rev.Cytol.* 47, 327-359.

55. FRIEDENSTEIN AJ, IVANOV-SMOLENSKI AA, CHAJLAKJAN RK *et al.* (1978) Origin of Bone Marrow Stromal Mechanocytes in Radiochimeras and Heterotopic Transplants. *Exp.Hematol.* 6, 440-444.

56. FRIEDENSTEIN AJ, PETRAKOVA KV, KUROLESOVA AI, & FROLOVA GP (1968) Heterotopic of Bone Marrow. Analysis of Precursor Cells for Osteogenic and Hematopoietic Tissues. *Transplantation* 6, 230-247.

57. FUJIBAYASHI S, NEO M, KIM HM, KOKUBO T, & NAKAMURA T (2004) Osteoinduction of Porous Bioactive Titanium Metal. *Biomaterials* 25, 443-450.

58. GERASIMOV AM, TOPOROVA SM, FURTSEVA LN *et al.* (1991) The Role of Lysosomes in the Pathogenesis of Unicameral Bone Cysts. *Clin.Orthop.Relat Res.* 53-63.

59. GETGOOD A, BROOKS R, FORTIER L, & RUSHTON N (2009) Articular Cartilage Tissue Engineering: Today's Research, Tomorrow's Practice? *J.Bone Joint Surg.Br.* 91, 565-576.

60. GIANNINI S, BUDA R, VANNINI F, CAVALLO M, & GRIGOLO B (2009) One-Step Bone Marrow-Derived Cell Transplantation in Talar Osteochondral Lesions. *Clin.Orthop.Relat Res.* 467, 3307-3320.

61. GLOBUS RK, DOTY SB, LULL JC *et al.* (1998) Fibronectin Is a Survival Factor for Differentiated Osteoblasts. *J.Cell Sci.* 111 (Pt 10), 1385-1393.

62. GREEN DW, BOLLAND BJ, KANCZLER JM *et al.* (2009) Augmentation of Skeletal Tissue Formation in Impaction Bone Grafting Using Vaterite Microsphere Biocomposites. *Biomaterials* 30, 1918-1927.

63. GREY A, MITNICK MA, SHAPSES S *et al.* (1996) Circulating Levels of Interleukin-6 and Tumor Necrosis Factor-Alpha Are Elevated in Primary Hyperparathyroidism and Correlate With Markers of Bone Resorption--a Clinical Research Center Study. *J.Clin.Endocrinol.Metab* 81, 3450-3454.

64. GRONTHOS S (2004) Reconstruction of Human Mandible by Tissue Engineering. *Lancet* 364, 735-736.

65. GRONTHOS S & ZANNETTINO AC (2008) A Method to Isolate and Purify Human Bone Marrow Stromal Stem Cells. *Methods Mol.Biol.* 449, 45-57.

66. HABIBOVIC P & DE GROOT K (2007) Osteoinductive Biomaterials--Properties and Relevance in Bone Repair. *J Tissue Eng Regen.Med.* 1, 25-32.

67. HABIBOVIC P, SEES TM, VAN DEN DOEL MA, VAN BLITTERSWIJK CA, & DE GROOT K (2006a) Osteoinduction by Biomaterials--Physicochemical and Structural Influences. *J Biomed.Mater Res.A* 77, 747-762.

68. HABIBOVIC P, YUAN H, VAN DEN DOEL M *et al.* (2006b) Relevance of Osteoinductive Biomaterials in Critical-Sized Orthotopic Defect. *J Orthop.Res.* 24, 867-876.

69. HALLIDAY BR, ENGLISH HW, TIMPERLEY AJ, GIE GA, & LING RS (2003) Femoral Impaction Grafting With Cement in Revision Total Hip Replacement. Evolution of the Technique and Results. *J.Bone Joint Surg.Br.* 85, 809-817.

70. HARTMANN EK, HEINTEL T, MORRISON RH, & WECKBACH A (2009) Influence of Platelet-Rich Plasma on the Anterior Fusion in Spinal Injuries: a Qualitative and Quantitative Analysis Using Computer Tomography. *Arch.Orthop.Trauma Surg.*

71. HECKMAN JD & SARASOHN-KAHN J (1997) The Economics of Treating Tibia Fractures. The Cost of Delayed Unions. *Bull.Hosp.Jt.Dis.* 56, 63-72.

72. HELIOTIS M, LAVERY KM, RIPAMONTI U, TSIRIDIS E, & DI SL (2006) Transformation of a Prefabricated Hydroxyapatite/Osteogenic Protein-1 Implant into a Vascularised Pedicled Bone Flap in the Human Chest. *Int.J.Oral Maxillofac.Surg.* 35, 265-269.

73. HER MAJESTY'S STATIONERY OFFICE. Human Tissue Act 2004. Chapter 30. 2004.

74. HERNIGOU P & BEAUJEAN F (2002) Treatment of Osteonecrosis With Autologous Bone Marrow Grafting. *Clin.Orthop.Relat Res.* 14-23.

75. HERNIGOU P, MATHIEU G, POIGNARD A *et al.* (2006) Percutaneous Autologous Bone-Marrow Grafting for Nonunions. Surgical Technique. *J.Bone Joint Surg.Am.* 88 Suppl 1 Pt 2, 322-327.

76. HERNIGOU P, POIGNARD A, BEAUJEAN F, & ROUARD H (2005a) Percutaneous Autologous Bone-Marrow Grafting for Nonunions. Influence of the Number and Concentration of Progenitor Cells. *J.Bone Joint Surg.Am.* 87, 1430-1437.

77. HERNIGOU P, POIGNARD A, MANICOM O, MATHIEU G, & ROUARD H (2005b) The Use of Percutaneous Autologous Bone Marrow Transplantation in Nonunion and Avascular Necrosis of Bone. *J.Bone Joint Surg.Br.* 87, 896-902.

78. HERNIGOU P, POIGNARD A, ZILBER S, & ROUARD H (2009) Cell Therapy of Hip Osteonecrosis With Autologous Bone Marrow Grafting. *Indian J.Orthop.* 43, 40-45.

79. HIBI H, YAMADA Y, UEDA M, & ENDO Y (2006) Alveolar Cleft Osteoplasty Using Tissue-Engineered Osteogenic Material. *Int.J.Oral Maxillofac.Surg.* 35, 551-555.

80. HINDLE P (2010) Winner of the Frank Horan Essay Prize: the Effect of War on the Evolution of the Treatment of Open Fractures. *J.Bone Joint Surg.Br.* 92, 1632-1635.

81. HOLLISTER SJ (2009) Scaffold Engineering: a Bridge to Where? *Biofabrication.* 1, 012001.

82. HORAN F, MARTI RK, SEDEL L, DICKSON RA, & RUSHTON N (1999) The Bone & Joint Decade - 2000 to 2010. *J.Bone Joint Surg.Br.* 81-B, 377-379.

83. HSU YH, TURNER IG, & MILES AW (2007) Fabrication and Mechanical Testing of Porous Calcium Phosphate Bioceramic Granules. *J Mater Sci Mater Med.* 18, 1931-1937.

84. HUANG CH, CHEN MH, YOUNG TH, JENG JH, & CHEN YJ (2009) Interactive Effects of Mechanical Stretching and Extracellular Matrix Proteins on Initiating Osteogenic Differentiation of Human Mesenchymal Stem Cells. *J.Cell Biochem.* 108, 1263-1273.

85. HUTMACHER DW, SCHANTZ JT, LAM CX, TAN KC, & LIM TC (2007) State of the Art and Future Directions of Scaffold-Based Bone Engineering From a Biomaterials Perspective. *J.Tissue Eng Regen.Med.* 1, 245-260.

86. INNOCENTI M, ABED YY, BELTRAMI G *et al.* (2009) Biological Reconstruction After Resection of Bone Tumors of the Proximal Tibia Using Allograft Shell and Intramedullary Free Vascularized Fibular Graft: Long-Term Results. *Microsurgery* 29, 361-372.

87. INTINI G (2009) The Use of Platelet-Rich Plasma in Bone Reconstruction Therapy. *Biomaterials* 30, 4956-4966.

88. ISHIMI Y, MIYAURA C, JIN CH *et al.* (1990) IL-6 Is Produced by Osteoblasts and Induces Bone Resorption. *J.Immunol.* 145, 3297-3303.

89. JONES AMH, FOONG TS, NEW AM *et al.* The Effect of Skeletal Stem Cells, Hydroxyapatite Coated Stem Cells and Collagen Coated Allograft on the Biomechanical Properties of Impacted Bone Graft. European Cells & Materials 18[Supp 2], 26. 2009. 8-7-2009.

90. KANAKARIS NK, PALIOBEIS C, NLANIDAKIS N, & GIANNOUDIS PV (2007) Biological Enhancement of Tibial Diaphyseal Aseptic Non-Unions: the Efficacy of Autologous Bone Grafting, BMPs and Reaming by-Products. *Injury* 38 Suppl 2, S65-S75.

91. KEIZER SB, KOCK NB, DIJKSTRA PD, TAMINIAU AH, & NELISSEN RG (2006) Treatment of Avascular Necrosis of the Hip by a Non-Vascularised Cortical Graft. *J Bone Joint Surg.Br.* 88, 460-466.

92. KHAN WS, JOHNSON DS, & HARDINGHAM TE (2010) The Potential of Stem Cells in the Treatment of Knee Cartilage Defects. *Knee.* 17, 369-374.

93. KILGORE ML, MORRISEY MA, BECKER DJ *et al.* (2009) Health Care Expenditures Associated With Skeletal Fractures Among Medicare Beneficiaries, 1999-2005. *J.Bone Miner.Res.* 24, 2050-2055.

94. KIM MS, DAY CJ, & MORRISON NA (2005) MCP-1 Is Induced by Receptor Activator of Nuclear Factor-{Kappa}B Ligand, Promotes Human Osteoclast Fusion, and Rescues Granulocyte Macrophage Colony-Stimulating Factor Suppression of Osteoclast Formation. *J.Biol.Chem.* 280, 16163-16169.

95. KIM MS, MAGNO CL, DAY CJ, & MORRISON NA (2006) Induction of Chemokines and Chemokine Receptors CCR2b and CCR4 in Authentic Human Osteoclasts Differentiated With RANKL and Osteoclast Like Cells Differentiated by MCP-1 and RANTES. *J.Cell Biochem.* 97, 512-518.

96. KITOH H, KITAKOJI T, TSUCHIYA H, KATOH M, & ISHIGURO N (2007) Distraction Osteogenesis of the Lower Extremity in Patients With Achondroplasia/Hypochondroplasia Treated With Transplantation of Culture-Expanded Bone Marrow Cells and Platelet-Rich Plasma. *J.Pediatr.Orthop.* 27, 629-634.

97. KLEIN B, WIJDENES J, ZHANG XG *et al.* (1991) Murine Anti-Interleukin-6 Monoclonal Antibody Therapy for a Patient With Plasma Cell Leukemia. *Blood* 78, 1198-1204.

98. KOMIYA S, KAWABATA R, ZENMYO M, HASHIMOTO S, & INOUE A (2000) Increased Concentrations of Nitrate and Nitrite in the Cyst Fluid Suggesting Increased Nitric Oxide Synthesis in Solitary Bone Cysts. *J.Orthop.Res.* 18, 281-288.

99. KOMIYA S, TSUZUKI K, MANGHAM DC, SUGIYAMA M, & INOUE A (1994) Oxygen Scavengers in Simple Bone Cysts. *Clin.Orthop.Relat Res.* 199-206.

100. KON E, MURAGLIA A, CORSI A *et al.* (2000) Autologous Bone Marrow Stromal Cells Loaded Onto Porous Hydroxyapatite Ceramic Accelerate Bone Repair in Critical-Size Defects of Sheep Long Bones. *J.Biomed.Mater.Res.* 49, 328-337.

101. KORDA M, BLUNN G, GOODSHIP A, & HUA J (2008) Use of Mesenchymal Stem Cells to Enhance Bone Formation Around Revision Hip Replacements. *J Orthop.Res.* 26, 880-885.

102. KORDA M, BLUNN G, PHIPPS K *et al.* (2006) Can Mesenchymal Stem Cells Survive Under Normal Impaction Force in Revision Total Hip Replacements? *Tissue Eng* 12, 625-630.

103. KOROMPILIAS AV, LYKISSAS MG, BERIS AE, URBANIAK JR, & SOUCACOS PN (2009) Vascularised Fibular Graft in the Management of Femoral Head Osteonecrosis: Twenty Years Later. *J Bone Joint Surg.Br.* 91, 287-293.

104. KUDO O, SABOKBAR A, POCOCK A *et al.* (2003) Interleukin-6 and Interleukin-11 Support Human Osteoclast Formation by a RANKL-Independent Mechanism. *Bone* 32, 1-7.

105. LAJTHA LG (1979) Stem Cell Concepts. *Differentiation* 14, 23-34.

106. LANGER R & VACANTI JP (1993) Tissue Engineering. *Science* 260, 920-926.

107. LEVINE BR, SPORER S, POGGIE RA, DELLA VALLE CJ, & JACOBS JJ (2006) Experimental and Clinical Performance of Porous Tantalum in Orthopedic Surgery. *Biomaterials* 27, 4671-4681.

108. LING RS, TIMPERLEY AJ, & LINDER L (1993) Histology of Cancellous Impaction Grafting in the Femur. A Case Report. *J Bone Joint Surg.Br.* 75, 693-696.

109. LOKIEC F, EZRA E, KHERMOSH O, & WIENTROUB S (1996) Simple Bone Cysts Treated by Percutaneous Autologous Marrow Grafting. A Preliminary Report. *J.Bone Joint Surg.Br.* 78, 934-937.

110. LOWIK CW, VAN DER PLUIJM G, BLOYS H *et al.* (1989) Parathyroid Hormone (PTH) and PTH-Like Protein (PLP) Stimulate Interleukin-6 Production by Osteogenic Cells: a Possible Role of Interleukin-6 in Osteoclastogenesis. *Biochem.Biophys.Res.Commun.* 162, 1546-1552.

111. MANOLAGAS SC (1995) Role of Cytokines in Bone Resorption. *Bone* 17, 63S-67S.

112. MARCACCI M, KON E, MOUKHACHEV V *et al.* (2007) Stem Cells Associated With Macroporous Bioceramics for Long Bone Repair: 6- to 7-Year Outcome of a Pilot Clinical Study. *Tissue Eng* 13, 947-955.

113. MARINO JT & ZIRAN BH (2010) Use of Solid and Cancellous Autologous Bone Graft for Fractures and Nonunions. *Orthop.Clin.North Am.* 41, 15-26.

114. MARKOVIC B, CVIJETIC A, & KARAKASEVIC J (1988) Acid and Alkaline Phosphatase Activity in Bone-Cyst Fluid. *J.Bone Joint Surg.Br.* 70, 27-28.

115. MCCARTY RC, GRONTHOS S, ZANNETTINO AC, FOSTER BK, & XIAN CJ (2009) Characterisation and Developmental Potential of Ovine Bone Marrow Derived Mesenchymal Stem Cells. *J.Cell Physiol* 219, 324-333.

116. MCKEE MD, GARAY ME, SCHEMITSCH EH, KREDER HJ, & STEPHEN DJ (1998) Irreducible Fracture-Dislocation of the Hip: a Severe Injury With a Poor Prognosis. *J Orthop.Trauma* 12, 223-229.

117. MCLAIN RF, FLEMING JE, BOEHM CA, & MUSCHLER GF (2005) Aspiration of Osteoprogenitor Cells for Augmenting Spinal Fusion: Comparison of Progenitor Cell Concentrations From the Vertebral Body and Iliac Crest. *J.Bone Joint Surg.Am.* 87, 2655-2661.

118. MCNAMARA IR (2010) Impaction Bone Grafting in Revision Hip Surgery: Past, Present and Future. *Cell Tissue Bank.* 11, 57-73.

119. MERLE DR, POSTEL M, MAZABRAUD A *et al.* (1965) Idiopathic Necrosis of the Femoral Head in Adults. *J Bone Joint Surg.Br.* 47, 612-633.

120. MIRRA JM, BERNARD GW, BULLOUGH PG, JOHNSTON W, & MINK G (1978) Cementum-Like Bone Production in Solitary Bone Cysts. (So-Called "Cementoma" of Long Bones). Report of Three Cases. Electron Microscopic Observations Supporting a Synovial Origin to the Simple Bone Cyst. *Clin.Orthop.Relat Res.* 295-307.

121. MITCHELL DG, STEINBERG ME, DALINKA MK *et al.* (1989) Magnetic Resonance Imaging of the Ischemic Hip. Alterations Within the Osteonecrotic, Viable, and Reactive Zones. *Clin.Orthop.Relat Res.* 60-77.

122. MIZUNO M & KUBOKI Y (2001) Osteoblast-Related Gene Expression of Bone Marrow Cells During the Osteoblastic Differentiation Induced by Type I Collagen. *J.Biochem.* 129, 133-138.

123. MONT MA, CARBONE JJ, & FAIRBANK AC (1996) Core Decompression Versus Nonoperative Management for Osteonecrosis of the Hip. *Clin.Orthop.Relat Res.* 169-178.

124. MONT MA, ZYWIEL MG, MARKER DR, MCGRATH MS, & DELANOIS RE (2010) The Natural History of Untreated Asymptomatic Osteonecrosis of the Femoral Head: a Systematic Literature Review. *J Bone Joint Surg.Am.* 92, 2165-2170.

125. MORISHITA T, HONOKI K, OHGUSHI H *et al.* (2006) Tissue Engineering Approach to the Treatment of Bone Tumors: Three Cases of Cultured Bone Grafts Derived From Patients' Mesenchymal Stem Cells. *Artif.Organs* 30, 115-118.

126. MUNDY GR, BOYCE B, HUGHES D *et al.* (1995) The Effects of Cytokines and Growth Factors on Osteoblastic Cells. *Bone* 17, 71S-75S.

127. MURAMATSU K, IHARA K, SHIGETOMI M, & KAWAI S (2004) Femoral Reconstruction by Single, Folded or Double Free Vascularised Fibular Grafts. *Br.J.Plast.Surg.* 57, 550-555.

128. MUSCHLER GF, BOEHM C, & EASLEY K (1997) Aspiration to Obtain Osteoblast Progenitor Cells From Human Bone Marrow: the Influence of Aspiration Volume. *J Bone Joint Surg Am.* 79, 1699-1709.

129. MUSCHLER GF, NITTO H, BOEHM CA, & EASLEY KA (2001) Age- and Gender-Related Changes in the Cellularity of Human Bone Marrow and the Prevalence of Osteoblastic Progenitors. *J Orthop.Res.* 19, 117-125.

130. MUSHIPE MT, CHEN X, JENNINGS D, & LI G (2006) Cells Seeded on MBG Scaffold Survive Impaction Grafting Technique: Potential Application of Cell-Seeded Biomaterials for Revision Arthroplasty. *J.Orthop.Res.* 24, 501-507.

131. NATIONAL JOINT REGISTRY. 5th Annual Report. 2009.

132. NATIONAL JOINT REGISTRY. 7th Annual Report. 2010.

133. NILSDOTTER AK, TOKSVIG-LARSEN S, & ROOS EM (2009) Knee Arthroplasty: Are Patients' Expectations Fulfilled? A Prospective Study of Pain and Function in 102 Patients With 5-Year Follow-Up. *Acta Orthop.* 80, 55-61.

134. OFFICE FOR NATIONAL STATISTICS. 2008-Based Population Projections. 2008.

135. OHGUSHI H, KOTOBUKI N, FUNAOKA H *et al.* (2005) Tissue Engineered Ceramic Artificial Joint--Ex Vivo Osteogenic Differentiation of Patient Mesenchymal Cells on Total Ankle Joints for Treatment of Osteoarthritis. *Biomaterials* 26, 4654-4661.

136. ONO K. Annual Report of Japaneese Investigation Committee for Avascular Necrosis of the Femoral Head. 331-336. 1986.

137. OREFFO RO, BENNETT A, CARR AJ, & TRIFFITT JT (1998) Patients With Primary Osteoarthritis Show No Change With Ageing in the Number of Osteogenic Precursors. *Scand.J.Rheumatol.* 27, 415-424.

138. OREFFO RO, BORD S, & TRIFFITT JT (1998) Skeletal Progenitor Cells and Ageing Human Populations. *Clin.Sci.(Lond)* 94, 549-555.

139. OREFFO RO, GEORGE S, RASSOULIAN H *et al.* Musculoskeletal Biology, Biomechanics, Disease and Regeneration. 2007. University of Southampton. Basic Science Regional Course.

140. OREFFO RO, MUNDY GR, SEYEDIN SM, & BONEWALD LF (1989) Activation of the Bone-Derived Latent TGF Beta Complex by Isolated Osteoclasts. *Biochem.Biophys.Res.Commun.* 158, 817-823.

141. OYAJOBI BO, FRANCHIN G, WILLIAMS PJ *et al.* (2003) Dual Effects of Macrophage Inflammatory Protein-1alpha on Osteolysis and Tumor Burden in the Murine 5TGM1 Model of Myeloma Bone Disease. *Blood* 102, 311-319.

142. PARSONS B & STRAUSS E (2004) Surgical Management of Chronic Osteomyelitis. *The American Journal of Surgery* 188, 57-66.

143. POLITOU M, TERPOS E, ANAGNOSTOPOULOS A *et al.* (2004) Role of Receptor Activator of Nuclear Factor-Kappa B Ligand (RANKL), Osteoprotegerin and Macrophage Protein 1-Alpha (MIP-1a) in Monoclonal Gammopathy of Undetermined Significance (MGUS). *Br.J.Haematol.* 126, 686-689.

144. QUARTO R, MASTROGIACOMO M, CANCEDDA R *et al.* (2001) Repair of Large Bone Defects With the Use of Autologous Bone Marrow Stromal Cells. *N.Engl.J.Med.* 344, 385-386.

145. REICHERT JC, SAIFZADEH S, WULLSCHLEGER ME *et al.* (2009) The Challenge of Establishing Preclinical Models for Segmental Bone Defect Research. *Biomaterials* 30, 2149-2163.

146. RIDGWAY J, BUTCHER A, CHEN PS, HORNER A, & CURRAN S (2010) Novel Technology to Provide an Enriched Therapeutic Cell Concentrate From Bone Marrow Aspirate. *Biotechnol.Prog.*

147. RIPAMONTI U, CROOKS J, KHOALI L, & RODEN L (2009) The Induction of Bone Formation by Coral-Derived Calcium Carbonate/Hydroxyapatite Constructs. *Biomaterials* 30, 1428-1439.

148. ROODMAN GD & WINDLE JJ (2005) Paget Disease of Bone. *J.Clin.Invest* 115, 200-208.

149. ROPOSCH A, SARAPH V, & LINHART WE (2000) Flexible Intramedullary Nailing for the Treatment of Unicameral Bone Cysts in Long Bones. *J.Bone Joint Surg.Am.* 82-A, 1447-1453.

150. ROPOSCH A, SARAPH V, & LINHART WE (2004) Treatment of Femoral Neck and Trochanteric Simple Bone Cysts. *Arch.Orthop.Trauma Surg.* 124, 437-442.

151. ROUGRAFF BT & KLING TJ (2002) Treatment of Active Unicameral Bone Cysts With Percutaneous Injection of Demineralized Bone Matrix and Autogenous Bone Marrow. *J.Bone Joint Surg.Am.* 84-A, 921-929.

152. ROZBRUCH SR & ILIZAROV S (2007) *Limb Lengthening and Reconstruction Surgery, Part 1* Informa Healthcare.

153. SACCHETTI B, FUNARI A, MICHIENZI S *et al.* (2007) Self-Renewing Osteoprogenitors in Bone Marrow Sinusoids Can Organize a Hematopoietic Microenvironment. *Cell* 131, 324-336.

154. SAGI HC, YOUNG M, GERSTENFELD LC, & TORNETTA P (2009) Quantitative differences between bone graft obtained with a Reamer/Irrigator/Aspirator and from the Iliac Crest.

155. SALASZNYK RM, WILLIAMS WA, BOSKEY A, BATORSKY A, & PLOPPER GE (2004) Adhesion to Vitronectin and Collagen I Promotes Osteogenic Differentiation of Human Mesenchymal Stem Cells. *J.Biomed.Biotechnol.* 2004, 24-34.

156. SALEH M, YANG L, & SIMS M (1999) Limb Reconstruction After High Energy Trauma. *Br.Med.Bull.* 55, 870-884.

157. SCAGLIETTI O, MARCHETTI PG, & BARTOLOZZI P (1979) The Effects of Methylprednisolone Acetate in the Treatment of Bone Cysts. Results of Three Years Follow-Up. *J.Bone Joint Surg.Br.* 61-B, 200-204.

158. SCHEP NW, VAN LIESHOUT EM, PATKA P, & VOGELS LM (2009) Long-Term Functional and Quality of Live Assessment Following Post-Traumatic Distraction Osteogenesis of the Lower Limb. *Strategies.Trauma Limb.Reconstr.* 4, 107-112.

159. SCHREURS BW, BOLDER SB, GARDENIERS JW *et al.* (2004) Acetabular Revision With Impacted Morsellised Cancellous Bone Grafting and a Cemented Cup. A 15- to 20-Year Follow-Up. *J.Bone Joint Surg.Br.* 86, 492-497.

160. SCHREURS BW, KEURENTJES JC, GARDENIERS JW *et al.* (2009) Acetabular Revision With Impacted Morsellised Cancellous Bone Grafting and a Cemented Acetabular Component: a 20- to 25-Year Follow-Up. *J.Bone Joint Surg.Br.* 91, 1148-1153.

161. SCHUMACHER M, UHL F, DETSCH R, DEISINGER U, & ZIEGLER G (2010) Static and Dynamic Cultivation of Bone Marrow Stromal Cells on Biphasic Calcium Phosphate Scaffolds Derived From an Indirect Rapid Prototyping Technique. *J.Mater.Sci.Mater.Med.* 21, 3039-3048.

162. SHAH NN, EDGE AJ, & CLARK DW (2009) Hydroxyapatite-Ceramic-Coated Femoral Components in Young Patients Followed-Up for 16 to 19 Years: an Update of a Previous Report. *J Bone Joint Surg Br* 91, 865-869.

163. SHEARER JR, ROACH HI, & PARSONS SW (1992) Histology of a Lengthened Human Tibia. *J.Bone Joint Surg.Br.* 74, 39-44.

164. SHEPPERD JA & APTHORP H (2005) A Contemporary Snapshot of the Use of Hydroxyapatite Coating in Orthopaedic Surgery. *J Bone Joint Surg Br* 87, 1046-1049.

165. SHINDELL R, HUURMAN WW, LIPPIELLO L, & CONNOLLY JF (1989) Prostaglandin Levels in Unicameral Bone Cysts Treated by Intralesional Steroid Injection. *J.Pediatr.Orthop.* 9, 516-519.

166. SLOOFF TJ, HUISKES R, VAN HJ, & LEMMENS AJ (1984) Bone Grafting in Total Hip Replacement for Acetabular Protrusion. *Acta Orthop.Scand.* 55, 593-596.

167. SOBAJIMA S, VADALA G, SHIMER A *et al.* (2008) Feasibility of a Stem Cell Therapy for Intervertebral Disc Degeneration. *Spine J.* 8, 888-896.

168. SPIEGELBERG BG, SEWELL MD, ASTON WJ *et al.* (2009) The Early Results of Joint-Sparing Proximal Tibial Replacement for Primary Bone Tumours, Using Extracortical Plate Fixation. *J.Bone Joint Surg.Br.* 91, 1373-1377.

169. SPONER P & URBAN K (2004) [Treatment of Juvenile Bone Cysts by Curettage and Filling of the Cavity With BAS-0 Bioactive Glass-Ceramic Material]. *Acta Chir Orthop.Traumatol.Cech.* 71, 214-219.

170. STEINBERG ME (1995) Core Decompression of the Femoral Head for Avascular Necrosis: Indications and Results. *Can.J Surg.* 38 Suppl 1, S18-S24.

171. STEINBERG ME, BRIGHTON CT, STEINBERG DR, TOOZE SE, & HAYKEN GD (1984) Treatment of Avascular Necrosis of the Femoral Head by a Combination of Bone Grafting, Decompression, and Electrical Stimulation. *Clin.Orthop.Relat Res.* 137-153.

172. STEINBERG ME, HAYKEN GD, & STEINBERG DR (1984) A New Method for the Evaluation and Staging of Avascular Necrosis of the Femoral Head. In: *Bone Circulation* (eds. J Arlet, RP Ficat, & DS Hungerford), 398-403. Williams & Wilkins, Baltimore.

173. STENDERUP K, JUSTESEN J, ERIKSEN EF, RATTAN SI, & KASSEM M (2001) Number and Proliferative Capacity of Osteogenic Stem Cells Are Maintained During Aging and in Patients With Osteoporosis. *J.Bone Miner.Res.* 16, 1120-1129.

174. STEVENSON S, EMERY SE, & GOLDBERG VM (1996) Factors Affecting Bone Graft Incorporation. *Clin.Orthop.Relat Res.* 66-74.

175. SUDA T, UDAGAWA N, NAKAMURA I, MIYAURA C, & TAKAHASHI N (1995) Modulation of Osteoclast Differentiation by Local Factors. *Bone* 17, 87S-91S.

176. SUGANO N, ATSUMI T, OHZONO K *et al.* (2002) The 2001 Revised Criteria for Diagnosis, Classification, and Staging of Idiopathic Osteonecrosis of the Femoral Head. *J Orthop.Sci* 7, 601-605.

177. SWENNEN G, SCHLIEPHAKE H, DEMPF R, SCHIERLE H, & MALEVEZ C (2001) Craniofacial Distraction Osteogenesis: a Review of the Literature. Part 1: Clinical Studies. *International Journal of Oral and Maxillofacial Surgery* 30, 89-103.

178. TAKAHASHI K & YAMANAKA S (2006) Induction of Pluripotent Stem Cells From Mouse Embryonic and Adult Fibroblast Cultures by Defined Factors. *Cell* 126, 663-676.

179. TAMURA T, UDAGAWA N, TAKAHASHI N *et al.* (1993) Soluble Interleukin-6 Receptor Triggers Osteoclast Formation by Interleukin 6. *Proc.Natl.Acad.Sci.U.S.A* 90, 11924-11928.

180. TARE RS, BABISTER JC, KANCZLER J, & OREFFO RO (2008) Skeletal Stem Cells: Phenotype, Biology and Environmental Niches Informing Tissue Regeneration. *Mol.Cell Endocrinol.* 288, 11-21.

181. TARE RS, KANCZLER J, AARVOLD A *et al.* (2010) Skeletal Stem Cells and Bone Regeneration: Translational Strategies From Bench to Clinic. *Proc.Inst.Mech.Eng H.* 224, 1455-1470.

182. TAYLOR GI, MILLER GD, & HAM FJ (1975) The Free Vascularized Bone Graft. A Clinical Extension of Microvascular Techniques. *Plast.Reconstr.Surg.* 55, 533-544.

183. THAWRANI D, THAI CC, WELCH RD, COPLEY L, & JOHNSTON CE (2009) Successful Treatment of Unicameral Bone Cyst by Single Percutaneous Injection of Alpha-BSM. *J.Pediatr.Orthop.* 29, 511-517.

184. TILLEY S, BOLLAND BJ, PARTRIDGE K *et al.* (2006) Taking Tissue-Engineering Principles into Theater: Augmentation of Impacted Allograft With Human Bone Marrow Stromal Cells. *Regen.Med.* 1, 685-692.

185. TRIKHA SP, SINGH S, RAYNHAM OW *et al.* (2005) Hydroxyapatite-Ceramic-Coated Femoral Stems in Revision Hip Surgery. *J.Bone Joint Surg.Br.* 87, 1055-1060.

186. TROUVIN AP & GOEB V (2010) Receptor Activator of Nuclear Factor-KappaB Ligand and Osteoprotegerin: Maintaining the Balance to Prevent Bone Loss. *Clin.Interv.Aging* 5, 345-354.

187. TSAI KS, KAO SY, WANG CY *et al.* (2010) Type I Collagen Promotes Proliferation and Osteogenesis of Human Mesenchymal Stem Cells Via Activation of ERK and Akt Pathways. *J.Biomed.Mater.Res.A* 94, 673-682.

188. UDAGAWA N, TAKAHASHI N, KATAGIRI T *et al.* (1995) Interleukin (IL)-6 Induction of Osteoclast Differentiation Depends on IL-6 Receptors Expressed on Osteoblastic Cells but Not on Osteoclast Progenitors. *J.Exp.Med.* 182, 1461-1468.

189. UEDA M, YAMADA Y, OZAWA R, & OKAZAKI Y (2005) Clinical Case Reports of Injectable Tissue-Engineered Bone for Alveolar Augmentation With Simultaneous Implant Placement. *Int.J.Periodontics.Restorative.Dent.* 25, 129-137.

190. VACANTI CA, BONASSAR LJ, VACANTI MP, & SHUFFLEBARGER J (2001) Replacement of an Avulsed Phalanx With Tissue-Engineered Bone. *N.Engl.J.Med.* 344, 1511-1514.

191. VADALA G, DI MA, TIRINDELLI MC, DENARO L, & DENARO V (2008) Use of Autologous Bone Marrow Cells Concentrate Enriched With Platelet-Rich Fibrin on Corticocancellous Bone Allograft for Posterolateral Multilevel Cervical Fusion. *J.Tissue Eng Regen.Med.* 2, 515-520.

192. VAN DER DONK S, BUMA P, SLOOFF TJ, GARDENIERS JW, & SCHREURS BW (2002) Incorporation of Morselized Bone Grafts: a Study of 24 Acetabular Biopsy Specimens. *Clin.Orthop.Relat Res.* 131-141.

193. VAN HAAREN EH, HEYLIGERS IC, ALEXANDER FG, & WUISMAN PI (2007) High Rate of Failure of Impaction Grafting in Large Acetabular Defects. *J.Bone Joint Surg.Br.* 89, 296-300.

194. VAYEGO SA, DE CONTI OJ, & VARELLA-GARCIA M (1996) Complex Cytogenetic Rearrangement in a Case of Unicameral Bone Cyst. *Cancer Genet.Cytogenet.* 86, 46-49.

195. VEILLETTE CJ, MEHDIAN H, SCHEMITSCH EH, & MCKEE MD (2006) Survivorship Analysis and Radiographic Outcome Following Tantalum Rod Insertion for Osteonecrosis of the Femoral Head. *J.Bone Joint Surg.Am.* 88 Suppl 3, 48-55.

196. VIGORITA VJ, GHELMAN B, & MINTZ D (2007) Basic Science of Bone. In: *Orthopaedic Pathology* Lippincott, Williams & Wilkins.

197. VON WILMOWSKY C, SCHWARZ S, KERL JM *et al.* (2009) Reconstruction of a Mandibular Defect With Autogenous, Autoclaved Bone Grafts and Tissue Engineering: An in Vivo Pilot Study. *J.Biomed.Mater.Res.A* 93, 1510-1518.

198. VOTTA BJ, WHITE JR, DODDS RA *et al.* (2000) CKbeta-8 [CCL23], a Novel CC Chemokine, Is Chemotactic for Human Osteoclast Precursors and Is Expressed in Bone Tissues. *J.Cell Physiol* 183, 196-207.

199. WANG BL, SUN W, SHI ZC *et al.* (2010) Treatment of Nontraumatic Osteonecrosis of the Femoral Head Using Bone Impaction Grafting Through a Femoral Neck Window. *Int.Orthop.* 34, 635-639.

200. WARNKE PH, SPRINGER IN, WILTFANG J *et al.* (2004) Growth and Transplantation of a Custom Vascularised Bone Graft in a Man. *Lancet* 364, 766-770.

201. WARNKE PH, WILTFANG J, SPRINGER I *et al.* (2006) Man As Living Bioreactor: Fate of an Exogenously Prepared Customized Tissue-Engineered Mandible. *Biomaterials* 27, 3163-3167.

202. WATT FM & DRISKELL RR (2010) The Therapeutic Potential of Stem Cells. *Philos.Trans.R.Soc.Lond B Biol.Sci.* 365, 155-163.

203. XU C, SU P, CHEN X *et al.* (2011) Biocompatibility and Osteogenesis of Biomimetic Bioglass-Collagen-Phosphatidylserine Composite Scaffolds for Bone Tissue Engineering. *Biomaterials* 32, 1051-1058.

204. YAMASAKI T, YASUNAGA Y, ISHIKAWA M, HAMAKI T, & OCHI M (2010) Bone-Marrow-Derived Mononuclear Cells With a Porous Hydroxyapatite Scaffold for the Treatment of Osteonecrosis of the Femoral Head: a Preliminary Study. *J Bone Joint Surg.Br.* 92, 337-341.

205. YANG XB, ROACH HI, CLARKE NM *et al.* (2001) Human Osteoprogenitor Growth and Differentiation on Synthetic Biodegradable Structures After Surface Modification. *Bone* 29, 523-531.

206. YU J, CHANG SS, SURATWALA S *et al.* (2005) Zoledronate Induces Apoptosis in Cells From Fibro-Cellular Membrane of Unicameral Bone Cyst (UBC). *J.Orthop.Res.* 23, 1004-1012.

207. YUAN H, FERNANDES H, HABIBOVIC P *et al.* (2010) Osteoinductive Ceramics As a Synthetic Alternative to Autologous Bone Grafting. *Proc.Natl.Acad.Sci U.S.A* 107, 13614-13619.

208. YUAN H, YANG Z, DE BRUIJ JD, DE GROOT K, & ZHANG X (2001) Material-Dependent Bone Induction by Calcium Phosphate Ceramics: a 2.5-Year Study in Dog. *Biomaterials* 22, 2617-2623.